

Polymers and Surfactants in Solution and at Interfaces

A model study on detergency

Promotor: dr. J. Lyklema,
emeritus hoogleraar in de fysische chemie,
met bijzondere aandacht voor de grensvlak- en kolloïdchemie

Co-promotoren: dr. ir. L. K. Koopal,
universitair hoofddocent bij de leerstoelgroep Fysische Chemie en
Kolloïdkunde

dr. A. de Keizer,
universitair docent bij de leerstoelgroep Fysische Chemie en
Kolloïdkunde

1102701.2134

Polymers and Surfactants in Solution and at Interfaces

A model study on detergency

Bert Torn

Proefschrift

ter verkrijging van de graad van doctor

op gezag van de rector magnificus

van Wageningen Universiteit,

dr. ir. L. Speelman,

in het openbaar te verdedigen

op woensdag 13 september 2000

des namiddags te vier uur in de Aula.

UW 6-21001

Torn, L. H.

Polymers and Surfactants in Solution and at Interfaces: a model study on
detergency/ L. H. Torn

Thesis Wageningen University

ISBN 90-5808-264-4

Subject headings: polymer adsorption/surfactant adsorption/polymer-
surfactant interactions

Omslag: Marije Verkerk

Het in dit proefschrift beschreven onderzoek is mogelijk gemaakt door
Unilever Research Vlaardingen.

BIBLIOTHEEK
LANDBOUWUNIVERSITEIT
WAGENINGEN

Stellingen

1. De preferente specifieke adsorptie van protonen ten opzichte van natriumionen op de platen van kaoliniet, leidt tot een verhoging van de adsorptie van poly(vinylpyrrolidon) op dit oppervlak.

Dit proefschrift hoofdstuk 2

2. Bij de interactie tussen poly(vinylpyrrolidon) en natrium dodecylbenzeensulfonaat treedt bij hoge surfactantconcentraties een conformatieverandering van het complex op, die gepaard gaat met een verlies aan hydrofobe binding.

Dit proefschrift hoofdstuk 3

4. De adsorptiekinetiek van polyethyleenglycol alkylethers op cellulose is zeer gevoelig voor kleine veranderingen in de grootte van de kop en de staart van de surfactanten.

Dit proefschrift hoofdstuk 6

5. De door Biswas en Chattoraj waargenomen negatieve adsorptie van alkyltrimethylammonium bromide op cellulose kan worden verklaard door de porositeit van de cellulosedeeftjes in de discussie te betrekken.

S. C. Biswas and D. K. Chattoraj, Langmuir 13, 4505, 1997

6. In hun microcalorimetrische onderzoek naar de interactie tussen ongeladen cellulose ethers en natrium dodecylsulfaat nemen Singh and Nilsson ten onrechte geen kop-kopwisselwerking mee in hun bespreking.

S. K. Singh and S. Nilsson, J. Colloid Interface Sci. 213, 133, 1999

7. Ondanks het veelvuldige gebruik van microcalorimetrie bij de bestudering van polymeer-surfactantinteracties, worden de mogelijkheden van deze techniek doorgaans onvolledig benut doordat er slechts bij één temperatuur wordt gemeten.

8. De wet van de afnemende meeropbrengst gaat niet op voor het adsorberen van surfactants en het spelen van een snelschaakpartij.

9. De positie en het werkterrein van Wageningen URC die in de nota 'Strategische visie' worden beschreven door 'twee hoofdassen', 'drie kernactiviteiten', en 'een viertal thema's onderverdeeld in subthema's', is na lezing niet duidelijk.

Strategische visie Wageningen Universiteit en Research Centrum, juni 1998.

10. Het is niet vreemd dat mensen niet geloven in een zelfbedachte God.

11. Het feit dat politici het bestaan van een kiezerskloof niet begrijpen is juist de oorzaak ervan.

12. Tijdsgebrek is, als algemeen erkende volksziekte, niet zozeer het gevolg van een groeiend aantal mogelijkheden, alswel van een toename van ambities.

13. In een bekende variant van de Oostenrijkse aanval van de Pirc-verdediging, ontstaat na 1. e4 d6 2. d4 Pf6 3. Pc3 g6 4. f4 Lg7 5. Pf3 c5 6. dxc5 Da5 7. Ld3 Dxc5 8. De2 Lg4 9. Le3 Da5 10. 0-0 Pc6 11. h3 Lxf3 12. Dxf3 0-0 13. a3 Pd7 14. Ld2 Db6+ 15. Kh1 Pc5 16. Tab1 Pxd3 17. cxd3 'een kritieke stelling' (The Ultimate Pirc, J. Nunn, Batsford, 1998, 63) die zwart volgens de huidige stand van de theorie gelijke kansen biedt. Wit kan echter met 16. Pd5! in het voordeel komen.

14. De waarneming dat bij de afhaal-Chinees op de vraag "Sambal bij?" het antwoord niet wordt afgewacht, zegt meer over de aard van de gemiddelde Nederlander dan over de Chinese beheersing van de Nederlandse taal.

15. Om termen als 'witte energie' en blauwe kracht' te voorkomen, verdient het aanbeveling om wetenschappers in te schakelen bij het maken van reclame voor wasmiddelen.

Stellingen behorende bij het proefschrift "Polymers and surfactants in solution and at interfaces: a model study on detergency" van Bert Torn, Wageningen Universiteit, 13 september 2000.

‘Uit deze massa, uit dit grove mengelmoes dat aan de pen kleefde en uit alle hoeken en gaten van zijn geheugen kwam getuimeld, elke herinnering onderend en het vrije denken blokkerend, moest hij noodgedwongen, onvermijdelijk, voorzichtig, en stukje bij beetje, het beeld, compleet en ongeschonden, te voorschijn halen.....’

Vladimir Nabokov, *De verdediging*

Ter herinnering aan mijn oma

- Chapter 2: published in Prog. Colloid Polym. Sci. **109**, 153 (1998).
- Chapter 3: published in Colloids Surf. A: Physicochem. Eng. Aspects **160**, 237 (1999).
- Chapter 4: submitted to J. Colloid Interface Sci.
- Chapter 5: submitted to Colloids Surf. A
- Chapter 6: submitted to Langmuir

Contents

Chapter 1: Introduction	1
1.1 Polymers in aqueous solution and at solid-liquid interfaces	1
1.2 Surfactants	3
1.2.1 Introduction	3
1.2.2 Surfactants in aqueous solutions	4
1.2.3 Surfactants at solid-liquid interfaces	7
1.3 Detergency	7
1.3.1 Introduction	9
1.3.2 Soil removal	10
1.3.2.1 Oily soil removal	11
1.3.2.2 Particulate soil removal	12
1.4 Aims and contents of this thesis	13
References	15
Chapter 2: Adsorption of poly(vinylpyrrolidone) on kaolinite	21
2.1 Introduction	22
2.2 Experimental	24
2.2.1 Materials	24
2.2.2 Methods	24
2.3 Results and Discussion	25
2.3.1 Potentiometric titrations	25
2.3.2 Adsorption of PVP	28
2.4 Conclusions	36
References	37
Chapter 3: Interaction between poly(vinylpyrrolidone) and sodium dodecylbenzenesulphonate in aqueous solutions	39
3.1 Introduction	40
3.2 Experimental	41
3.2.1 Materials	41
3.2.2 Methods	41

3.3 Results and discussion	42
3.3.1 Micellization of SDBS	42
3.3.2 Interaction between PVP and SDBS in solution	44
3.3.2.1 General trends	44
3.3.2.2 Effect of the amount of polymer	52
3.3.2.3 Effect of the electrolyte concentration	54
3.4 Conclusions	55
References	56

Chapter 4: Mixed adsorption of poly(vinylpyrrolidone) and sodium dodecylbenzenesulphonate on kaolinite

4.1 Introduction	60
4.2 Experimental	61
4.2.1 Materials	61
4.2.2 Methods	62
4.3 Results and discussion	63
4.3.1 Single adsorption isotherms	63
4.3.2 Interaction in solution	64
4.3.3 Mixed adsorption isotherms	65
4.3.3.1 Effect of pH	65
4.3.3.2 Effect of the electrolyte concentration	69
4.3.3.3 Effect of the amount of polymer	72
4.4 Conclusions	75
References	76

Chapter 5: Cellulose Films as Model Systems for Adsorption Studies

5.1 Introduction	80
5.2 Experimental	81
5.2.1 Materials	81
5.2.2 Preparation of the films	81
5.2.3 Methods	83
5.3 Results and Discussion	85
5.3.1 Characterization	85

5.3.1.1 Ellipsometry	85
5.3.1.2 Contact angle measurements	85
5.3.1.3 Atomic force microscopy	86
5.3.1.4 Streaming potential measurements	88
5.3.2 Adsorption	89
5.3.2.1 Stability and swelling	89
5.3.2.2 Polymer adsorption	91
5.3.2.3 Surfactant adsorption	92
5.4 Conclusions	93
References	93

Chapter 6: Nonionic Surfactants approaching Cellulose Surfaces:

Kinetics and Adsorbed Amount	97
6.1 Introduction	98
6.2 Experimental	100
6.2.1 Materials	100
6.2.2 Methods	101
6.3 Results and discussion	102
6.3.1 Kinetic aspects	102
6.3.1.1 Adsorption and desorption as a function of time	102
6.3.1.2 Initial adsorption and desorption kinetics	104
6.3.1.3 Modelling and discussion	105
6.3.2 Equilibrium aspects	113
6.3.2.1 Adsorbed amount	113
6.3.2.2 Molecular packing at the surface	117
6.4 Conclusions	118
References	118
Summary	123
Samenvatting	129
Levensloop	135
Dankwoord	137

Chapter 1

Introduction

This thesis deals with the behaviour of polymers and surfactants in solution and at solid-liquid interfaces. Both types of molecules play a role in the removal and subsequent stabilization of soil from a substrate, i.e. detergency. This chapter gives an introduction on their characteristic behaviour. The main features of detergency are also shortly discussed.

1.1 Polymers in aqueous solution and at solid-liquid interfaces

Polymers are large molecules consisting of a great number of repeating, covalently linked segments. These segments can have a variety of compositions, ranging from hydrophilic to hydrophobic, and uncharged to charged, thereby governing the specific properties of a polymer chain¹. However, the main feature of polymers is their large spatial extent which endows them with unique properties. Some important adsorption aspects will be shortly outlined. Reviews can be consulted for a more thorough treatment²⁻⁴.

If carefully selected, polymers can be dissolved in several solvents. They may be water-soluble when they have enough ionic and/or hydrophilic groups. The conformation of the chains in solution is balanced by segment-segment and segment-solvent interactions. For uncharged water-soluble polymers, a random coil is the most common conformation.

Polymers can adsorb at surfaces by a variety of mechanisms such as hydrogen bonding, hydrophobic interactions, dipolar interactions, and coulombic attractions. Remind adsorption as an exchange process, polymers tend to adsorb when the attractive segment-surface interactions exceed the solvent-surface interactions. However, this picture is not the whole story. In solution, a polymer chain has a great number of degrees of

freedom, i.e. *conformational entropy*. When adsorbed, at least some polymer segments are in intimate contact with the surface. This leads to a lower conformational entropy. Furthermore, the *mixing energy* (which is related to the solvent quality) and the *mixing entropy* (which decreases upon polymer adsorption) have to be taken into account. In order to adsorb, the *polymer adsorption energy* with respect to the solvent, has to overcome the above-mentioned contributions by favourable segment-surface contacts. As a result, there is a critical adsorption energy which must be surpassed before chains adsorb⁴.

Although the interaction energy per segment may be small, usually less than 1 kT, the total Gibbs energy contribution per molecule may be large enough compensate the incurred entropy loss, provided that loops and tails are formed (figure 1.1). An accompanying feature is that polymer adsorption isotherms usually show typical high affinity behaviour.

If a large number of segments are close to the surface, the macromolecule adopts a flat conformation resulting in a large entropic penalty. A compromise between high conformational entropy and low Gibbs energy is found in a thick adsorbed layer⁵ (order of nanometers), where trains, loops, and tails can be distinguished⁶ (figure 1.1).

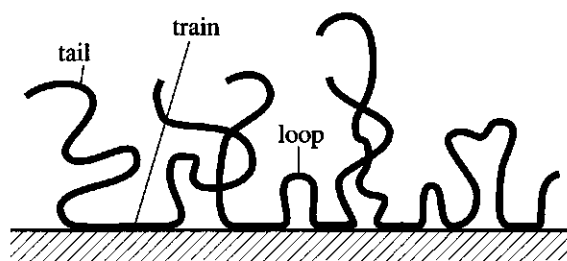


Figure 1.1: Schematic representation of a polymer adsorbed at a surface.

Additional phenomena come into play in the case of polyelectrolyte adsorption. The segment-surface interaction energy is influenced by charges as expected. Repulsive segment-segment interactions have consequences for both the conformation of chains in solution and that at a surface. A random coil conformation is unlikely for charged polymers

since that would contain many intramolecular contacts. Polyelectrolytes will therefore be more rigid and swollen⁷, i.e. they adopt a more stretched conformation compared to uncharged polymers. Near a surface, loops and tails protruding into the solution repel each other, so they do not develop, resulting in a flat adsorbed layer. An attendant consequence is that once a polyelectrolyte is adsorbed it is more difficult for incoming chains to approach the surface^{8,9}. An electrostatic barrier is formed which strongly influences the adsorption kinetics.

A last feature typical for polymers which has implications for adsorption is their polydispersity, i.e. they display a molecular mass distribution rather than a single value. With respect to adsorption, short polymer chains adsorb faster than longer ones, but at equilibrium high molecular mass polymers preferentially adsorb, thereby replacing the smaller molecules. This last feature originates from the entropy of mixing in solution which strongly decreases with increasing chain length⁴. The consequences for adsorption isotherms are twofold. Firstly, instead of a high affinity isotherm a more rounded isotherm, gradually ascending towards a plateau value, may be found^{4,10}. Secondly, it may take very long before equilibrium is reached.

Polymers adsorbed at solid-liquid interfaces are used in a great variety of processes, either as stabilizing¹¹⁻¹³ (electrostatically and/or sterically) or destabilizing agents^{13,14}. Stabilization can be provided by a thick adsorbed layer on a saturated surface. Destabilization (flocculation) can take place at low polymer concentrations, when long chains simultaneously adsorb onto two or more surfaces.

1.2 Surfactants

1.2.1 Introduction

The term 'surfactant' is a contraction from SURFace ACTive Agent. This name covers the most prominent property of these class of molecules: the tendency to accumulate at interfaces¹⁵⁻¹⁷. The origin of this behaviour is

revealed by their molecular structure: surfactants are ambivalent, having a water-loving ('hydrophilic') part, usually referred to as head group, and a water-fearing ('hydrophobic') part, called tail (figure 1.2). In aqueous systems the latter is mostly a hydrocarbon which can either be branched or unbranched, and saturated or unsaturated. In non-aqueous systems fluorocarbons and polydimethylsiloxanes are used as hydrophobes. Classification of surfactant molecules is usually based on the charge of the polar head group, resulting in the categories of nonionic, anionic, cationic, and zwitterionic surfactants.



Figure 1.2: Schematic picture of a surfactant molecule.

Most surfactants have one polar and one apolar group. In recent years, there is growing interest in so-called gemini surfactants, consisting of two hydrophilic and two hydrophobic groups per molecule separated by a spacer^{18,19}.

Besides the word 'surfactant' there are many synonyms used for these molecules. The term which unravels its nature equally well is 'amphiphile' ("loving both sides"). Furthermore, they are called detergents, soaps, (de)wetting agents, (d)emulsifiers, and dispersants, according to their function. In all cases, it is their dual nature which makes them indispensable for a great variety of industrial, technological, and biological processes. Recently, two very readable textbooks^{17,20} have been published covering important aspects of surfactant systems, a few of which will be shortly discussed below.

1.2.2 Surfactants in aqueous solutions

Surfactant molecules dissolved in an aqueous solution experience two opposing forces: the hydrophobic part is expelled by water molecules whereas the hydrophilic part wants to remain hydrated²¹. If the latter force is weak, the system will undergo a macroscopic phase separation, which

occurs for long chain alcohols in water. If hydration of the head group is strong compared to the hydrophobic effect, dissolved single monomers will be the most stable form. An example of this is an aqueous solution of a short chain alcohol. An intermediate situation arises when the hydrophobic and hydrophilic forces are roughly balanced. In this case, the composition of the system lies in between that of macroscopic phase separation and complete mixing. As early as 1913 McBain²² suggested the (initially controversial) self-association of surfactant molecules into what he called 'micelles'. In aqueous solution these are aggregates with an apolar core surrounded by polar head groups (figure 1.3). Currently, the existence of surfactant associates has been proven beyond any doubt, in both extensive experimental and theoretical research^{16,23,24}.

The overall composition of a surfactant solution is roughly constant in time, meaning that there exist dynamic equilibria between monomers and micelles in solution, and between adsorbed molecules and bulk molecules (figure 1.3).

Micellization diminishes contact between water and hydrophobic groups and occurs if the surfactant molecules can form tightly-packed aggregates. This requires a minimum amount of surfactant molecules, usually expressed as critical micelle concentration (c.m.c.).

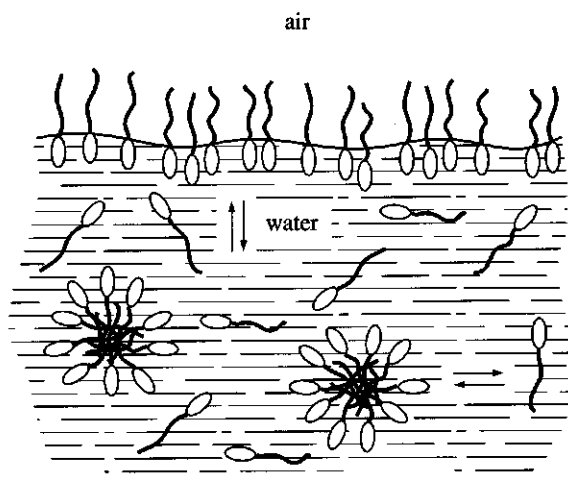


Figure 1.3: Schematic picture of an aqueous surfactant solution above the c.m.c..

A variety of physical properties, such as the surface tension, osmotic pressure, light scattering, and solubilization, abruptly change at the c.m.c.²⁵ which makes this quantity easily experimentally accessible. It may be noted that these physical properties depend either on the concentration of surfactant monomers, as in the case of surface tension, or on that of micelles, as seen in solubilization.

The c.m.c. is probably the most characteristic property of a surfactant. It depends both on molecular (e.g. the length of the hydrocarbon tail, the size and the charge of the head group, and the type of counterion) and solution (e.g. the electrolyte concentration, the presence of co-solutes and the temperature) properties^{15,17,26}. Rules of thumb for the direction into which the c.m.c. changes are:

- Surfactants with a longer hydrocarbon chain have a lower c.m.c. because they are more strongly repelled by water molecules.
- The c.m.c. of ionic surfactants can be considerably lowered by indifferent ions or co-solutes, since these can screen the charges of neighbouring head groups in a micelle.
- Increasing the temperature of a nonionic surfactant solution, leads to dehydration of the hydrophilic (ethylene oxide) groups, resulting in a lowering of the c.m.c..

Micelles can be characterized by a (mutually related) size and shape. The former is usually expressed by an average number of monomers in a micelle and can be experimentally determined by several different techniques²⁶ of which fluorescence spectroscopy²⁷ and nuclear magnetic resonance²⁸ are most popular. For charged surfactants this number is usually between 60 and 100, whereas nonionic surfactants can have a much broader range of aggregation numbers¹⁵.

In the absence of energetic constraints, micellar shape is determined by the monomer architecture, i.e. the relative size of the hydrophilic and hydrophobic parts. Based on geometric packing constraints only, Israelachvili introduced a dimensionless critical packing parameter^{29,30}:

$$CPP = \frac{v}{a_0 l_c} \quad [1.1]$$

where v is the volume of the hydrocarbon chain in a micellar core, a_0 the optimum cross-sectional surface area of the head group in an aggregate, and l_c the extended length of the hydrocarbon chain. This parameter is a useful tool to see how molecular geometry influences aggregate shape.

For surfactants with a relatively large head group, $CPP < 1/3$, and micelles will be spherical. Examples of this type are anionic surfactants at low salt concentrations, and the nonionic penta-ethylene glycol *n*-dodecylether, $C_{12}E_7$. For $1/2 < CPP < 1/3$, cylindrical structures are preferred; this occurs, for example, for the nonionic surfactant $C_{12}E_5$. If $CPP \approx 1$, head group and tail have roughly the same cross-sectional area and molecules can pack parallel to each other forming lamellar or bilayer structures. Examples are nonionic surfactants with a short head group and double-chain surfactants. If the critical packing parameter exceeds unity, reverse micelles will form, the continuous phase being apolar.

Although this packing concept is a very valuable tool, it should be kept in mind that the solution properties and the surfactant concentration also influence micellar shape. The structures just discussed are preferred for concentrations not too far above the c.m.c.. Various other complex morphologies exist in concentrated surfactant solutions^{17,31}. The composition of surfactant aggregates as a function of the concentration is usually expressed in a phase diagram³¹.

1.2.3 Surfactants at solid-liquid interfaces

For a similar reason that surfactant molecules concentrate at air-water interfaces, they do so at solid-water interfaces. The molecular orientation at the former is easily depicted, whereas this is far less obvious at the latter. Ignoring for the moment coulombic effects, the polarity of the surface determines in principle whether it preferably attracts the head group or the tail of a surfactant. Once molecules are adsorbed on a surface, it is favourable for incoming molecules to interact laterally, leading to the

formation of surface aggregates at concentrations well below the c.m.c.^{5,32,33}. The adsorption process can be looked upon as a surface-induced self-assembly.

The specific structure of surface aggregates is balanced by surfactant-surface interaction on the one hand, and hydrophobic attraction between the aliphatic tails at the other¹⁷. If the latter is much larger than the former, discrete structures are formed which strongly resemble those formed in solution, i.e. half-micelles on hydrophobic substrates³⁴ and surface micelles on hydrophilic ones³⁵. In the other case, when surfactant-surface attractions are dominant, the surface imposes the structure of the adsorbed layer, i.e. monolayers at hydrophobic substrates³⁵, and bilayers on hydrophilic surfaces^{32,33}. These structures are commonly referred to as 'hemimicelles'³⁶ and 'admicelles'³⁷, respectively.

The introduction of charges on both adsorbate and adsorbent, influences both surfactant-surface and surfactant-surfactant interactions. In the case of oppositely charged surface and surfactant, their affinity increases compared to that of uncharged species, whereas the opposite holds when they are of like charge. Charge influences surfactant-surfactant interactions in the formation of aggregates, i.e. neighbouring charged head groups repel each other. In general this leads to aggregate shapes where the head group distance is maximized, i.e. small spherical associates.

Numerous models have been proposed for surfactant adsorption at solid-liquid interfaces, ranging from simple to very elaborate ones³⁸⁻⁴⁰. Often they are based on the Frumkin-Fowler-Guggenheim (FFG) equation^{41,42} which adds lateral interactions to the Langmuir isotherm in the Bragg-Williams approximation. This equation can be extended by including electrostatic interactions⁴³⁻⁴⁵, surface heterogeneity⁴⁵⁻⁴⁷, and chain characteristics of the surfactant^{43,48}. A different and widely applicable model was proposed by Gu et al.⁴⁹⁻⁵¹ which distinguishes two stages in the adsorption process: (1) single molecules adsorb according to the Langmuir model, which then (2) act as nuclei for surface aggregates.

Adsorption isotherms of ionic surfactants on polar surfaces have received a lot of attention^{47,52,53}. Typically, they are interpreted on the basis of a four-region log-log plot, which accounts for singly adsorbed monomers at low surfactant concentrations (Henry-region) and bilayer structures at higher concentrations. Disagreement on the evolution of these aggregates^{37,52,54,55} resulted in a variety of proposed models, such as the reverse orientation model⁵², the bilayer model³⁷, and the two-step model⁵⁰. To further complicate matters, a recent detailed NMR study on the adsorption of isomer-free sodium *n*-decylbenzenesulphonate onto alumina⁵⁵ suggests that the truth may be close to an intermediate model.

A completely different approach is the use of a mean-field lattice model. Originally developed for polymer adsorption^{56,57}, it has been extended to study the adsorption and micellization of surfactants^{40,53,58}. Results obtained with this type of model can be compared with experimentally observed trends, but absolute fitting of data is not conclusive because of the great number of adjustable parameters.

In conclusion, it can be said that all these models provide a reasonable insight into surfactant adsorption at solid-liquid interfaces. However, significant experimental progress is currently offered by in-situ techniques such as atomic force microscopy (AFM)⁵⁹⁻⁶⁶, yielding direct information on the structure of surface aggregates.

1.3 Detergency

1.3.1 Introduction

Detergency is generally defined as the removal of soil ("matter out of place"⁶⁷) from a substrate. It will be used here in a more restricted sense, referring to systems having the following characteristics: (1) cleaning is carried out in an aqueous medium and (2) cleaning is primarily caused by interfacial forces acting between liquid, substrate, and soil. Hence, hydrodynamic (due to agitation) and chemical forces (e.g. due to enzymes and bleaching agents) are not considered. Looking through the eyes of a

physical chemist, the detergency process is an eldorado. It may include various interfacial phenomena such as wetting, adsorption, double layer repulsion, (de)micellization, soil detachment, solubilization, emulsification, and redeposition, which can occur simultaneously. As a result, detergency is an extremely complex process and far too complicated to be qualitatively treated by classical theories of colloid science. The majority of the extensive literature covers the experimental side of sub-systems, a topic on which already several books and reviews have been published⁶⁷⁻⁷⁴. The following short introduction is mainly based on the reviews of Schwartz⁶⁸ and Carroll⁷³ which focus on physico-chemical aspects of detergency.

1.3.2 Soil removal

Numerous different soils can be encountered in a cleaning process. Basically, they can be divided into two types: solid (particulate) and liquid (oily) soil. These types can also be combined, resulting in mixed soil, for instance particulate soil with an oily shell.

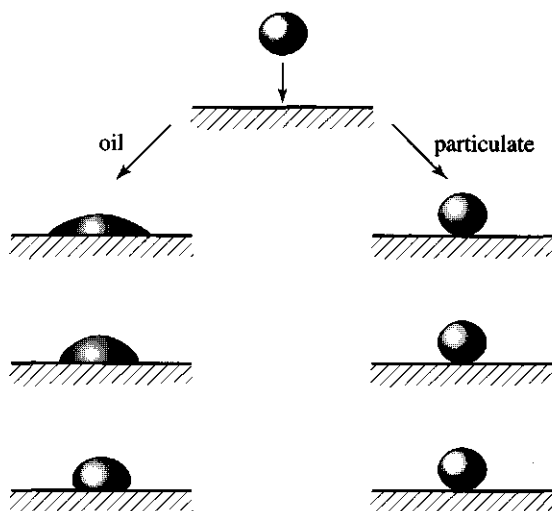


Figure 1.4: Interactions of oily and particulate soil with a substrate: in air, in water, and in aqueous surfactant solution, respectively (redrawn from B. J. Carroll⁷³).

Particulate and oily soils differ in shape and rheological properties. The former retain their shapes throughout the washing process, whereas those

of the latter can be altered by, for example, changes in temperature, capillary forces induced by the (fibrous) nature of the substrate, and differences in the composition of the liquid medium (figure 1.4). As a result, the driving force for the removal of these soil types differs and a separate discussion is required.

1.3.2.1 Oily soil removal

Three different types of removal mechanisms for oily soils are reported: roll up, emulsification, and solubilization⁶⁸. Originated by Adam⁷⁵, the *roll up* process is probably the primary mechanism of oily soil removal from hydrophilic surfaces. On such surfaces, oily soil does not readily spread but rather forms droplets. It is possible to identify the equilibrium contact angle θ between soil, substrate and water (figure 1.5) which is a measure of the wettability.



Figure 1.5: Illustration of roll-up by an increasing contact angle θ .

This angle can be related to the interfacial tensions between substrate and water (γ_{sw}), substrate and oil (γ_{so}), and oil and water (γ_{ow}), by Young's equation:

$$\cos \theta = \frac{\gamma_{sw} - \gamma_{so}}{\gamma_{ow}} \quad [1.2]$$

When surfactants are added to an oily-soiled substrate, adsorption may occur at the substrate-water and oil-water interface, whereby both γ_{sw} and γ_{ow} are expected to decrease. If the decrease of $(\gamma_{sw} - \gamma_{so})$ is large compared to that of γ_{ow} , θ increases (figure 1.5) and roll up is facilitated. Spontaneous roll up occurs if $\gamma_{so} > \gamma_{sw} + \gamma_{ow}$. Soil detachment is thus accomplished by an increase of the equilibrium contact angle. Cleaning may be enhanced by wetting and/or swelling of the fabric by water molecules, thereby lifting the soil from the surface into solution.

The contact angle of oily soil on a hydrophobic surface will be much lower than that on a hydrophilic one. As a result, oily soil readily spreads on hydrophobic substrates. In this case, surfactant molecules are not able to undercut the soil and hence they cannot increase the contact angle. Soil removal can be enhanced by surfactants due to a decreasing oil/water interfacial tension which allows the liquid film to be easily deformed into small emulsion droplets (*emulsification*).

Direct *solubilization* of oily soils in micelles may occur when there is a large excess of surfactant relative to oil present. Surfactant aggregates pick up oil from the substrate and desorb into solution. The last two mechanisms are important for the removal of oily soil from hydrophobic surfaces. For more information on emulsification and solubilization the excellent review of Miller and Rainey can be consulted⁷².

1.3.2.2 Particulate soil removal

Whereas the removal of oily soil can be discussed in terms of the equilibrium contact angle and/or the oil-water interfacial tension, this is not possible in case of particulate soil. Particulate soil is more difficult to remove than liquid soil for two reasons. The first is the great variety in particle sizes and shapes; the second is that particles usually consist of agglomerates of smaller particles. As a response to mechanical forces applied with the intention to detach the particle, it may either be removed as a whole, or it may be dispersed into the smaller aggregates, thereby encountering the risk of leaving residues onto the substrate.

Particulate soil adhered to a substrate can be looked at as an aggregated colloidal system. Soil removal is then just the opposite, i.e. dispersion of these aggregates. Detergent systems are thus commonly approached from the viewpoint of colloid stability. Consequently, they are described on the basis of the classical DLVO-theory^{76,77}, which incorporates London - Van der Waals attraction and electrical double layer overlap, and assumes that these contributions are additive. Other types of interactions, for example due to steric repulsion, are ignored in this classical treatment, but can be

added. The total interaction energy is a complex expression which can be analytically solved by making assumptions. More information about the DLVO-theory can be found in general textbooks^{20,30,78}, or in specialized treatises applied to detergency^{73,74,79}. The distinction between common colloidal solutions and deterative ones is that in the latter, one of the components (the substrate) has an infinite size.

1.4 Aims and contents of this thesis

The cleaning of fabrics is for an important part determined by physico-chemical phenomena. Simplified, a washing process can be divided into two parts: (1) detachment of soil from a substrate and (2) stabilization of soil against re-attachment (i.e. anti-redeposition). In both processes, polymers and surfactants play a major role. Since a washing formulation contains a large number of different components, the specific action of single components or a combination of components is often very difficult to address. Added to this, literature is not abundant on fundamental adsorption studies of multi-component systems.

The aim of this thesis was to study the effect of mixtures of polymers and surfactants on detergency-related adsorption phenomena. In order to control complexity, a model detergency system was chosen, consisting of a polymer, a surfactant, a substrate and particulate soil. This complex system does not readily lend itself directly to a detailed study, and therefore a division is made into a set of sub-systems, each covering specific interactions of two or more of the model components.

Since clays are major constituents of particulate soil⁶⁹, the clay mineral kaolinite was chosen as a model soil system. The surface of kaolinite is patchwise heterogeneous with respect to its charge and chemical composition^{80,81} which makes it an interesting object for study. The adsorption of the water-soluble uncharged polymer polyvinylpyrrolidone (PVP) (see figure 1.6) onto this surface is studied in chapter 2. An interpretation in terms of the adsorption on different surface types is put forward.

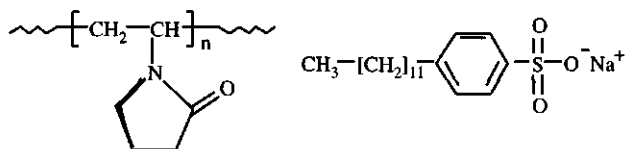


Figure 1.6: Structural formulas of poly(vinylpyrrolidone) (PVP) and sodium dodecylbenzenesulphonate (SDBS).

In order to understand the mixed adsorption of polymers and surfactants at particulate soil, knowledge of their interaction in solution is indispensable. This is the subject of chapter 3, where titration microcalorimetry is used as a sensitive technique. The interaction between PVP and the anionic surfactant sodium-dodecylbenzenesulphonate (SDBS, a global workhorse in detergency formulations) (see figure 1.6) in aqueous solutions is studied. Emphasis is put on the temperature dependence of the enthalpy of interaction, since this provides useful information on the nature of the polymer-surfactant interactions.

The results, obtained in this way, were used in the investigation of the mixed adsorption of PVP and SDBS on kaolinite, which is covered in chapter 4. This very complex process highly depends on the pH, the electrolyte concentration, and the amounts of polymer and surfactant. By careful looking at the resulting adsorption due to variation of these variables, a fairly detailed picture of the adsorption process is obtained.

After a thorough look at the solution side of the washing process, we focused on the substrate. Chapter 5 describes the development and the characterization of rapidly-prepared, smooth, stable and well-defined cellulose films on Si-wafers. These cellulose surfaces can be used in a flow cell as model adsorption substrates for cotton.

Detergency is a very dynamic process, and therefore process rates are very important. The kinetics and the equilibrium adsorbed amount of nonionic surfactants onto the model cellulose surface is dealt with in chapter 6. The use of homodisperse surfactants with a different molecular composition, together with stagnation point reflectometry in a flow cell, gives a fairly detailed picture of the influence of molecular composition on the

adsorption and desorption rates of nonionic amphiphiles. The using of the model cellulose substrates in a flow cell allows us to carry out accurate kinetic and equilibrium studies of multi-component, detergency-related systems, of which an illustration is shown in the summary.

References

- 1 G. Odian, *Principles of Polymerization*, John Wiley & Sons, New York (1991).
- 2 G. J. Fleer and J. Lyklema, in *Adsorption from Solution at the Solid/Liquid Interface*, edited by G. D. Parfitt and C. H. Rochester, Academic Press, London (1983), 153.
- 3 M. Kawaguchi and A. Takahashi, *Adv. Colloid Interface Sci.* **37**, 219 (1992).
- 4 G. J. Fleer, M. A. Cohen Stuart, J. M. H. M. Scheutjens, T. Cosgrove, and B. Vincent, *Polymers at Interfaces*, Chapman & Hall, London (1993).
- 5 J. Lyklema, *Fundamentals of Interface and Colloid Science, Vol. II*, Academic Press, London (1995) Chapter 5, 2.
- 6 E. Jenkel and B. Rumbach, *Z. Elektrochem* **55**, 612 (1951).
- 7 J. Lyklema, *Fundamentals of Interface and Colloid Science, Vol. II*, Academic Press, London (1995) Chapter 5, 14.
- 8 H. A. van der Schee and J. Lyklema, *J. Phys. Chem.* **88**, 6661 (1984).
- 9 J. G. Göbel, N. A. M. Besseling, M. A. Cohen Stuart, and C. Poncet, *J. Colloid Interface Sci.* **209**, 129 (1999).
- 10 M. A. Cohen Stuart, J. M. H. M. Scheutjens, and G. J. Fleer, *J. Polym. Sci., Polym. Phys. Ed.* **12**, 559 (1980).
- 11 T. F. Tadros, *The Effect of Polymers on Dispersion Properties*, Academic Press, London (1981).
- 12 T. Sato and R. Ruch, *Stabilization of Colloidal Dispersions by Polymer Adsorption*, Marcel Dekker, New York (1980).
- 13 D. H. Napper, *Polymeric Stabilization of Colloidal Dispersions*, Academic Press, London (1983).
- 14 K. J. Ives, *The Scientific Bases of Flocculation*, Sijthoff & Noordhoff, Alphen aan de Rijn (1978).

- 15 M. J. Rosen, *Surfactants and Interfacial Phenomena*, second ed., John Wiley & Sons, New York (1989).
- 16 J. H. Clint, *Surfactant Aggregation*, Blackie & Son, Glasgow (1992).
- 17 B. Jönsson, B. Lindmann, K. Holmberg, and B. Kronberg, *Surfactants and Polymers in Aqueous Solution*, John Wiley & Sons, Chichester (1998).
- 18 F. M. Menger and C. A. Littau, *J. Am. Chem. Soc.* **115**, 10083 (1993).
- 19 R. Zana, *Curr. Opinion Colloid Interface Sci.* **1**, 566 (1996).
- 20 D. F. Evans and H. Wennerström, *The Colloidal Domain, where physics, chemistry and biology meet*, VCH Publishers, New York (1994).
- 21 C. Tanford, *The Hydrophobic Effect*, John-Wiley, New York (1980).
- 22 J. W. McBain, *Trans. Faraday Soc.* **9**, 99 (1913).
- 23 W. M. Gelbart, A. Ben-Shaul, and D. Roux, *Micelles, membranes, microemulsions, and monolayers*, Springer, New York (1994).
- 24 M. N. Jones and D. Chapman, *Micelles, monolayers, and biomembranes*, Wiley, New York (1995).
- 25 B. Lindman, in *Surfactants*, edited by T. F. Tadros, Academic Press, New York (1984).
- 26 K. P. Ananthapadmanabhan, in *Interactions of Surfactants with Polymers and Proteins*, edited by E. D. Goddard and K. P. Ananthapadmanabhan, CRC Press, Boca Raton (1993), 5.
- 27 R. Zana, in *Surfactant Solutions, Surfactant Science Series; Vol. 22*, edited by R. Zana, Marcel Dekker, New York (1987), 241.
- 28 P.-G. Nilsson, H. Wennerström, and B. Lindman, *J. Phys. Chem.* **87**, 1377 (1983).
- 29 J. N. Israelachvili, D. J. Mitchell, and B. W. Ninham, *J. Chem. Soc., Faraday Trans. 2* **72**, 1525 (1976).
- 30 J. Israelachvili, *Intermolecular and Surface Forces*, second ed., Academic Press, San Diego (1991).
- 31 R. G. Laughlin, *The Aqueous Phase Behaviour of Surfactants*, Academic Press, London (1994).
- 32 J. S. Clunie and B. T. Ingram, in *Adsorption from Solution at the Solid/Liquid Interface*, edited by G. D. Parfitt and C. H. Rochester, Academic Press, London (1983), 105.

- 33 F. Tiberg, *J. Chem. Soc., Faraday Trans.* **92**, 531 (1996).
- 34 A. Gellan and C. H. Rochester, *J. Chem. Soc., Faraday Trans. I* **81**, 1503 (1985).
- 35 L. M. Grant, T. Ederth, and F. Tiberg, *Langmuir* **16**, 2285 (2000).
- 36 G. D. Gaudin and D. W. Fuerstenau, *Trans. AIME* **202**, 958 (1955).
- 37 J. H. Harwell, J. C. Hoskins, R. S. Schechter, and W. H. Wade, *Langmuir* **1**, 251 (1985).
- 38 D. B. Hough and H. M. Rendall, in *Adsorption from Solution at the Solid/Liquid Interface*, edited by G. D. Parfitt and C. H. Rochester, Academic Press, London (1983), 247.
- 39 L. K. Koopal, in *Coagulation and Flocculation, Surfactant Science Series; Vol. 47*, edited by B. Dobias, Marcel Dekker, New York (1993), 101.
- 40 L. K. Koopal, in *Structure-performance Relationships in Surfactants, Surfactant Science Series; Vol. 70*, edited by K. Esumi and M. Ueno, Marcel Dekker, New York (1997), 395.
- 41 A. N. Frumkin, *Z. Phys. Chem.* **116**, 466 (1925).
- 42 R. H. Fowler and E. A. Guggenheim, *Statistical Thermodynamics*, University Press, Cambridge (1965).
- 43 L. K. Koopal and J. Ralston, *J. Colloid Interface Sci.* **112**, 362 (1986).
- 44 J. M. Cases and F. Villieras, *Langmuir* **8**, 1251 (1992).
- 45 J. Narkiewicz-Michalek, W. Rudzinski, and S. Partyka, *Langmuir* **9**, 2630 (1993).
- 46 J. M. Cases, G. Goujon, and S. Smani, *AIChE Symp. Ser.* **71**, 100 (1975).
- 47 J. F. Scamehorn, R. S. Schechter, and W. H. Wade, *J. Colloid Interface Sci.* **85**, 463 (1982).
- 48 B. Kronberg, *J. Colloid Interface Sci.* **96**, 55 (1983).
- 49 Y. Gao, J. Du, and T. Gu, *J. Chem. Soc., Faraday Trans. I* **83**, 2671 (1987).
- 50 B.-Y. Zhu and T. Gu, *Adv. Colloid Interface Sci.* **37**, 1 (1991).
- 51 B.-Y. Zhu and T. Gu, *J. Chem. Soc. Faraday Trans. I* **85**, 3813 (1991).
- 52 P. Somasundaran and D. W. Fuerstenau, *J. Phys. Chem.* **70**, 90 (1966).
- 53 M. R. Böhmer and L. K. Koopal, *Langmuir* **8**, 2649 (1992).
- 54 A. Fan, P. Somasundaran, and N. J. Turro, *Langmuir* **13**, 506 (1997).
- 55 K. Nagashima and F. D. Blum, *J. Colloid. Interface Sci.* **214**, 8 (1999).
- 56 J. M. H. M. Scheutjens and G. J. Fleer, *J. Phys. Chem.* **83**, 1619 (1979).

- 57 J. M. H. M. Scheutjens and G. J. Fleer, *J. Phys. Chem.* **84**, 178 (1980).
- 58 M. R. Böhmer and L. K. Koopal, *Langmuir* **6**, 1478 (1990).
- 59 H. N. Patrick, G. G. Warr, S. Manne, and I. A. Aksay, *Langmuir* **13**, 4349 (1994).
- 60 S. Manne and H. E. Gaub, *Science* **270**, 1480 (1995).
- 61 L. M. Grant and W. A. Ducker, *J. Phys. Chem.* **101**, 5337 (1997).
- 62 H. N. Patrick, G. G. Warr, S. Manne, and I. A. Aksay, *Langmuir* **15**, 1685 (1999).
- 63 H. N. Patrick and G. G. Warr, *Colloids Surf., A: Physicochem. Eng. Aspects* **162**, 149 (2000).
- 64 S. B. Velegol, B. D. Fleming, S. Biggs, E. J. Wanless, and R. D. Tilton, *Langmuir* **16**, 2548 (2000).
- 65 J. C. Schulz and G. G. Warr, *Langmuir* **16**, 2995 (2000).
- 66 J. L. Wolgemuth, R. K. Workman, and S. Manne, *Langmuir* **16**, 3077 (2000).
- 67 W. G. Cutler and E. Kissa, *Detergency: Theory and Technology*, *Surfactant Science Series*, Vol. 20, Marcel Dekker, New York (1972).
- 68 A. M. Schwartz, in *Surface and Colloid Science*; Vol. 5, edited by E. Matijevic, Wiley-Interscience, New York (1972), 195.
- 69 M. J. Schick, in *Nonionic Surfactants - Physical Chemistry*, *Surfactant Science Series*; Vol. 23, edited by M. J. Schick, Marcel Dekker, New York (1987), 753.
- 70 M. J. Schwuger, in *Anionic Surfactants, Physical Chemistry of Surfactant Action*, *Surfactant Science Series*; Vol. 11, edited by E. H. Lucassen-Reinders, Marcel Dekker, New York (1981), 267.
- 71 L. K. Koopal, *Neth. Milk Dairy J.* **39**, 127 (1985).
- 72 C. A. Miller and K. H. Raney, *Colloids Surf., A: Physicochem. Eng. Aspects* **74**, 169 (1993).
- 73 B. J. Carroll, *Colloids Surf., A: Physicochem. Eng. Aspects* **74**, 131 (1993).
- 74 M. Tagawa and K. Gotoh, in *Electrical Phenomena at Interfaces*, *Surfactant Science Series*; Vol. 76 Marcel Dekker, New York (1998), 359.
- 75 N. K. Adam, *J. Soc. Dyers Colour.* **53**, 121 (1937).
- 76 E. J. W. Verwey and J. T. G. Overbeek, *The Theory of the Stability of Lyophobic Colloids*, Elsevier, Amsterdam (1948).
- 77 B. V. Derjaguin and L. Landau, *Acta Physiochim.* **14**, 633 (1941).

- 78 R. J. Hunter, *Foundations of Colloid Science, Volume I and II*, Clarendon Press, Oxford (1989).
- 79 Lange, in *Adsorption at Interfaces*, edited by K. L. Mittal, American Chemical Society, Washington (1975), 270.
- 80 B. Braggs, D. Fornasiero, J. Ralston, and R. S. Smart, *Clays Clay Miner.* **42**, 123 (1994).
- 81 P. V. Brady, R. T. Cygan, and K. L. Nagy, *J. Colloid Interface Sci.* **183**, 356 (1996).

Chapter 2

Adsorption of Poly(VinylPyrrolidone) on Kaolinite

Abstract

The adsorption of the uncharged polymer poly(vinylpyrrolidone) (PVP) on a homo-ionic Na-kaolinite has been studied. Potentiometric acid-base titrations of kaolinite were performed on samples at different concentrations of sodium chloride. An interpretation in terms of the contributions of the individual surface types has been given. Protons are strongly favoured over sodium ions at the basal planes. Some striking similarities were observed between the results of the acid-base titrations and the PVP adsorption experiments. PVP readily adsorbs on at least part of the kaolinite surface showing a high affinity character and an adsorbed amount at the plateau of about 1 mg m^{-2} total area. The influence of the pH, electrolyte concentration and multivalent ions on the amount adsorbed at the plateau has been investigated. Increasing the pH or the electrolyte concentration leads to a decrease in adsorption. A model is proposed in which PVP adsorbs on edges and basal planes by different mechanisms. The adsorption of PVP on the edges is strongly pH dependent, that of the plates only weakly. Specifically adsorbed protons at the plates act as anchor sites for PVP segments. Multivalent ions do not influence the proposed adsorption mechanism directly but primarily change the surface area accessible for PVP.

2.1 Introduction

Clay minerals are used in a number of industrial processes, for example as paper fillers and coating pigments, to improve the properties of the material. For these purposes, stable dispersions are needed and therefore the adsorption of polymers on clays becomes of interest.

The adsorption of uncharged polymers on clay minerals is very complex due to the heterogeneous character of the clay surface. The overall interaction is the result of a subtle balance of forces determined by polymer-surface, polymer-solvent and surface-solvent interactions. Most of the published work of uncharged polymer adsorption on clay minerals is restricted to polyvinylalcohol (PVA) and polyacrylamide (PAM) on kaolinite and montmorillonite¹⁻⁶. Two French research groups^{5,6} were the first trying to interpret results of PAM adsorption on kaolinite by accounting for the different types of surfaces present. Their main discussion point was the extent of adsorption of PAM on the basal planes of the gibbsite surface.

Less attention has been paid to the adsorption of polyvinylpyrrolidone (PVP), although it is an often used dispersant. Due to the presence of both hydrophilic and hydrophobic functional groups, PVP is soluble in water and a wide variety of organic solvents⁷. In solution it probably occurs as a random coil. The adsorption of PVP on hydrophilic⁸⁻¹² (mostly mineral oxides) and hydrophobic surfaces¹³⁻¹⁶ has been reported. PVP hardly adsorbs on metal oxides, except for silica.

Clay minerals consist of sheets of silicon-oxygen tetrahedra and aluminium- or magnesium oxygen-hydroxyl octahedra¹⁷. They can be classified according to the arrangement of these layers. The kaolinite group represents clay minerals with a 1:1-unit layer structure consisting of a Si-tetrahedron sheet and an Al-octahedron sheet. These minerals are non-swelling and form flat, hexagonal particles. Three types of surfaces can be distinguished: siloxane plates, gibbsite plates, and edges. Much research has been carried out to reveal the surface chemical and charge characteristics of kaolinite¹⁷⁻²⁴. It is generally accepted that the (surface)

charge of the clay particles can be separated in a permanent and a variable part. A permanent negative charge is present on the basal planes due to isomorphous substitution of Al^{3+} and Si^{4+} -ions inside the solid by ions of lower valency, while the edges possess a pH dependent charge caused by (de)protonation of surface hydroxyl groups. The two basal planes show a much lower affinity for the H^+ and OH^- -ions^{25,26}.

For homo-ionic kaolinite samples, many values determined by different techniques have been reported for the point of zero charge of the edges (epzc) and the overall isoelectric point (iep). The epzc is difficult to establish by titration because only sums of H^+ and OH^- -consumptions on the three types of surfaces are measurable. Measured values for the epzc fall in the range 5-9; most of them are around 7. The papers of Rand and Melton¹⁹, and Herrington et al.²² can be consulted for a discussion of the observed discrepancies. The overall iep is in principle measurable but difficult to interpret in terms of edge and plate properties. Values around five^{22,27} and below two^{28,29} have been reported. In general it can be stated that important causes of these discrepancies involve problems in obtaining reproducible pure samples and finding suitable experimental techniques. Most data are obtained by electrophoretic measurements^{22,27,28,30}. The difficulty of converting mobilities into zeta-potentials for kaolinite samples is well known; it is caused by non-uniformity of charge and shape, and the occurrence of large surface conductance around the particles³⁰⁻³².

To our knowledge, the literature contains only two examples of the adsorption of PVP on kaolinite. In the early seventies, Francis³³ studied it on reference clay minerals by gravimetry. Hardly any adsorption of PVP on kaolinite was detectable and no adsorption isotherms were given. Since then, researchers seemed to have lost their interest in this system for a long time. However, very recently Hild et al.³⁴ studied it again, emphasizing the solution side of the system. Their findings will be discussed below.

The aim of this chapter is to advance our understanding of the interaction between PVP and the three types of surfaces of kaolinite by comparing it with the uptake of protons, which also differs between these faces. To that

end, the PVP adsorption measurements are extended by potentiometric titrations at different electrolyte concentrations. The influence of multivalent ions on the adsorption of PVP on kaolinite is also studied.

2.2 Experimental

2.2.1 Materials

Kaolinite was obtained from Sigma Company. Extensive characterisation of this sample by Mehrian^{28,35} showed it to be very pure. According to Mehrian, the particle size range of the sample is 0.1 – 4 μm and its BET (N_2) surface area amounted to 17.7 $\text{m}^2 \text{g}^{-1}$. For the cation exchange capacities (c.e.c.) she found: 30 $\mu\text{mol g}^{-1}$ (determined by the silver thiourea method) and 57 $\mu\text{mol g}^{-1}$ (measured by the ammonium acetate method). It was assumed that the latter values also include the surface sites of the edges. An edge/plate area ratio of 0.25 was found by argon adsorption.

Poly(vinylpyrrolidone) with a number average molar mass of 17.4 $\cdot 10^3 \text{ g mol}^{-1}$ ($M_w/M_n = 1.9$) was obtained from BASF and used as received. HCl, NaOH, and NaCl were all of analytical grade. Water is purified by passing it over a mixed bed ion exchanger, a carbon column, and a microfilter.

2.2.2 Methods

Potentiometric titrations were performed on Na-kaolinite samples prepared according to the procedure described by Mehrian^{28,35}. The titration vessel is filled with 0.5 g of clay dispersed in 30 ml electrolyte solution. First, the pH is lowered to pH = 4 and five titration curves were measured between pH = 4 and 10 (three upwards, two downwards). After completion, the pH is lowered to around 7, the electrolyte concentration is raised, the resulting change in pH recorded, and the same procedure is followed at the higher concentration. Blank titrations were performed under similar conditions.

The surface charge was calculated from the difference between the amount of H^+ and OH^- adsorbed, taken up by the samples and the blank experiments. The charge obtained in this way is the relative surface charge which is the change in the total surface charge. The absolute surface charge cannot be unambiguously determined because the absolute amount of permanent negative charge due to isomorphous substitution is not well established. It can be estimated to be $30 \mu\text{mol g}^{-1}$. Curves at different electrolyte concentrations are mutually positioned by accounting for the effect of an increasing electrolyte concentration on the surface charge.

Adsorption isotherms of PVP were determined by depletion measurements at 25°C . The PVP-concentration was determined by UV-absorption at 204 nm. Centrifuge tubes are filled with 0.4 g kaolinite, 30 ml demineralised water and 5 ml polymer solution of the desired concentration. The tubes were shaken end-over-end for 16 hours at 30 rpm. Preliminary kinetic experiments showed that an almost constant adsorbed amount is reached within one hour; thereafter the adsorption increases slightly. After six hours, there is no detectable change in the adsorbed amount anymore. The pH of the solution is repeatedly adjusted. The solids were separated by centrifugation for 30 minutes at 20,000 rpm.

2.3 Results and Discussion

2.3.1 Potentiometric titrations

Characteristic acid-base titration curves of homo-ionic Na-kaolinite samples at three electrolyte concentrations are shown in figure 2.1. This set of relative surface charge curves is arbitrarily referred to the charge being zero for the curve with the lowest electrolyte concentration at the pH where the effect of indifferent electrolyte is smallest: $\Delta\sigma \equiv 0$ at $\text{pH} = 7$ for the 10^{-3} M-curve.

Successive titrations at one electrolyte concentration showed a small hysteresis effect. In accordance with Mehrian²⁸, this phenomenon can be attributed to a retardation effect in the formation and destruction of the

card-house structure. This open structure is formed by coagulation of negatively charged plates and positively charged edges. The fact that the hysteresis increases slightly with decreasing electrolyte concentration supports this explanation. The hysteresis is too small to influence the essential characteristics of the surface charge curves.

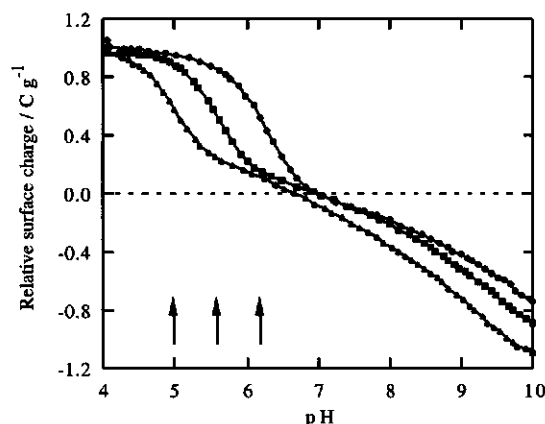


Figure 2.1: Relative surface charge of Na-kaolinite at different NaCl-concentrations: ●: 10^{-3} M, ■: 10^{-2} M, ▲: 10^{-1} M; the arrows are explained in the text.

To explain the observations in figure 2.1, it is useful to divide the total relative surface charge into additive contributions of edges and plates, ignoring overspill at the edge-plate border:

$$\Delta\sigma_{\text{H}^+/\text{OH}^-}^{\text{total}} = \Delta\sigma_{\text{H}^+/\text{OH}^-}^{\text{plates}} + \Delta\sigma_{\text{H}^+/\text{OH}^-}^{\text{edges}} \quad [2.1]$$

The negative charge of the plates is compensated by an excess of counterions and a deficit of co-ions in the electrical double layer. The contribution $\Delta\sigma_{\text{H}^+/\text{OH}^-}^{\text{plates}}$ is the result of counterion exchange against specifically adsorbed protons^{18,28} and depends on the electrolyte concentration and pH. At high pH, the proton concentration is too low (compared to the counterion concentration) to contribute to the charge on the plates. Therefore, any further proton desorption stems from the edges. The charge on the edges is caused by either adsorption or desorption of protons or hydroxyl ions, resulting in a variable-charge surface. For

isolated variable-charge surfaces, the absolute value of the charge increases with increasing concentration of indifferent electrolyte. Curves at different concentrations of indifferent electrolyte cross each other at a common intersection point (cip) which corresponds to the pzc³⁶.

In figure 2.1, no common intersection point can be observed. Recently, this was also reported by Braggs et al.²³ but subsequently ignored in their discussion. On the other hand, Herrington et al.²² did find common intersection points for different kaolinite samples with potassium chloride as the indifferent electrolyte. A reason for this discrepancy may be found in their pretreatment, using acid and hydrogen peroxide.

In our experiments, it is observed that with decreasing pH the curves approach each other, although the cip is masked by the superimposed exchange on the plates. Extrapolation of the edge part of the charges suggests a cip of about 7. This may be identified with the epzc, in good agreement with literature values^{22,27,28}.

Below pH = 7, compared to the behaviour of variable-charge surfaces, an additional contribution to the proton uptake can be observed, which sets in at higher pH at lower electrolyte concentrations. Considering the Na⁺/H⁺-exchange, the preference of the surface for either protons or sodium ions manifests itself in the non-diffuse part of the double layer. The resulting change in the Gibbs free energy, ΔG^* , due to this exchange can be expressed as:

$$\Delta G^* = RT \ln K \quad [2.2]$$

with

$$K = \frac{\phi_{Na^+} c_{H^+}}{\phi_{H^+} c_{Na^+}} \quad [2.3]$$

where ϕ_{H^+} and ϕ_{Na^+} are the volume fractions of the ions adsorbed at the surface, and c_{H^+} and c_{Na^+} are their bulk concentrations. A more detailed interpretation of K is deferred to a future publication. Values for K can be determined from the steepest part of the curves of figure 2.1 (the arrows in the figure mark these points) where $\phi_{H^+} = \phi_{Na^+} = 0.5$, assuming $c_{Na^+} \approx$ the

initial electrolyte concentration. Table 2.1 shows the corresponding pH, ($\text{pH}_{0.5}^{\Delta\sigma}$), and K for each electrolyte concentration.

Table 2.1: $\text{pH}_{0.5}^{\Delta\sigma}$ and K at different Na^+ -concentrations.

$[\text{Na}^+]$ (M)	$\text{pH}_{1/2}^{\Delta\sigma}$	K (-)
10^{-3}	6.2	$10^{-3.2}$
10^{-2}	5.6	$10^{-3.6}$
10^{-1}	4.9	$10^{-3.9}$

It follows that $\Delta G^* = -7$ to -9 RT, which expresses the specific preference of the plate surface for protons over sodium ions. Apparently, protons start to displace sodium ions at the plates if $[\text{H}^+] > 10^{-4} [\text{Na}^+]$.

It can be concluded that no cip or intersecting curves are found when (1) the contribution of the H^+/Na^+ exchange is significant and (2) this exchange occurs close enough to the epzc. The titration curves can be well interpreted as reflecting the consecutive titration of edges and plates. The question to which extent the two types of plates contribute remains to be addressed.

2.3.2 Adsorption of PVP

Adsorption isotherms of PVP on kaolinite at three different pH values in 10^{-2} M NaCl are shown in figure 2.2. PVP shows in all cases a fairly strong affinity for at least part of the kaolinite surface. The graphs show a steep initial rise followed by a pseudo plateau. The polydispersity of the samples is reflected in the bending of the curves and the reluctance to attain the plateau^{37,38}. The amount adsorbed at the plateau is somewhat low for uncharged polymers (the adsorbed amount can be $1.5 - 2.5 \text{ mg m}^{-2}$). However, the amount adsorbed at $\text{pH} = 5.5$ is comparable to values reported for PVP on silica^{10,37} and PAM on kaolinite^{1,3,39}.

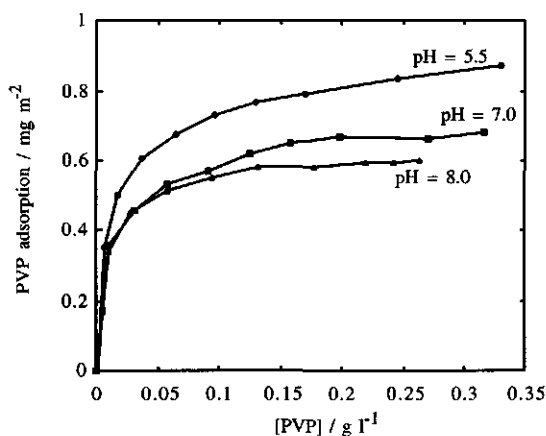


Figure 2.2: Adsorption of PVP on kaolinite: ●: pH = 5.5, ■: pH = 7, ▲: pH = 8; $I = 10^{-2}$ M NaCl.

A significant pH-dependence is observed in the present system, while in earlier studies, there was hardly a pH-dependence^{3,37} or the influence of the pH was not investigated^{1,10,39}. In order to gain more insight into the adsorption mechanism, adsorption at the plateau was determined as a function of pH at different electrolyte concentrations. To assure plateau adsorption, the initial PVP concentration is chosen sufficiently high (i.e. 0.5 g l^{-1}). The results are presented in figure 2.3.

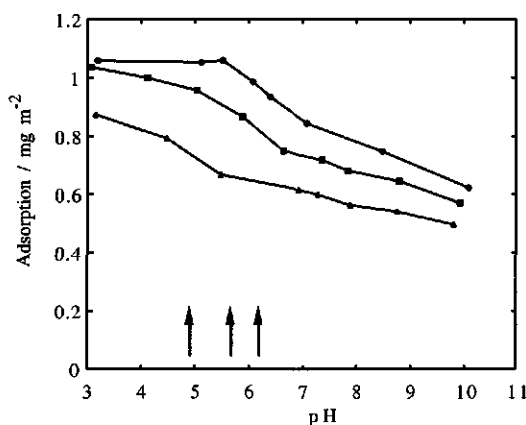


Figure 2.3: Plateau adsorption of PVP on kaolinite as a function of pH at different NaCl-concentrations: ●: $2 \cdot 10^{-3}$ M, ■: 10^{-2} M, ▲: 10^{-1} M; $[PVP]_0 = 0.50 \text{ g l}^{-1}$, $[PVP]_{eq} = 0.30 - 0.40 \text{ g l}^{-1}$; the arrows are explained in the text.

Three observations can be made. First, there is a monotonous but discontinuous decrease of the adsorption with pH. At 10^{-3} M NaCl, the adsorbed amount is constant between pH = 6 and pH = 3. Perhaps here complete coverage of the adsorbing surface type(s) has been attained. Second, even at high pH values (pH > p_{zc}) a significant adsorption persists. Third, the addition of electrolytes decreases the adsorbed amount. In order to explain these observations, two questions must be answered:

- (1) What is/are the driving force(s) for adsorption?
- (2) On which surface type(s) does adsorption occur?

Since PVP is not charged in the pH-range 4-10, coulombic interactions cannot be responsible for the adsorption, and other physical or chemical interactions must be considered. In studies of PAM adsorption on clay minerals, hydrogen bonding was considered to be the major driving force for adsorption^{2,3,39}. It could in principle take place in the actual system between surface hydroxyl groups of the clay and the carbonyl group of the pyrrolidone ring. Furthermore, PVP is known to be strongly attracted by hydrophobic surfaces^{13-15,40}, so hydrophobic interactions are also possible. With these possible mechanisms in mind, it is useful to look separately at the different surface types of kaolinite (a siloxane and a gibbsite as plate surfaces, and metal oxide type edges) for possible adsorption sites.

First, the siloxane surface is considered. PVP readily adsorbs on silica^{8,10}. In both studies, hydrogen bonding to silanol groups as well as hydrophobic interactions contributed to the adsorbed amount. The siloxane surface of the kaolinite particles carries no silanol groups, its composition is expected not to vary with pH and it has a permanent negative charge. Adsorption of PVP on this surface type is expected to occur by hydrophobic bonding. As a consequence, this contribution will be independent of pH.

Let us now look at the gibbsite surface part. PVP hardly adsorbs on gibbsite^{41,42} although pure gibbsite possesses many hydroxyl groups. This general observation for metal oxide surfaces other than silica is probably caused by their strongly hydrophilic character: hydrogen bonding with

water molecules is preferred over that with the carbonyl groups of the pyrrolidone ring. Otherwise stated, the critical exchange Gibbs energy for polymer adsorption⁴³ is not surpassed on these surfaces. It is therefore expected that substantial adsorption onto the gibbsite surface of the clay is absent or very small.

Finally, the edges are considered. They consist of exposed aluminol and silanol groups. The silanols have an acidic character (the pzc of silica is around 2-3)³⁶ with a variable charge. The aluminols are basic groups (the pzc of gibbsite is about 9)³⁶ also behaving like a variable-charge surface. Their behaviour is different from that of the aluminols on the basal faces, due to a different coordination of these surface groups²⁶. As a consequence, a pH dependent (de)protonation takes place at both the silanol and the aluminol sites. Figure 2.4 shows schematically some surface characteristics of the edges at different pH values^{6,23}. Adsorption on the edges can occur by hydrogen bonding to (di)protonated surface oxygens. The number of these groups increases with decreasing pH. It is therefore likely that adsorption on the edges will gradually increase with decreasing pH.

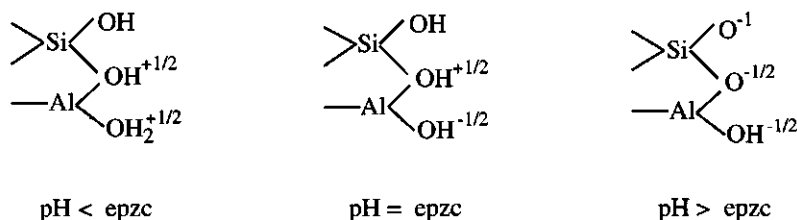


Figure 2.4: Surface charge characteristics of the edges of kaolinite at different pH values^{6,23}.

Summing up the expected effects of edges and plates on the adsorption of PVP, some insight into the curves of figure 2.3 can be obtained. At high pH when all surface types of kaolinite are negatively charged and the edge hydroxyl groups are ionized, adsorption can only take place by hydrophobic bonding on the siloxane plates. This amount will be independent of pH and the electrolyte concentration. When the curves in

figure 2.3 are extrapolated, they merge around $\text{pH} = 13$ at an adsorbed amount of about 0.45 mg m^{-2} of the total surface. Converting this value to mg m^{-2} siloxane surface leads to an adsorbed amount of about 1.2 mg m^{-2} , in good agreement with PVP adsorption values on a silica surface^{8,10}. Upon decreasing the pH, in addition to the adsorption on the siloxane plates, hydrogen bonding to (di)protonated surface oxygens will lead to further adsorption. This amount increases gradually from zero at high pH till about 0.45 mg m^{-2} total area at $\text{pH} = 3$ which is about 1.8 mg m^{-2} edge area. These contributions are estimated from the 10^{-2} M -curve in figure 2.3. In figure 2.5 the two contributions are schematically shown by the curves a and b, and their sum is represented by curve c. Comparing curve c of figure 2.5 with the 10^{-2} M -curve in figure 2.3, it follows that the PVP adsorption is not yet fully explained. In each curve of figure 2.3, a stepwise contribution to the adsorption can be seen around $\text{pH} = 5$ to 7. This contribution is more pronounced at lower electrolyte concentrations and it shifts to lower pH values at increased electrolyte concentrations. The pH halfway these additional contributions is marked by arrows in figure 2.3 and given in table 2.2.

Table 2.2: $\text{pH}_{0.5}^{\Delta\Gamma_{\text{PVP}}}$ at different Na^+ -concentrations.

$[\text{Na}^+]$ (M)	$\text{pH}_{0.5}^{\Delta\Gamma_{\text{PVP}}}$
$2 \cdot 10^{-3}$	6.2
10^{-2}	5.6
10^{-1}	4.9

Although we are aware that the $\text{pH}_{0.5}^{\Delta\Gamma_{\text{PVP}}}$ -values are not highly accurate, comparison with the $\text{pH}_{0.5}^{\Delta\sigma}$ -values of table 2.1 reveals a close correspondence: the exchange of sodium ions for protons at the plates (figure 2.1 and table 2.1) parallels the additional increase in PVP adsorption (figure 2.3 and table 2.2). Apparently, the specific adsorption of protons on the plates creates adsorption sites for PVP. It is most likely that

this additional adsorption occurs on the siloxane plates, for example to newly formed silanol groups. According to the titration curves, the Na^+/H^+ exchange occurs over about one pH-unit. When the process is completed, the number of anchor points for PVP adsorption will also not increase any more. The contribution of these additional adsorption sites is estimated from the 10^{-2} M-curve of figure 2.3 and it is included in figure 2.5 as curve d; the resulting curve is curve e.

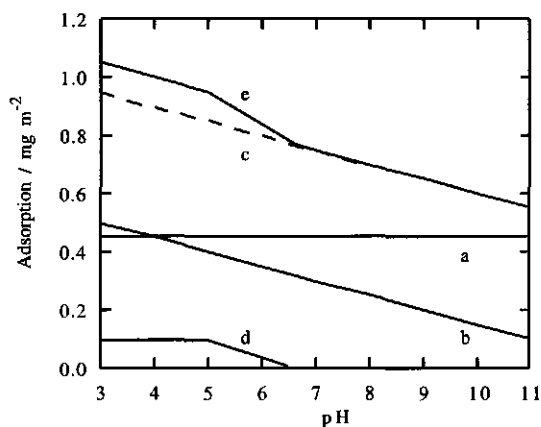


Figure 2.5: Schematic contributions of the different surface types of kaolinite to the plateau adsorption of PVP as a function of pH; a: siloxane contribution; b: edge contribution; c: a + b; d: additional siloxane contribution; e: overall contribution = a + b + d.

The shape of the PVP adsorption curves is now well explained. Adsorption occurs on the siloxane plates by hydrophobic bonding and to a lesser extent (if bridged by specifically adsorbed protons) also by hydrogen bonding; adsorption on the edges takes place by hydrogen bonding. As a result, the surface of kaolinite is only partly covered by PVP, the degree of coverage depending on both pH and the electrolyte concentration. An indication of the incomplete coverage could already be seen in the amount adsorbed at the plateau which is quite low for an uncharged polymer. This finding will have consequences for the stability of PVP-coated kaolinite.

The influence of the electrolyte concentration on the adsorption is twofold. First, an increasing number of edge surface hydroxyl groups will be ionized at higher electrolyte concentration. As a result, fewer sites are available for hydrogen bonding, so adsorption on the edges will decrease and also the total adsorbed amount. Second, at a higher electrolyte concentration, less protons will be adsorbed at the plates leading to fewer additional adsorption sites for PVP. Overall, increasing the electrolyte concentration lowers the adsorption both at the edges and the plates.

The experimental results of Hild et al.³⁴ mainly concern the adsorbed amount and the layer thickness measured by microelectrophoresis. With respect to the adsorbed amount their results are in good agreement with the present ones. The plateau values are comparable and by looking carefully the additional contributions we found in figure 2.3 can also be seen in their results. However in their interpretation they consider a complete, averaged coverage of the kaolinite surface by PVP which is not supported by our observations.

Plateau adsorption experiments for PVP were also carried out in the presence of phosphate and calcium ions, additional to 10^{-2} M NaCl. The results are shown in figure 2.6.

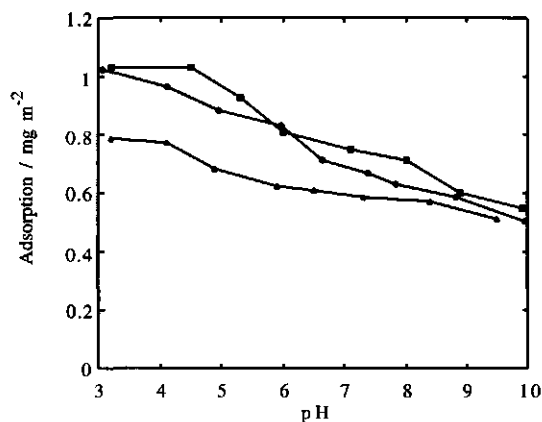


Figure 2.6: Plateau adsorption of PVP on kaolinite in the presence of multivalent ions: ●: 10^{-2} M NaCl, ■: 10^{-2} M NaCl, 10^{-2} M Na_2HPO_4 , ▲: 10^{-2} M NaCl, $2 \cdot 10^{-2}$ M CaCl_2 ; $[\text{PVP}]_0 = 0.5 \text{ g l}^{-1}$.

At high pH, the differences between the curves are very small, indicating that the adsorption mechanism in this range is hardly influenced by multivalent ions. This is in line with our proposed adsorption mechanism of hydrophobic bonding at the siloxane plates. At lower pH values, the presence of calcium ions leads to a decrease in adsorption whereas phosphate ions slightly increase the adsorbed amount. In the latter case, the adsorbed amount below $\text{pH} = 4.5$ is constant at about 1 mg m^{-2} , indicating saturation of adsorption sites.

Calcium ions are known for their specific adsorption on kaolinite^{4,18} but no systematic study of their adsorption on the different surface types of kaolinite could be found. The results of Atesok et al.⁴ suggest a major contribution of the edges to the total adsorbed amount, and ion exchange between calcium and sodium ions. Calcium ions are expected to adsorb on negatively charged edge sites and on the basal planes. Edge adsorption of calcium ions on ionized hydroxyl groups is not expected to hinder the PVP adsorption on the edge hydroxyl groups by hydrogen bonding substantially. Adsorbed Ca^{2+} -ions at the plates may compete more strongly with protons than Na^{+} -ions do, leading to a reduction in the amount of polymer adsorbed at the plates. However, an additional property of calcium ions is their valency effect on coagulation. Two particles can be coagulated by Ca^{2+} -ions, thereby reducing the total available surface area for PVP. We observed that the presence of calcium ions greatly destabilizes the kaolinite dispersions. This reduced surface accessibility effect may be another cause of the decreased adsorption for PVP.

Phosphate ions specifically adsorb on the edges of kaolinite^{44,45}. It is therefore likely that these ions will influence only the adsorption of PVP on the edges, i.e. they have to compete with hydrogen-bonded PVP segments. Figure 2.6 shows overall a slight increase in the adsorbed amount as a function of pH. Obviously, the presence of phosphate ions does not substantially hinder adsorption of PVP, and even seems to create slightly more adsorption sites. This can be attributed to an increased

electrostatic repulsion between the kaolinite particles due to the presence of (adsorbed) phosphate ions. This results in an increased surface area accessible for PVP and therefore in an enhanced adsorption.

2.4 Conclusions

The combination of potentiometric titrations and uncharged polymer adsorption measurements yields information that helps to unravel the heterogeneity of the kaolinite surface. The key element is that specifically adsorbed protons on the basal planes act as anchor sites for PVP-segments, so that the pH and electrolyte concentration dependence of the PVP adsorption runs parallel to that of protons.

Potentiometric titrations show that surface oxygens of the edges are titrated in the entire pH range. At $\text{pH} < 7$, sodium ions adsorbed at the basal planes are exchanged for protons leading to an additional proton charge.

Poly(vinylpyrrolidone) adsorbs on the individual faces of kaolinite by different mechanisms. Adsorption occurs on the edges by hydrogen bonding. This amount increases with decreasing pH. Adsorption takes place on the siloxane plates by hydrophobic bonding and below $\text{pH} = 7$ also by hydrogen bonding to specifically adsorbed protons. The first contribution is independent of pH, whereas the latter decreases with increasing electrolyte concentration. The influence of multivalent ions is rather indirect and mainly caused by changes in the surface accessibility for PVP.

Acknowledgements

Mr. P. L. M. Theunissen is greatly acknowledged for performing the potentiometric titration experiments.

References

- 1 B. K. G. Theng, *Formation and Properties of Clay-Polymer Complexes*, Elsevier, Amsterdam (1979) .
- 2 E. Pefferkorn, L. Nabzar, and R. Varoqui, *Colloid Polym. Sci.* **265**, 889 (1987).
- 3 A. F. Hollander, P. Somasundaran, and C. C. Gryte, *J. Appl. Polym. Sci.* **26**, 2123 (1981).
- 4 G. Atesok, P. Somasundaran, and L. J. Morgan, *Colloids Surf.* **32**, 127 (1988).
- 5 L. T. Lee, R. Rahbari, J. Lecourtier, and G. Chauveteau, *J. Colloid Interface Sci.* **147**, 351 (1991).
- 6 E. Pefferkorn, L. Nabzar, and A. Carroy, *J. Colloid Interface Sci.* **106**, 94 (1985).
- 7 R. Meza and L. Gargallo, *Eur. Polym. J.* **13**, 235 (1977).
- 8 M. A. Cohen Stuart, G. J. Fleer, and B. H. Bijsterbosch, *J. Colloid Interface Sci.* **90**, 310 (1982).
- 9 K. Esumi and M. Oyama, *Langmuir* **9**, 2020 (1993).
- 10 R. S. Parnas, M. Claimberg, V. Taepaisitphongse, and Y. Cohen, *J. Colloid Interface Sci.* **129**, 441 (1989).
- 11 T. Sato and S. Kohnosu, *Colloids Surf.* **88**, 197 (1994).
- 12 Y. Ishimaru and T. Lindström, *J. Appl. Polym. Sci.* **29**, 1675 (1984).
- 13 M. Kawaguchi, I. Hayashi, and A. Takahashi, *Polym. J.* **13**, 783 (1981).
- 14 J. N. Smith, J. Meadows, and P. A. Williams, *Langmuir* **12**, 3773 (1996).
- 15 I. W. Kellaway and N. M. Najib, *Int. J. Pharm.* **6**, 285 (1980).
- 16 M. Sugiura, *Bull. Chem. Soc. Jap.* **43**, 2604 (1970).
- 17 H. van Olphen, *An Introduction to Clay Colloid Chemistry*, second ed., Wiley-Interscience, New York (1977) .
- 18 A. P. Ferris and W. B. Jepson, *J. Colloid Interface Sci.* **51**, 245 (1975).
- 19 B. Rand and I. E. Melton, *J. Colloid Interface Sci.* **60**, 308 (1977).
- 20 M. D. A. Bolland, A. M. Posner, and J. P. Quirk, *Clays Clay Miner.* **28**, 412 (1980).
- 21 Z. H. Zhou and W. D. Gunter, *Clays Clay Miner.* **40**, 365 (1992).
- 22 T. M. Herrington, A. Q. Clarke, and J. C. Watts, *Colloids Surf.* **68**, 161 (1992).
- 23 B. Braggs, D. Fornasiero, J. Ralston, and R. S. Smart, *Clays Clay Miner.* **42**, 123 (1994).
- 24 P. V. Brady, R. T. Cygan, and K. L. Nagy, *J. Colloid Interface Sci.* **183**, 356 (1996).

- 25 K. A. Wierer and B. Dobias, *J. Colloid Interface Sci.* **122**, 171 (1988).
- 26 T. Hiemstra, W. H. Van Riemsdijk, and G. H. Bolt, *J. Colloid Interface Sci.* **133**, 105 (1989).
- 27 B. Alince and T. G. M. van de Ven, *J. Colloid Interface Sci.* **155**, 465 (1993).
- 28 T. Mehrian Isfahany, Thesis, Wageningen Agricultural University, 1992.
- 29 L. Järnström and P. Stenius, *Colloids Surf.* **50**, 47 (1990).
- 30 D. J. A. Williams and K. P. Williams, *J. Colloid Interface Sci.* **65**, 79 (1978).
- 31 M. C. Fair and J. L. Anderson, *J. Colloid Interface Sci.* **127**, 388 (1989).
- 32 R. W. O'Brien and W. N. Rowlands, *J. Colloid Interface Sci.* **159**, 471 (1993).
- 33 C. W. Francis, *Soil Sci.* **115**, 40 (1973).
- 34 A. Hild, J.-M. Sequaris, H.-D. Narres, and M. Schwuger, *Colloids Surf. A: Physicochem. Eng. Aspects* **123-124**, 515 (1997).
- 35 T. Mehrian, A. de Keizer, and J. Lyklema, *Langmuir* **7**, 3094 (1991).
- 36 J. Lyklema, *Fundamentals of Interface and Colloid Science, volume II*, Academic Press, London (1995).
- 37 M. A. Cohen Stuart, J. M. H. M. Scheutjens, and G. J. Fleer, *J. Polym. Sci., Polym. Phys. Ed.* **18**, 559 (1980).
- 38 L. K. Koopal, *J. Colloid Interface Sci.* **83**, 116 (1981).
- 39 P. J. Dodson and P. Somasundaran, *J. Colloid Interface Sci.* **97**, 481 (1984).
- 40 K. Esumi, K. Takamine, M. Ono, T. Osada, and S. Ichikawa, *J. Colloid Interface Sci.* **161**, 321 (1993).
- 41 K. Ishiduki and K. Esumi, *J. Colloid Interface Sci.* **185**, 274 (1997).
- 42 L. H. Torn, *Unpublished results* (1997).
- 43 G. J. Fleer, M. A. Cohen Stuart, J. M. H. M. Scheutjens, T. Cosgrove, and B. Vincent, *Polymers at Interfaces*, Chapman & Hall, London (1993).
- 44 F. A. M. De Haan, Thesis, Wageningen Agricultural University, 1965.
- 45 J. W. Lyons, *J. Colloid Interface Sci.* **19**, 399 (1964).

Chapter 3

Interaction between Poly(VinylPyrrolidone) and Sodium DodecylBenzeneSulphonate in Aqueous Solutions

Abstract

Microcalorimetric titrations are carried out on solutions containing the anionic surfactant sodium dodecylbenzenesulphonate (SDBS), and mixtures of SDBS and the uncharged polymer poly(vinylpyrrolidone) (PVP). Measurements are taken at different temperatures. Micellization of SDBS is driven by hydrophobic bonding. The interaction enthalpy of mixed PVP/SDBS systems shows clearly a consecutive endothermic and exothermic region with increasing surfactant concentration. The endothermic part can be looked upon as an incremental binding isotherm and reflects the number of surfactant molecules involved in the association process. The exothermic region features inverse hydrophobic bonding behaviour. This is related to the flexible nature of the adsorbent, i.e. the polymer. Electrostatic repulsion between neighbouring surfactant molecules causes at increased surfactant concentrations structural rearrangements of the polymer-surfactant complexes. This is accompanied by losing inter- and intrachain linking. Additional surfactants continue to adsorb on the vacant hydrophobic adsorption sites. The influence of the initial amount of polymer and the electrolyte concentration support our proposals.

3.1 Introduction

A large number of properties of polymer-surfactant mixtures in aqueous solutions like surface tension, viscosity, critical aggregation concentration, aggregation number, structure of the complexes, and thermodynamic data have been determined by various experimental techniques. As a result, the subject has become well documented¹⁻⁷. Most studied systems consist of an uncharged aqueous polymer and a charged surfactant. Water-soluble polymers can be divided into hydrophilic polymers and hydrophobically modified polymers. The latter can form hydrophobic microdomains in which hydrocarbon tails of surfactants can adhere to or solubilize in.

The interaction of surfactants with hydrophilic polymers is quite different^{6,8}. A general picture for a hydrophilic polymer-charged surfactant complex is currently accepted, in which the polymer wraps itself around surfactant aggregates thereby lowering the head group repulsion and screening the contacts between water and the hydrophobic core⁹. Despite this general picture, the details of the interaction mechanism are not yet known.

In recent times, due to the development of calorimeters with an increased sensitivity, titration microcalorimetry is put forward as a powerful and easily applicable technique to investigate polymer-surfactant interactions¹⁰⁻¹⁸. However, the interpretation of the data is not always obvious. The excellent overview of Olofsson and Wang¹⁷ can be consulted for a current discussion. In this chapter we contribute to the discussion and propose some new viewpoints. Our microcalorimetric study deals with the interaction between poly(vinylpyrrolidone) (PVP) and sodium dodecylbenzenesulphonate (SDBS). Titrations are carried out at different temperatures, and different polymer and electrolyte concentrations to obtain insight into the interaction mechanisms. The discriminating feature is that the enthalpy of hydrophobic interactions strongly depends on the temperature, whereas other interactions are essentially far less temperature-sensitive.

3.2 Experimental

3.2.1 Materials

Sodium dodecylbenzenesulphonate (SDBS) was supplied by Fluka and used as received. This product consists of a 85 wt% mixture of homologues (determined by comparison with isomerically pure sodium 4-dodecylbenzenesulphonate by UV-spectroscopy). The critical micelle concentration in 10^{-2} M NaCl at 293 K amounts to 0.7 mM (surface tension and surfactant selective electrode measurements; the surface tension showed no minimum as a function of the concentration). Poly(vinylpyrrolidone) with a number average molar mass of $17.4 \cdot 10^3 \text{ g mol}^{-1}$ ($M_w/M_n = 1.9$) was obtained from BASF and is used as received. HCl, NaOH, and NaCl were all of analytical grade.

3.2.2 Methods

Calorimetric measurements were carried out on the isothermal microcalorimeter from MicroCal, Inc. (Northampton, MA, USA). A 13.4 mM solution of SDBS is titrated into a 1.3 ml cell containing a solution with or without PVP. After each successive addition of 8.9 μl of SDBS solution, the heat q was directly monitored by the calorimeter. The partial molar enthalpy (per mole of surfactant monomers) is for each injection calculated from:

$$\Delta H_{\text{obs}} = \frac{q}{([SDBS]_{\text{titrant}} - \text{CMC})\Delta V_{\text{titrant}}} \quad [3.1]$$

where $[SDBS]_{\text{titrant}}$ is the concentration of the SDBS solution added to the cell, c.m.c. is the critical micelle concentration of SDBS, and $\Delta V_{\text{titrant}}$ is the volume of the injection. The time between two injections was 5 minutes; it was checked that this was sufficient for the system to reach equilibrium. Both the titrant solution and the titration cell contain in every experiment the same NaCl concentration.

3.3 Results and discussion

3.3.1 Micellization of SDBS

Figure 3.1 shows microcalorimetric titration curves of micellar SDBS solutions into 10^{-2} M NaCl at three temperatures. All figures show the observed enthalpy change for each addition of SDBS (ΔH_{obs}) as a function of the total SDBS concentration present in the cell.

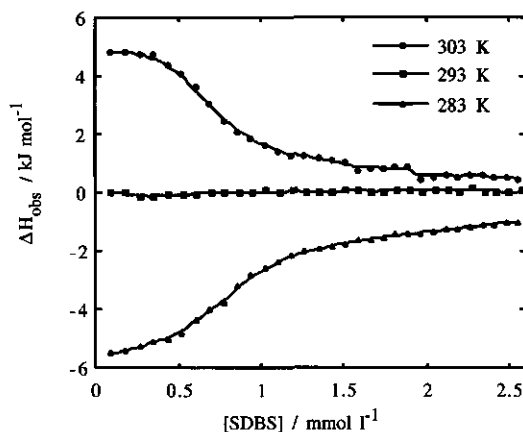


Figure 3.1: Microcalorimetric titrations of 13.4 mM SDBS into 10^{-2} M NaCl at different temperatures.

The observed enthalpies increase considerably with increasing temperature, being exothermic at 283 K, nearly zero at 293 K, and endothermic at 303 K. The trend in the curves at 283 and 303 K is that an initial (pseudo-)plateau is followed by a transition to a second plateau.

When a micellar solution is titrated into a solvent, the micelles are diluted and may, depending on the final surfactant concentration, decompose. The observed enthalpy therefore consists of a dilution and a demicellization term:

$$\Delta H_{\text{obs}} = \Delta H_{\text{dil}} + \Delta H_{\text{demicel}} = \Delta H_{\text{dil}} - \Delta H_{\text{micel}} \quad [3.2]$$

These contributions can be easily derived from the titration curves¹⁹. The transition regions in the curves at 283 K and 303 K indicate the c.m.c.. Hence, ΔH_{micel} follows from the difference between the two plateaus. The transitions are not sharp because SDBS is not isomerically pure.

At high surfactant concentrations, the micelles do not break up any more, i.e. $\Delta H_{\text{micel}} = 0$. Therefore, the dilution term is the enthalpy of the second plateau. The c.m.c.'s are arbitrarily assigned to a SDBS concentration halfway the transition which physically means that 50% of the added micelles decomposes. Observed enthalpies ΔH_{obs} and actual c.m.c.'s are calculated by an iterative process (equation [3.1]). Errors in these estimated c.m.c.'s have no substantial consequences for the calculated values of ΔH_{obs} , since $[\text{SDBS}]_{\text{titrant}} \gg \text{c.m.c.}$. The c.m.c. at 293 K has been determined by surface tension and surfactant-selective electrode measurements. The obtained c.m.c.'s, and the enthalpies of micellization and dilution, are summarized in table 3.1.

Table 3.1: C.m.c.'s and enthalpic contributions of the microcalorimetric titrations of SDBS at different temperatures; $[\text{NaCl}] = 10^{-2} \text{ M}$.

temperature (K)	c.m.c. (10^{-3} M)	ΔH_{dil} (kJ mol^{-1})	ΔH_{micel} (kJ mol^{-1})
283	0.8	- 1.0	4.1
293	0.7	0.04	0.09
303	0.7	0.5	- 4.4

The enthalpy of micellization changes from endothermic to exothermic with increasing temperature. This trend has been observed before for both the micellization of cationic¹⁹ and anionic surfactants^{20,21}. The latter reference can be consulted for more examples. The change in the sign of the enthalpy of micellization with temperature is typical for hydrophobic bonding^{19,22,23}. The Gibbs energy of micellization, which is directly related to the c.m.c. by $\Delta G_{\text{micel}}^{\circ} = RT \ln(\text{c.m.c.}/55.5)$, is far less temperature-sensitive (see table 3.1). This is caused by enthalpy/entropy compensation²⁴⁻²⁶ which occurs whenever a large number of molecular configurations exist with a comparable free energy²². At low temperatures, the enthalpy of micellization is endothermic. Micellization is entropically driven. At higher temperatures where $\Delta H_{\text{micel}} < 0$, enthalpy also favours micellization and the entropy contribution decreases.

The transition temperature, where the enthalpy of micellization changes sign, is slightly lower than 293 K. At this temperature, an endothermic enthalpy contribution stemming from the head groups is counterbalanced by an exothermic contribution from the hydrocarbon tails. The former is independent of temperature while the latter decreases (i.e. becomes less positive, or more negative) with increasing temperature.

The observation that the enthalpy of dilution slightly depends on the temperature is probably a hydrophobic bonding effect caused by the impurity of the surfactant.

3.3.2 Interaction between PVP and SDBS in solution

3.3.2.1 General trends

It is curious that in the literature only in two microcalorimetric studies of the interaction between polymers and surfactants, titration measurements were carried out at different temperatures^{14,27}. In the very first study²⁷, the expected trends for hydrophobic interactions were not found. This may have been caused by the used calorimeter²⁴ which had a lower sensitivity and resolution than current devices^{17,28}. These results may be the reason that the temperature effect on the interaction between polymers and surfactants has received remarkable little attention. The work of Wang and Olofsson¹⁴ showed no noticeable effect of temperature from 25°C to 45°C on the extent of binding of ionic surfactants to ethyl(hydroxyethyl)cellulose (EHEC).

Figures 3.2 – 3.4 show SDBS titration curves in the absence and presence of PVP at three temperatures and 10^{-2} M NaCl. The presence of polymer drastically changes the observed enthalpy, especially at 283 and 293 K.

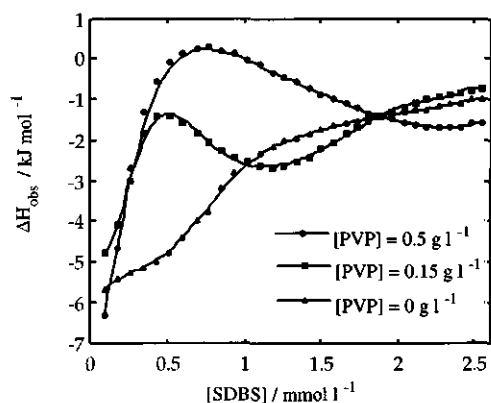


Figure 3.2: Microcalorimetric titrations of 13.4 mM SDBS into solutions of PVP; temperature = 283 K, 10^{-2} M NaCl.

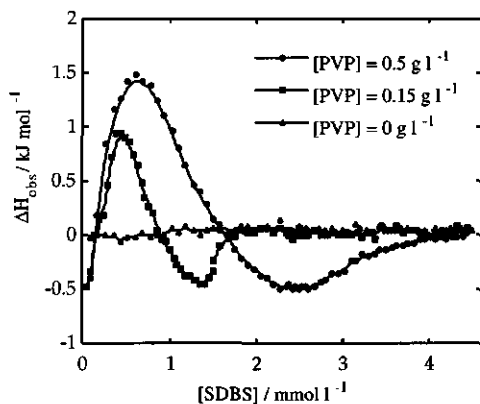


Figure 3.3: Microcalorimetric titrations of 13.4 mM SDBS into solutions of PVP; temperature = 293 K, 10^{-2} M NaCl.

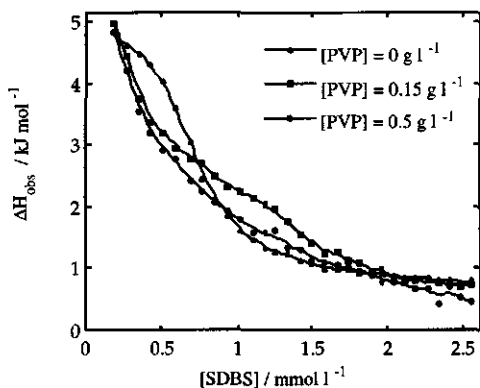


Figure 3.4: Microcalorimetric titrations of 13.4 mM SDBS into solutions of PVP; temperature = 303 K, 10^{-2} M NaCl.

In order to get insight into the enthalpic interaction between PVP and SDBS, the curves in figures 3.2 – 3.4 with and without PVP are subtracted at each surfactant concentration. The curves, thus constructed, are collected for two polymer concentrations and shown in figures 3.5 and 3.6.

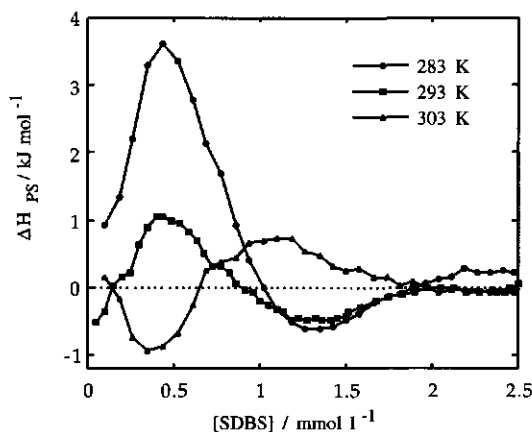


Figure 3.5: Differential interaction enthalpy of PVP and SDBS as a function of the total SDBS concentration; $[\text{SDBS}]_{\text{titrant}} = 13.4 \text{ mM}$, $[\text{PVP}]_0 = 0.15 \text{ g l}^{-1}$, 10^{-2} M NaCl .

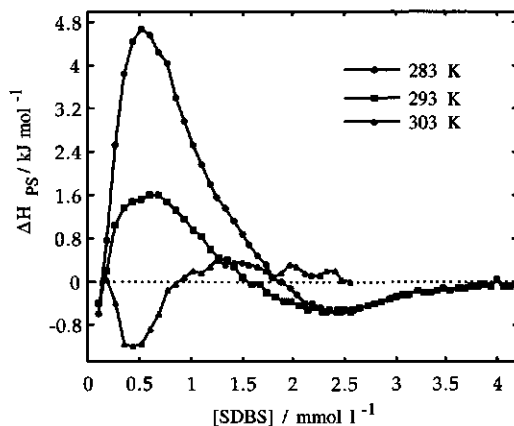


Figure 3.6: Differential interaction enthalpy of PVP and SDBS as a function of the total SDBS concentration; $[\text{SDBS}]_{\text{titrant}} = 13.4 \text{ mM}$, $[\text{PVP}]_0 = 0.5 \text{ g l}^{-1}$, 10^{-2} M NaCl .

The constructed enthalpy, ΔH_{diff} is basically an enthalpy difference between the micellization of SDBS, and the association between PVP and SDBS, at the same overall surfactant concentration. Remarkably similar

shaped curves emerge as a function of temperature and SDBS concentration. These similarities indicate the same underlying interaction mechanism and it supports the validity of our subtraction procedure to obtain the curves. All curves intersect two or three times the x-axis, where $\Delta H_{\text{diff}} = 0$, thereby passing through endothermic and exothermic extrema. The concentrations at which the extrema occur are hardly dependent on the temperature. It is emphasized that ΔH_{diff} changes sign between $T = 293 \text{ K}$ and 303 K , being endothermic at 293 K and exothermic at 303 K . The transition temperature, $T_{\text{trans'}}$ can be estimated by interpolation of the enthalpy at the first peak and yields for both polymer concentrations about 298.5 K , close to that of demicellization. This is a strong evidence for the occurrence of a process similar to micelle formation in bulk solution. The transition temperature increases from 293 K for the bulk micellization to 298.5 K for the association process in the presence of PVP. The hydrophobic bonding contribution in the presence of PVP is obviously smaller than the endothermic head group contribution. This may be caused by a decreased contribution of the hydrocarbon chain of the surfactant associating with PVP. This is in line with the observation that the transition temperature of micellization of *n*-alkylpyridinium chlorides increases with decreasing hydrocarbon chain length¹⁹.

The discussion will now be focused on the ΔH_{diff} -curves of 293 K because at that temperature the sum of the contributions ΔH_{dil} and ΔH_{micel} is approximately zero for the micellization of SDBS (see figure 3.1). Since these are non-zero in the presence of PVP, this temperature is well suited to study qualitatively the interaction enthalpy of SDBS on a polymer chain (ΔH_{PS}). Interpretation of the curves of 283 K and 303 K is more complex, since it is desirable to know the free monomer concentrations in order to obtain accurate ΔH_{PS} values at these temperatures. These curves will therefore just be used as a guide to monitor temperature effects. Since $\Delta H_{\text{obs}} \approx \Delta H_{\text{diff}} = \Delta H_{\text{PS}}$ at 293 K , no new figure is needed and the discussion is conducted on the basis of the curves of figure 3.3.

The association process of polymers and surfactants can be regarded as an exchange of surfactants and water molecules around the polymer chain. In general, the interaction enthalpy can be split up into a contribution due to specific polymer-surfactant interactions (ΔH_{spec}) and one because of mutual surfactant interactions. The latter consists of a hydrophobic contribution from the tails (ΔH_{hb}) and one from the head groups (ΔH_{hg}). As a result,

$$\Delta H_{\text{PS}} = \Delta H_{\text{PVP-SDBS}} + \Delta H_{\text{SDBS-SDBS}} = \Delta H_{\text{spec}} + \Delta H_{\text{hb}} + \Delta H_{\text{hg}} \quad [3.3]$$

The contribution ΔH_{hg} is typically weakly dependent of temperature, while ΔH_{hb} decreases strongly with increasing temperature.

With equation [3.3] in mind we will look at figure 3.3. With increasing surfactant concentration the curves in the presence of polymer show initially a small favourable enthalpy followed by an unfavourable and a favourable one respectively, and finally merging of the curves. These three regions will now be successively discussed.

(i) initial part

At very low surfactant concentrations, a small exothermic enthalpy is seen which becomes less exothermic with increasing temperature. As a result, it is not likely originated by hydrophobic bonding. In this region, single molecules associate with the polymer and there is no mutual interaction between bound surfactant molecules yet, i.e. $\Delta H_{\text{hb}} = 0$ and $\Delta H_{\text{hg}} = 0$. The observed exothermic enthalpy must therefore stem from association of single surfactant molecules with the polymer. It may be useful to look more closely at the origins of this association. A probable cause is attraction between the surfactant and the pyrrolidone ring. Ion-dipole interactions (between the surfactant head group and the pyrrolidone ring) have to be rejected because in the literature in none of the systems SDS-PVP^{10,27,29}, SDS-PEO¹⁴, SDS-PPO²⁹, and SDS-EHEC^{14,29} such an initial exothermic part is found. Apparently, initial attraction is driven by specific interactions between the pyrrolidone-ring and the surfactant head

group, or between the pyrrolidone-ring and the benzene-ring. In general, the extent of specific interactions decreases with increasing temperature, in line with the observations.

It is interesting to note that in the majority of systems studied, no interaction is observed at low surfactant concentrations^{11,14,15}, while for the combination PVP/SDS^{10,18} and our system, the enthalpy curves with and without PVP instantly differ. In the latter systems, polymer and surfactant interact right from the first addition of surfactants, while in the former a minimum surfactant concentration is needed before association occurs. This minimum surfactant concentration is often called critical aggregation concentration (c.a.c.) analogous to the critical micellization concentration (c.m.c.) in solution. As a result, it is not possible to identify a c.a.c. for the system SDBS/PVP.

(ii) endothermic part

Addition of successive small amounts of surfactant molecules results in an increasing endothermic enthalpy till $[SDBS] \approx 0.5$ mM which decreases to zero at intermediate SDBS concentrations. In this endothermic region, an increasing amount of surfactants will bind to the polymer and these molecules mutually interact. Neighbouring charged head groups repel, whereas hydrocarbon chains attract each other. As stated before, the sum of ΔH_{hb} and ΔH_{hg} results in an endothermic enthalpy for the mixed system at 293 K. Obviously, the head group contribution dominates the hydrophobic contribution. This is enthalpically unfavourable and the polymer-surfactant association is entropically driven. Compared to the micellization of SDBS in bulk solution (with $\Delta H_{micel} \approx 0$ kJ mol⁻¹ at 293 K), the endothermic effect of the mixture may be due to a decreased contribution of the hydrocarbon chain of SDBS when interacting with PVP.

To understand the shape of the curves till the concentration where $\Delta H_{obs} = 0$ kJ mol⁻¹, we suggest that they can be looked upon as incremental binding isotherms. Upon each surfactant addition, the enthalpy scales with

the number of surfactant molecules associating with the polymer molecules. This number is highest at the top of the endothermic peak and decreases when the enthalpy decreases. The maximum of the endothermic peak may therefore correspond to the inflection point of the binding isotherm. This can be clearly shown when the incremental titration curves are converted in cumulative enthalpy plots. In that case, sigmoidally shaped curves are obtained. This behaviour is comparable to that observed for the adsorption of ionic surfactants at solid/liquid interfaces^{30,31} and characterise a cooperative adsorption process. In addition, the temperature effect on the interaction enthalpy (see figures 3.5 and 3.6) shows that the association is driven by hydrophobic bonding.

(iii) exothermic part

At higher surfactant concentrations, the curves show an exothermic part at 293 K. According to figures 3.5 and 3.6 this effect is again strongly temperature dependent, suggesting that hydrophobic bonding is involved. However, in this region the trend is opposite compared to the usually observed hydrophobic bonding effect, i.e. ΔH_{obs} becomes more endothermic with increasing temperature. Therefore, there is a strong indication for a decrease in hydrophobic bonding. In our opinion, this is related to the flexibility of the adsorbent, i.e. the polymer chain. Structural rearrangements in the polymer-surfactant complexes occur accompanied by a decrease in hydrophobic interactions. This may be seen as follows. Initially, single PVP molecules will have a random coiled shape. Association with charged surfactant molecules will have two opposite effects on the polymer conformation. On the one hand, electrostatic repulsions between neighbouring surfactant molecules tend to swell the chain. On the other hand, an increase in the extent of hydrophobic bonding will contract the chain. These two effects may be more or less balanced till intermediate surfactant concentrations, leading to aggregates with intra- and interchain interactions. Support for the occurrence of these

interactions at intermediate surfactant concentrations can be found in viscosity measurements^{29,32}.

At increased binding of surfactants, the electrostatic repulsion between neighbouring charged head groups becomes too high, and the polymer chain considerably expands thereby breaking up associated surfactant aggregates. This is seen in the inverse-hydrophobic temperature dependence of figures 3.5 and 3.6. Figure 3.7 shows a schematic representation of the polymer-surfactant interaction with increasing surfactant concentration.

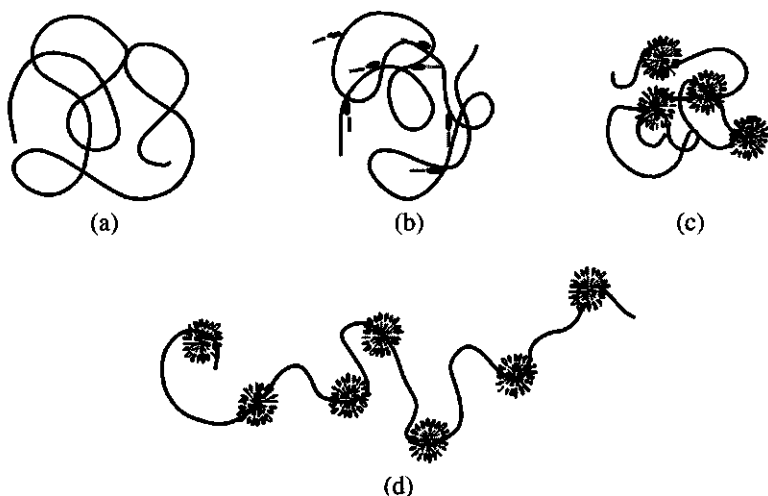


Figure 3.7: Schematic representation of the association of SDBS and PVP with increasing surfactant concentration: (a) random coil conformation, (b) single molecules associated with the chain, (c) polymer-surfactant aggregate with intrachain interactions, (d) expanded polymer-surfactant aggregate.

At even higher surfactant concentrations, the loss of hydrophobic bonding is made up for by adsorption of newly added surfactant molecules. As a result, the enthalpic effect goes through a minimum and increases somewhat till the expanded chain is saturated with surfactant. The resulting structure, surfactant aggregates associated on a polymer chain, is often called the pearl-necklace model.

Once the polymer is saturated with surfactant, the contribution ΔH_{obs} will go to zero since the number of surfactants bound to the polymer

approximately remains constant. At even higher surfactant concentrations pure micelles coexist in dynamic equilibrium with single surfactants and polymer-surfactant aggregates.

A change in the size of the polymer-surfactant complexes has been observed by Maltesh and Somasundaran³³ who studied the interaction between poly(ethylene glycol) (PEG) and SDS by fluorescence spectroscopy. They detected a contraction of the polymer coil at low SDS concentrations and an expansion at higher concentrations, in line with our interpretation of the results of the PVP/SDBS-system.

Similar shaped curves to our ΔH_{obs} curves have been observed in several polymer-surfactant systems^{12,14,15,17,29}. However, hardly any definite conclusions have been drawn with respect to a more detailed interpretation. The behaviour is a matter of discussion. Wang and Olofsson¹⁴ put forward an interpretation based on a parallel between the solubilization of uncharged molecules in ionic micelles³⁴ and the interaction between polymers and surfactants. The latter is then looked upon as the solubilization of polymer segments in surfactant aggregates. The consecutive occurrence of an endothermic and exothermic region is interpreted in terms of the dehydration and rehydration of polar polymer segments, respectively. Although the (re)hydration of polar segments is intimately related to hydrophobic bonding, we think our results suggest that the shape of the curves directly reflects the number of surfactant molecules associating with the polymer. Looking upon the results in this way allows us to explain the whole shape of the titration curve. Our analysis takes enthalpy changes into account of all interactions occurring in the presence of the polymer, i.e. ΔH_{spec} , ΔH_{hb} , and ΔH_{hg} .

3.3.2.2 Effect of the amount of polymer

Figure 3.3 shows titration curves at two polymer concentrations. If more PVP is present, both the endothermic and exothermic enthalpy peaks are larger, and merging takes place at higher surfactant concentrations. These observations can be qualitatively understood realising that an increased

amount of polymer leads to an increased number of associating surfactant molecules.

As a first approach, the areas enclosed by the endothermic and the exothermic peak, and the x-axis may be used as a relative measure of the number of bound surfactant molecules. The ratio of the areas are numerically determined and shown in table 3.2.

Table 3.2: Ratios between different areas of the titration curves at different polymer concentrations.

$\left(\frac{A_{[\text{PVP}]=0.5 \text{ g l}^{-1}}}{A_{[\text{PVP}]=0.15 \text{ g l}^{-1}}} \right)_{\text{endo}}$	$\left(\frac{A_{[\text{PVP}]=0.5 \text{ g l}^{-1}}}{A_{[\text{PVP}]=0.15 \text{ g l}^{-1}}} \right)_{\text{exo}}$	$\left(\frac{A_{[\text{PVP}]=0.5 \text{ g l}^{-1}}}{A_{[\text{PVP}]=0.15 \text{ g l}^{-1}}} \right)_{\text{total}}$	$\frac{[\text{PVP}]_{0.50}}{[\text{PVP}]_{0.15}}$
3.0	3.5	3.2	3.3

The ratios $\left(\frac{A_{[\text{PVP}]=0.5 \text{ g l}^{-1}}}{A_{[\text{PVP}]=0.15 \text{ g l}^{-1}}} \right)_i$ correspond to the areas of the endothermic, exothermic, and the total enthalpic effect (i.e. the sum of the absolute values of the aforementioned contributions), respectively. The last column is the ratio of the polymer concentrations. The ratio of the indicated areas under the curves fairly well correspond with this polymer ratio. Looking in somewhat more detail, the ratio of the areas of the endothermic peaks is somewhat lower than 3.3, while the opposite is found for that of the exothermic effect. These deviations may be caused by a decreased accessible area for surfactants at $[\text{PVP}]_0 = 0.5 \text{ g l}^{-1}$ due to inter- and intra-chain linking. These interactions will occur to a greater extent at increased polymer concentration. With an increasing number of charged molecules bound to the chains, both intra- and inter-chain interactions become less favourable. The complexes attain a more stretched conformation and formerly non-accessible sites become available for SDBS molecules. As a result, for the binding region (endothermic part) a somewhat lower ratio is found than for the rearrangement region (exothermic part). The ratio of the sum of these effects is 3.2 which comes very close to the ratio of the initial polymer concentrations. This supports our proposed model in which the area enclosed by the curves reflects the number of associated molecules.

3.3.2.3 Effect of the electrolyte concentration

Figure 3.8 shows titration curves at two different electrolyte concentrations (at $T = 293\text{ K}$ where $\Delta H_{\text{obs}} \approx \Delta H_{\text{ps}}$). The amount of salt does not influence the shape of the curves but shifts them to lower surfactant concentrations. Obviously, the interaction mechanism is not changed. Increasing the NaCl concentration decreases the double layer repulsion, so that co-operative binding of surfactant molecules is promoted. At first glance, this might seem to be all, but two effects need to be mentioned. Firstly, it is known that the enthalpy of micellization slightly decreases with increasing electrolyte concentration¹⁹. Secondly, with increasing electrolyte concentration, the aggregation number of SDS micelles³⁵⁻³⁷, and SDS-aggregates of SDS-uncharged polymer complexes³⁷⁻⁴⁰ increases somewhat. These two effects influence the interaction enthalpy in opposite direction. It is therefore likely that the similarity of shape of the enthalpy curves corresponds to a slightly increased number of associated SDBS molecules with a corresponding lower endothermic interaction enthalpy per molecule.

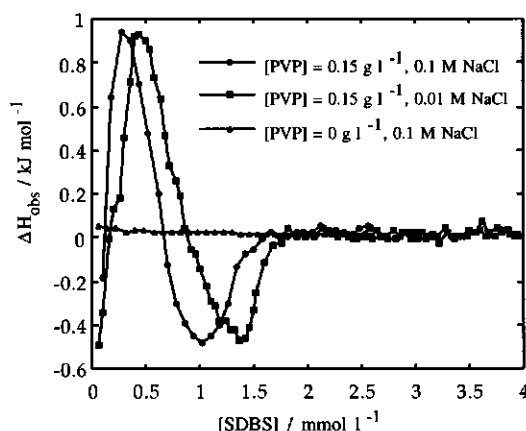


Figure 3.8: Microcalorimetric titrations of 13.4 mM SDBS to solutions with different amounts of polymer and electrolyte; temperature = 293 K.

3.4 Conclusions

Micellization of the anionic surfactant SDBS is driven by hydrophobic bonding. Microcalorimetric titrations of SDBS in the presence of PVP at different temperatures revealed the same driving force for the surfactant association around the polymer chain. The interaction between the uncharged polymer PVP and the anionic surfactant SDBS can be looked upon as a polymer-induced micellization starting at $[SDBS] < c.m.c.$. Titration curves at 293 K show distinct endothermic and exothermic regions. We offer a new interpretation of these curves, suggesting to look upon them as differential binding curves of surfactant molecules to the polymer chains. Initially, single SDBS molecules interact with PVP by non-hydrophobic interactions. At higher concentrations, adsorbed surfactant molecules act as nucleation sites for cluster formation. This is an endothermic process at 293 K, driven by hydrophobic bonding.

The subsequent exothermic region displays typical inverse hydrophobic bonding behaviour. In our opinion, this is due to conformational changes of the polyelectrolyte complexes, caused by electrostatic repulsion of neighbouring surfactant head groups. The chains considerably expand thereby decreasing the extent of hydrophobic bonding. This rearrangement offers additional adsorption sites for surfactant molecules.

At a well defined surfactant concentration PVP becomes saturated with SDBS. Further increase of the SDBS concentration leads to a dynamic equilibrium in which single surfactants, polymer-surfactant complexes, and surfactant micelles coexist. The final structure of the complex is that of a polymer wrapped around the micellar surface, thereby stabilising the hydrocarbon-water interface. Changing the initial PVP concentration allows us to quantify the relative contributions to the endothermic and exothermic effect. Electrolytes do not change the interaction mechanism but promote association of PVP and SDBS. Both results support our proposed model. The knowledge thus obtained will be used to understand the behaviour of PVP and SDBS at solid/liquid interfaces.

Microcalorimetry at different temperatures is a powerful tool to get insight into the nature of the polymer-surfactant binding process and the structure of the resulting aggregates. However, for a detailed quantitative analysis, binding isotherms are needed. This will be the subject of a future publication.

References

- 1 I. P. Robb, in *Anionic Surfactants, Surfactant Science Series; Vol. 11*, edited by E. H. Lucassen-Reynders, Marcel Dekker, New York (1981), 109.
- 2 E. D. Goddard, *Colloids Surf.* **19**, 255 (1986).
- 3 K. Hayakawa and J. C. T. Kwak, in *Cationic Surfactants, Surfactant Science Series; Vol. 37*, edited by D. N. Rubingh and P. M. Holland, Marcel Dekker, New York (1991), 189.
- 4 J. C. Brackman and J. B. F. N. Engberts, *Chem. Soc. Rev.* **22**, 85 (1993).
- 5 B. Lindman and K. Thalberg, in *Interactions of Surfactants with Polymers and Proteins*, edited by E. D. Goddard and K. P. Ananthapadmanabham, CRC Press, Boca Raton (1993), 203.
- 6 P. Hansson and B. Lindman, *Current Opinion Colloid Interface Sci.* **1**, 604 (1996).
- 7 B. Jönsson, B. Lindman, K. Holmberg, and B. Kronberg, *Surfactants and Polymers in Aqueous Solution*, Wiley, Chichester (1998).
- 8 L. F. G. Piculell, K. Thuresson, V. Shubin, and O. Ericsson, *Adv. Colloid Interface Sci.* **63**, 1 (1996).
- 9 B. Cabane, *J. Phys. Chem.* **81**, 1639 (1977).
- 10 G. Olofsson and G. Wang, *Pure Appl. Chem.* **66**, 527 (1994).
- 11 D. M. Bloor, J. F. Holzwarth, and E. Wyn-Jones, *Langmuir* **11**, 2312 (1995).
- 12 D. M. Bloor, Y. Li, and E. Wyn-Jones, *Langmuir* **11**, 3778 (1995).
- 13 G. J. Fox, D. M. Bloor, J. F. Holzwarth, and E. Wyn-Jones, *Langmuir* **14**, 1026 (1998).
- 14 G. Wang and G. Olofsson, *J. Phys. Chem.* **99**, 5588 (1995).
- 15 K. Thuresson, B. Nyström, G. Wang, and B. Lindman, *Langmuir* **11**, 3730 (1995).
- 16 Y. Wang, B. Han, H. Yan, and J. C. T. Kwak, *Langmuir* **13**, 3119 (1997).

- 17 G. Olofsson and G. Wang, in *Polymer-Surfactant Systems, Surfactant Science Series; Vol. 77*, edited by J. C. T. Kwak, Marcel Dekker, (1998), 317.
- 18 G. Wang and G. Olofsson, *J. Phys. Chem. B* **102**, 9276 (1998).
- 19 T. Mehrian, A. de Keizer, A. J. Korteweg, and J. Lyklema, *Colloids Surf. A: Physicochem. Eng. Aspects* **71**, 255 (1993).
- 20 I. Johnson, G. Olofsson, and B. J. Jönsson, *J. Chem. Soc., Faraday Trans. I* **83**, 3331 (1987).
- 21 N. M. Van Os, G. J. Daane, and T. A. B. M. Bolsman, *J. Colloid Interface Sci.* **115**, 402 (1987).
- 22 D. F. Evans, *Langmuir* **4**, 3 (1988).
- 23 C. Tanford, *The Hydrophobic Effect*, John-Wiley, New York (1980).
- 24 G. C. Kresheck and W. A. Hargraves, *J. Colloid Interface Sci.* **48**, 481 (1974).
- 25 R. Lumry and S. Rajender, *Biopolymers* **9**, 1125 (1970).
- 26 L.-J. Chen, S.-Y. Lin, and C.-C. Huang, *J. Phys. Chem.* **102**, 4350 (1998).
- 27 G. C. Kresheck and W. A. Hargraves, *J. Colloid Interface Sci.* **83**, 1 (1981).
- 28 T. Wiseman, S. Williston, J. F. Brandts, and L.-N. Lin, *Anal. Biochem.* **179**, 131 (1989).
- 29 D. M. Bloor, W. M. Z. Wan-Yunus, W. A. Wan-Badhi, Y. Li, J. F. Holzwarth, and E. Wyn-Jones, *Langmuir* **11**, 3395 (1995).
- 30 L. K. Koopal, in *Coagulation and Flocculation, Surfactant Science Series; Vol. 47*, edited by B. Dobias, Marcel Dekker, New York (1993), 101.
- 31 B. T. Ingram and R. H. Ottewil, in *Cationic Surfactants, Surfactant Science Series; Vol. 37*, edited by D. N. Rubingh and P. M. Holland, Marcel Dekker, New York (1991).
- 32 S. Biggs, J. Selb, and F. Candau, *Langmuir* **8**, 838 (1992).
- 33 C. Maltesh and P. Somasundaran, *Langmuir* **8**, 1926 (1992).
- 34 I. Johnson, G. Olofsson, M. Landgren, and B. Jönsson, *J. Chem. Soc., Faraday Trans. I* **85**, 4211 (1989).
- 35 S. Hayashi and S. Ikeda, *J. Phys. Chem.* **84**, 744 (1980).
- 36 P. J. Missel, N. A. Mazer, G. B. Benedek, and C. Y. Young, *J. Phys. Chem.* **84**, 1044 (1980).
- 37 F. M. Witte and J. B. F. N. Engberts, *Colloids Surf.* **36**, 417 (1989).

- 38 T. Gilányi and E. Wolfram, *Colloids Surf.* **3**, 181 (1981).
- 39 E. A. Lissi and E. Abuin, *J. Colloid Interface Sci.* **105**, 1 (1985).
- 40 J. Xia, P. L. Dubin, and Y. J. Kim, *J. Phys. Chem.* **96**, 6805 (1992).

Chapter 4

Mixed Adsorption of Poly(VinylPyrrolidone) and Sodium DodecylBenzeneSulphonate on Kaolinite

Abstract

The mixed adsorption of the nonionic polymer poly(vinylpyrrolidone) (PVP) and the anionic surfactant sodium dodecylbenzenesulphonate (SDBS) on kaolinite has been studied. Both components adsorb from their mixture on the clay mineral. The overall adsorption process is sensitive to the pH, the electrolyte concentration, and the amounts of polymer and surfactant. Interpretation of the experimental data is hampered by the patchwise heterogeneous surface of the clay. In the absence of PVP, SDBS adsorbs on kaolinite by electrostatic and hydrophobic interactions. When PVP is present, surfactant adsorption is at 10^{-2} M NaCl mainly driven by charge compensation of the edges. The adsorption of PVP from the mixture shows similar behaviour under different conditions. Three regions can be distinguished which display the changing character of charge of polymer-surfactant complexes in solution with increasing SDBS concentration. At low surfactant content, PVP adsorbs by hydrogen bonding and hydrophobic interactions, whereas coulombic effects dominate at higher surfactant concentrations. Over the entire surfactant concentration range, polymer-surfactant aggregates are present at the edges. The composition of these surface complexes differs from that in solution, and is controlled by the surface charge.

4.1 Introduction

Mixed adsorption of polymers and surfactants at solid/liquid interfaces has both practical (cosmetics, detergency, pharmaceuticals, enhanced oil recovery, etc.) and scientific interest. A mixed adsorption process is determined by a delicate balance of interactions between polymers, surfactants, solvent molecules, and adsorbent. In order to interpret mixed adsorption isotherms, knowledge of (1) the polymer-surfactant interaction in bulk solution¹⁻⁶ and (2) the single adsorption of polymers^{7,8} and surfactants^{9,10}, is essential. Despite the fact that these topics have received a lot of attention, relatively few studies are concerned with the mixed adsorption of polymers and surfactants at solid/liquid interfaces. This may be caused by the complexity of these systems. In general, the adsorption of two different solutes can be additive, cooperative and competitive.

Recently, Otsuka and Esumi¹¹ reviewed mixed polymer-surfactant adsorption, mainly on oxide surfaces. They made a classification of the studied systems based on the charges of both the polymer and the surfactant. It may be more fundamental to make a subdivision according to their mutual affinities, leading to the following groups:

(1) Individually both the polymer and the surfactant adsorb on the surface, but they do not (significantly) interact in solution. These systems typically show competitive adsorption behaviour. The component with the highest affinity preferentially adsorbs, and may be able to displace the other component. Either the polymer¹²⁻¹⁴ or the surfactant^{12,15-17} can have the highest surface affinity. If the polymer and the surfactant adsorb onto different sites of surfaces with a patchwise heterogeneity, additive adsorption has been observed¹⁴.

(2) Only one of the components adsorbs, but in solution the polymer and the surfactant interact. By far the most studied systems of this category are oxide surfaces in the presence of an adsorbing ionic surfactant and a non-adsorbing polymer such as poly(vinylpyrrolidone), PVP¹⁸⁻²³, or poly(styrene sulphonate)^{16,24}. Common in these systems is an initial

adsorption of the polymer due to complexation with surfactant molecules at low surfactant concentrations, followed by a strong decrease in polymer adsorption for high surfactant concentrations.

(3) The polymer and the surfactant adsorb both on the surface, and they interact^{19,25-28}. The overall behaviour is determined by the relative strengths of both single adsorption energies, the adsorption Gibbs energy of the associates, and the polymer-surfactant interaction Gibbs energy. These systems are the most complicated ones. The adsorption of the two components is highly sensitive to their concentrations and their specific properties. In the case that one or both components have an ionic character also the pH and the electrolyte concentration become important parameters.

In passing it should be noted that the above-mentioned classification considers equilibrium behaviour. No attention is given to kinetic features, such as the very slow desorption rates which are often observed for adsorbed polymer chains.

This chapter involves a detailed study on the adsorption of the nonionic polymer PVP and the anionic surfactant sodium dodecylbenzenesulphonate (SDBS) on kaolinite. This system is an example of the third category with the additional difficulty that the surface is heterogeneous with respect to its surface charge and chemistry²⁹⁻³². Kaolinite is a clay mineral consisting of alternating siloxane and gibbsite sheets with a constant negative plate charge, and amphoteric edges with a variable charge caused by (de)protonation. This work is an extension of previous studies on the adsorption of PVP on kaolinite (chapter 2), and on the interaction between PVP and SDBS in aqueous solutions (chapter 3).

4.2 Experimental

4.2.1 Materials

Poly(vinylpyrrolidone) (PVP) and sodium dodecylbenzenesulphonate (SDBS) were purchased from BASF and Fluka, respectively. Both

products were used as received. The PVP sample had a number-average molar mass of $17.4 \cdot 10^3 \text{ g mol}^{-1}$ ($M_w/M_n = 1.9$). Surface tension measurements as a function of the SDBS concentration showed no minimum. The critical micelle concentration (c.m.c.) of SDBS in 10^{-2} M NaCl was 0.7 mM , a value that has been obtained with both surface tension and surfactant selective electrode measurements. Our kaolinite was obtained from Sigma Company and extensively characterized by Mehrian^{33,34}, showing an edge/plate area ratio of about 0.25. The cation exchange capacity (c.e.c.) was found to be $30 \mu\text{mol g}^{-1}$ by the silver-thiourea method and $57 \mu\text{mol g}^{-1}$ by the ammonium acetate method. It was assumed that the latter value also include the surface sites of the edges. The point of zero charge of the edges was around 7.0 (see chapter 2) and the BET (N_2) surface area of our sample was $17.7 \text{ m}^2 \text{ g}^{-1}$. HCl, NaOH, and NaCl were all of analytical grade. Water was purified by passing it through a mixed bed ion exchanger, a carbon column, and a microfilter.

4.2.2 Methods

Adsorption isotherms were determined by depletion measurements at 25°C . The concentrations of PVP and SDBS were determined by UV-absorption (Hitachi U-3210 spectrophotometer) at 204.0 and 223.6 nm, respectively. The equilibrium adsorbed amount of SDBS is reached within one hour; the PVP adsorption reaches instantly about 75% of the maximum adsorbed amount and thereafter increases slowly to this level in 10 hours.

For the mixtures, the contributions of polymer and surfactant were additive with respect to Lambert-Beer's law (experimental error = 2%): $A^\lambda = \epsilon_p^\lambda c_p + \epsilon_s^\lambda c_s$, where A is the absorbance, ϵ the absorption coefficient, l the pathlength of the sample, and c_p and c_s the concentration of PVP and SDBS, respectively. In order to determine c_p and c_s , measurements were carried out at two wavelengths λ using the following absorption coefficients: $\epsilon_p^{204} = 3.362 \text{ m}^2 \text{ g}^{-1}$, $\epsilon_s^{204} = 1.082 \text{ m}^2 \text{ mmol}^{-1}$, $\epsilon_p^{223.6} = 0.329 \text{ m}^2 \text{ g}^{-1}$, and $\epsilon_s^{223.6} = 1.178 \text{ m}^2 \text{ mmol}^{-1}$.

Centrifuge tubes are filled with 25 ml kaolinite dispersion, 5 ml polymer solution, an appropriate amount of surfactant and electrolyte solution, and an appropriate amount of demineralized water to assure an equal volume in each tube. The PVP and SDBS solutions are simultaneously added, but not premixed. Introductory kinetic experiments showed the difference between these two ways of adding to be within experimental error. To ensure equilibration, the tubes were shaken end-over-end for 16 hours at 30 rpm. The solids were separated from solution by centrifugation for 30 minutes at 20,000 rpm in a Beckman J2-MC centrifuge, after which the pH of the supernatant is measured. Experiments are carried out as a function of the SDBS concentration, at two electrolyte concentrations, three pH values, and two initial PVP concentrations.

Settling rates of the dispersions have been determined directly after end-over-end rotation by measuring the height of the dispersion/supernatant interface as a function of time for about one hour. This interface was observed as a sharp boundary. Initially, the interface height vs. time curve showed a linear part. The slope of this part is taken as the settling rate of the dispersions as a measure of the stability of the dispersion.

All lines in the graphs only serve as guides to the eye.

4.3 Results and discussion

4.3.1 Single adsorption isotherms

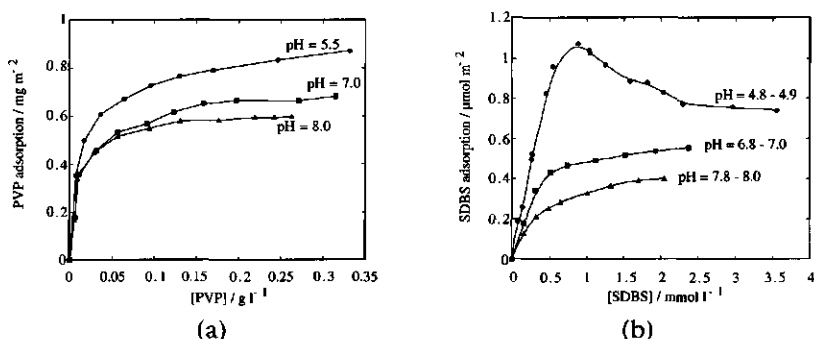


Figure 4.1: Adsorption of PVP (a) and SDBS (b) on kaolinite at different pH values; $I = 10^{-2}$ M NaCl.

The adsorption of PVP only and SDBS only at three pH values is presented in figures 4.1a and 1b, respectively. PVP readily adsorbs on kaolinite, the main contributions stemming from hydrogen bonding at the edges, and hydrophobic interactions at the siloxane plates (see chapter 2). The latter is independent of pH, while the former increases with decreasing pH.

The SDBS isotherms also show a decrease in adsorption with increasing pH. For negatively charged molecules this suggests an influence of coulombic interactions. However, even at high pH a fair amount of SDBS still adsorbs onto the clay, indicating that there is also a non-coulombic contribution. The maximum in the isotherm occurring at pH = 5 around 1 mmol l^{-1} is remarkable. This maximum has been observed for the adsorption of alkylbenzene sulphonates on kaolinite^{13,35-43}. Somasundaran and co-workers^{35,37-40} have investigated this complex system in detail. They concluded that mineral dissolution and precipitation may simultaneously occur, in addition to adsorption. The most probable cause for the observed maximum at pH = 5 seems to be precipitation of surfactants with Al^{3+} -ions leaching from the clay at low pH values. Above the critical micelle concentration these precipitates redissolve, thereby releasing monomers in solution³⁷.

4.3.2 Interaction in solution

The interaction between PVP and SDBS in solution is reported in chapter 3. One of the results relevant for the present study is that at 293 K, the micellization and dilution enthalpy of SDBS are nearly zero, which makes this temperature well suited to study the polymer-surfactant interaction. PVP and SDBS readily interact. This is clearly shown in figure 4.2 where the enthalpy of interaction is plotted versus the total surfactant concentration for two PVP concentrations and two electrolyte concentrations (data taken from chapter 3).

Initially, single molecules associate with the polymer chain by non-hydrophobic interactions. The endothermic peak at low

SDBS concentrations, corresponds with cooperative binding of molecules driven by hydrophobic interactions, i.e. a polymer-induced micellization. The exothermic region at intermediate concentrations features inverse hydrophobic bonding behaviour (see chapter 3). Electrostatic repulsion between neighbouring surfactant molecules causes structural rearrangements of the complexes. Newly added molecules can adsorb on vacant hydrophobic sites. At high SDBS concentrations, ΔH_{ps} approaches zero, indicating that the polymer is saturated with surfactant. Increasing the electrolyte concentration mainly promotes association of SDBS molecules on PVP due to a decreased lateral electrostatic repulsion.

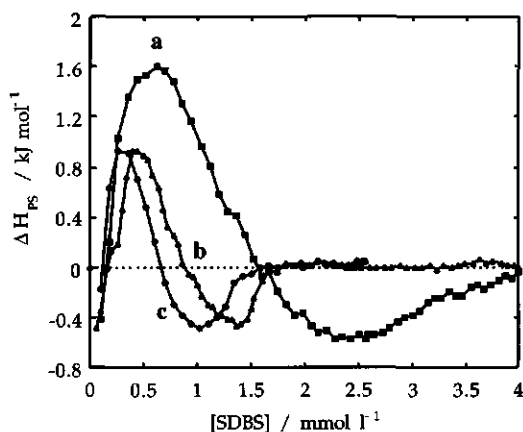


Figure 4.2: Microcalorimetric titrations of 13.4 mM SDBS to solutions with different concentrations of polymer and electrolyte, $T = 293\text{ K}$; a: $[PVP]_0 = 0.5\text{ g l}^{-1}$, 10^{-2} M NaCl ; b: $[PVP]_0 = 0.15\text{ g l}^{-1}$, 10^{-2} M NaCl ; c: $[PVP]_0 = 0.15\text{ g l}^{-1}$, 10^{-1} M NaCl .

4.3.3 Mixed adsorption isotherms

In order to structure this paper, the mixed adsorption isotherms are presented and discussed as a function of subsequently the pH, the electrolyte concentration, and the initial amount of polymer.

4.3.3.1 Effect of pH

Figure 4.3 shows mixed adsorption isotherms of PVP and SDBS as a function of the SDBS concentration at $\text{pH} = 5, 7$ and 8 . These pH values

correspond to positive, neutral, and negative charges on the clay edges, respectively. The trend is that with increasing pH, the adsorbed amount of both components decreases, similarly as observed for the individual adsorbate systems. The SDBS adsorption is drastically lowered compared to its single adsorption. Especially in the case of neutral or negatively charged edges, hardly any surfactant is adsorbed.

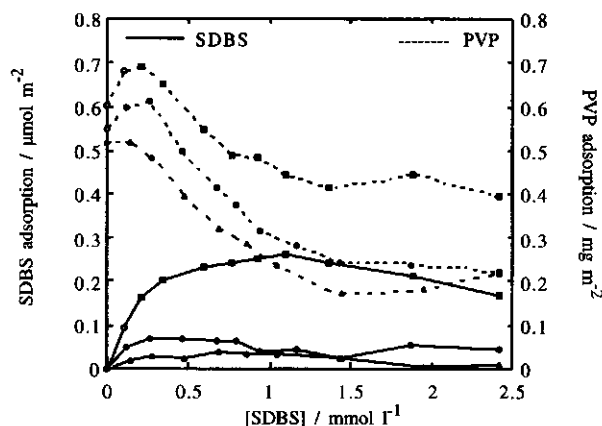


Figure 4.3: Effect of pH on the mixed adsorption of PVP and SDBS on kaolinite: ■: pH = 4.9-5.1; ●: pH = 6.8-7.0; ▲: pH = 7.8-8.0; 10^{-2} M NaCl, $[PVP]_0 = 0.15 \text{ g l}^{-1}$; open symbols indicate samples which settled within 30 minutes.

The general shape of the PVP curves is roughly independent of the pH. Three regions can be distinguished in these curves: (i) a small increase (pH = 5 and 7) or constant level (pH = 8) until $[SDBS] \approx 0.3 \text{ mM}$, followed by (ii) a substantial decrease until $[SDBS] \approx 1.5 \text{ mM}$, after which (iii) the curves level off to a (pseudo-)plateau. These regions correspond to different polymer-surfactant complexes present in solution (chapter 3): (i) slightly charged complexes, (ii) complexes with an increasing charge due to increased surfactant binding to PVP and (iii) saturated PVP-SDBS complexes, respectively. The results are discussed below on the basis of these regions.

Additional information on the behaviour of the systems are the settling rates that can be classified into two groups: stable dispersions and rapidly

settling dispersions. Stable dispersions are identified in figure 4.3 by closed symbols, while open symbols refer to rapid settling.

Region (i) The adsorption of polymers associated with a small number of surfactants is at pH = 5 and 7 somewhat higher than that of pure PVP chains. Since changes in pH only affect the charge on the clay edges, it is likely that this synergistic adsorption - which is more pronounced at lower pH - is an edge effect, caused by coulombic attraction between positive edges and slightly negatively charged PVP-SDBS complexes. So the surfactant acts as a bridge between hydrophobic polymer segments and the edges of the clay particles. Additional support for this conclusion is obtained from the settling rate measurements. Rapid settling of the dispersions takes place in 10^{-2} M NaCl for bare particles if edges and plates are oppositely charged. This is in agreement with measurements reported in literature^{44,45}. Moreover, under the given conditions the dispersions are unstable in the presence of PVP only. However, when a small amount of SDBS is added, the synergistic adsorption of PVP results in stable dispersions caused by negatively charged polymer-surfactant aggregates on the positive edges which inhibit edge-plate attraction.

Region (ii) In the second region ($0.3 \text{ mM} < [\text{SDBS}] < 1.5 \text{ mM}$), the adsorption of PVP considerably decreases while the SDBS adsorption hardly changes. In solution an increased number of surfactant molecules bind to the polymer, resulting in increasingly negatively charged PVP-SDBS complexes. Since the plates are also negatively charged, the affinity of these complexes for the plates will be lower than that of PVP only. The change in the edge adsorption will depend on the pH, i.e. a decrease at pH = 8 and likely a small increase at pH = 5. The curves of pH = 8 and pH = 5 show indeed the largest and smallest decrease, respectively.

The adsorbed amount of SDBS is hardly dependent on the SDBS concentration. To gain insight into the adsorption mechanism of SDBS a rough calculation can be made. Assuming plateau adsorption for SDBS in figure 4.3, an (average) difference in the adsorbed amount between pH = 5 and pH = 7 of about $0.17 \mu\text{mol m}^{-2}$ is found. Having about

0.35 g of kaolinite in each experiment this corresponds to a total charge difference of about 0.1 C. The difference in the edge charge going from pH = 5 to 7 can be estimated from the acid/base titration data of this kaolinite sample (see chapter 2). Since in this pH region part of the titrated protons are consumed by an exchange with sodium ions at the plates (chapter 2), this difference cannot be directly determined. It is therefore assumed that the number of edge charges are symmetrical around its point of zero charge (pH = 7). Thus, $\Delta\sigma_{\text{edge, pH7} - \text{pH5}} \approx \Delta\sigma_{\text{edge, pH7} - \text{pH9}}$, which results in a total charge of about 0.2 C (see chapter 2). This value is of comparable magnitude with the calculated difference in SDBS adsorption. As the total amount of SDBS adsorbed from the mixture, either as single molecules or as PVP-SDBS complexes, is mainly caused by charge compensation of the edges, we conclude that SDBS molecules which could adsorb in the absence of PVP (figure 4.1b) by specific (non-coulombic) interactions are displaced by the polymer.

Region (iii) The third region occurs at [SDBS] > 1.5 mM where the adsorbed amount of PVP flattens to a (pseudo-)plateau. Microcalorimetry measurements show saturated polymer-surfactant aggregates in solution at [SDBS] > 1.8 mM (figure 4.2). Addition of SDBS changes neither the composition of the associates in solution nor their affinity for the surface. As a result, the adsorption of both PVP and SDBS remains roughly constant in this region.

Insight in the composition of the surface aggregates can also be obtained from figure 4.3. The observation that the SDBS adsorption is mainly determined by edge charge compensation, and that it is roughly independent of the surfactant concentration (i.e. the composition of the solution aggregates), strongly indicates a difference in composition between the aggregates present in solution and those on the surface. Thus, weakly charged aggregates are likely present on the edges, whereas chains with no or hardly any surfactant may be adsorbed on the siloxane plates. In general, the charged complexes prefer the solution over the surface.

Mixed adsorption of systems consisting of non-adsorbing PVP and adsorbing surfactant^{18-20,23} onto metal oxides show PVP adsorption curves with shapes comparable to the ones we observe, i.e. an increase in adsorption followed by a decrease. However, synergistic effects are much more pronounced if metal oxides are used as the adsorbent^{18,20} since pure PVP does not adsorb on those surfaces (except for silica), whereas it does adsorb on kaolinite.

4.3.3.2 Effect of the electrolyte concentration

Figures 4.4 and 4.5 show the influence of the electrolyte concentration on the mixed adsorption at pH = 5 and pH = 8, respectively, at an initial PVP concentration of 0.15 g l^{-1} . At pH = 5 the adsorption of PVP decreases with increasing NaCl concentration over the entire concentration range and the synergistic effect in the PVP adsorption at low SDBS concentrations is absent at 10^{-1} M NaCl. The SDBS curves show an intersection point around 1.0 mmol l^{-1} SDBS. Electrolytes promote SDBS adsorption below this concentration but counteracts adsorption above it.

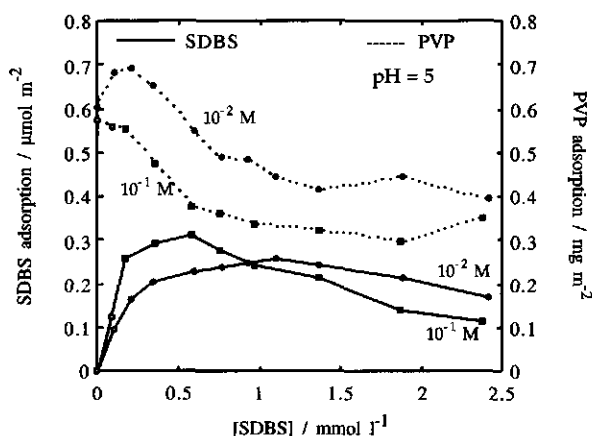


Figure 4.4: Effect of electrolytes on the mixed adsorption of PVP and SDBS on kaolinite: ■: 10^{-1} M NaCl; ●: 10^{-2} M NaCl; pH = 4.9-5.1, $[\text{PVP}]_0 = 0.15 \text{ g l}^{-1}$; open symbols indicate samples which settled within 30 minutes.

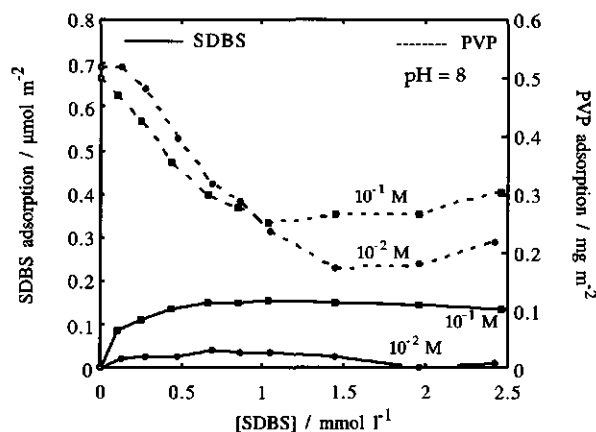


Figure 4.5: Effect of electrolytes on the mixed adsorption of PVP and SDBS on kaolinite: ■: 10^{-1} M NaCl; ●: 10^{-2} M NaCl; pH = 7.8-8.0, $[PVP]_0 = 0.15 \text{ g l}^{-1}$; open symbols indicate samples which settled within 30 minutes.

The adsorption pattern at pH = 8 differs from that at pH = 5 for both components. The main differences are that at high pH the PVP curves cross at 1 mmol l^{-1} SDBS, whereas over the entire surfactant range the SDBS adsorption is substantially higher in 10^{-1} M than in 10^{-2} M NaCl.

Before explaining these observations directly, a few remarks about the action of electrolytes are made. Electrolytes screen charges. This means that both the influence of electrostatic attractions and repulsions is suppressed at increased electrolyte concentrations. Non-electrostatic interactions are not affected by electrolytes, which makes these species suitable as a diagnostic tool.

With this in mind, it is useful to look at figure 4.5, since at pH = 8 both edges and plates are negatively charged. Enhanced screening (of both surfactant-surface and surfactant-surfactant interactions) has increased the SDBS adsorption over the entire concentration range. The adsorption of PVP at low surfactant content is reduced by electrolytes due to a decreased number of edge hydroxyl groups (chapter 2). At higher SDBS concentrations, adsorption of polymer-surfactant aggregates is enhanced in 10^{-1} M NaCl. The intersecting PVP-curves display therefore

the counteracting influence of electrolytes on the features dominating the adsorption process, i.e. hydrogen bonding at low surfactant concentrations and coulombic repulsion at increased surfactant concentrations.

The patchwise heterogeneous character of the clay particles must be taken into account to explain the behaviour of the mixed adsorption isotherms at pH = 5 (figure 4.4). Increasing the electrolyte concentration has opposite consequences for coulombic interactions on edges and plates, i.e. adsorption at the edges is reduced, whereas that on the plates is enhanced. The overall effect of an increased electrolyte concentration is determined by a sum of these two features. Since the adsorbed amount of PVP is lower in 10^{-1} M NaCl over the entire surfactant concentration range, it can be concluded that the enhanced adsorption at the plates is dominated by the reduced coulombic attraction between complexes and the edges. This is also inferred from the trends of the SDBS-curves at high surfactant content. Opposite trends are observed at low surfactant content, likely because weakly charged aggregates may well adsorb on the plates, whereas this is not possible anymore for highly charged complexes.

From the trends caused by an increase in the electrolyte concentration, it may be concluded that polymer-surfactant aggregates are present on the surface. In addition to the conclusions drawn on the composition of the surface aggregates in section 4.3.3.1, we suggest that with increasing electrolyte concentration, the composition of these aggregates increasingly resembles that of the complexes present in solution. Indications stem from figure 4.5, which shows an increased number of adsorbed surfactant molecules per gram of adsorbed polymer at increased electrolyte concentration.

In addition to the above-mentioned origin of the decreased PVP adsorption in region (ii), it should be noted that the conformation of an adsorbed uncharged polymer and an adsorbed polyelectrolyte differs. Uncharged PVP chains adsorb with loops and tails whereas charged PVP/SDBS complexes adopt a more stretched conformation⁴⁶, which is accompanied by a decreased adsorption. This feature may play a role but

cannot be a dominating factor since the decrease in the adsorbed amounts of PVP in region (ii) is roughly equal at both electrolyte concentrations.

4.3.3.3 Effect of the amount of polymer

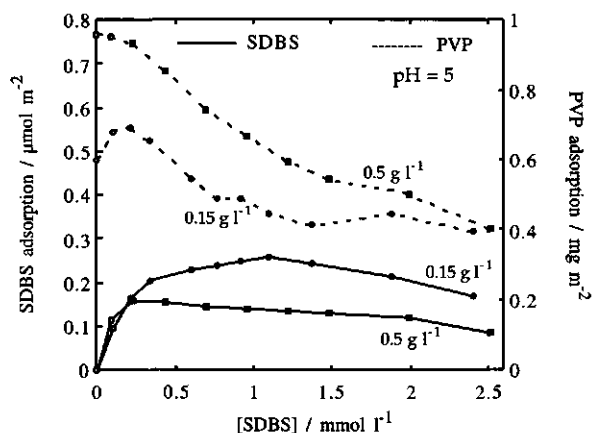


Figure 4.6: Effect of the initial amount of polymer on the mixed adsorption of PVP and SDBS on kaolinite: 10^{-2} M NaCl; pH = 4.9-5.1; ■: $[PVP]_0 = 0.50 \text{ g l}^{-1}$, ●: $[PVP]_0 = 0.15 \text{ g l}^{-1}$; open symbols indicate samples which settled within 30 minutes.

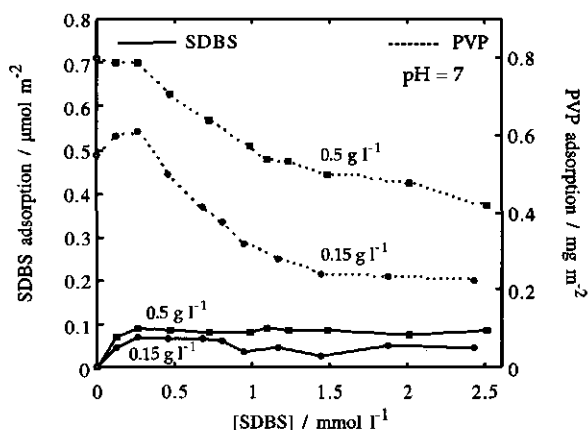


Figure 4.7: Effect of the initial amount of polymer on the mixed adsorption of PVP and SDBS on kaolinite: 10^{-2} M NaCl; pH = 6.8-7.0; ■: $[PVP]_0 = 0.50 \text{ g l}^{-1}$, ●: $[PVP]_0 = 0.15 \text{ g l}^{-1}$; open symbols indicate samples which settled within 30 minutes.

Figures 4.6 and 4.7 show the influence of the initial polymer concentration on the mixed adsorption at pH = 5 and 7, respectively, at 10^{-2} M NaCl. The PVP adsorption from the mixture always increases with polymer content. It is roughly constant until $[SDBS] = 0.3 \text{ mmol l}^{-1}$ and considerably decreases at higher surfactant concentrations. At pH = 5, the PVP adsorption curves approach each other at high surfactant concentrations, whereas at pH = 7, the difference remains roughly 0.2 mg m^{-2} over the entire measured surfactant range. The SDBS adsorption at pH = 7 is slightly higher in the case of $[PVP]_0 = 0.5 \text{ g l}^{-1}$, whereas at pH = 5 the SDBS adsorption reaches a significantly higher value at the lower polymer content.

The discussion focuses now on new aspects. The absence of a synergistic PVP adsorption at low surfactant content at $[PVP]_0 = 0.5 \text{ g l}^{-1}$ is likely because the plateau adsorption of PVP was reached at this concentration (figure 4.1a). To understand the difference in behaviour of the PVP curves at pH = 5 and 7, one should realise that two physical quantities differ between these curves, i.e. the surface charge of the edges (due to differences in pH) and the average charge of the complexes per monomer (due to differences in the initial polymer concentration). The last feature is inferred from figure 4.2. The SDBS concentration at which PVP is saturated with surfactant in bulk solution, depends on the initial amount of polymer. Figure 4.2 shows that in the case of $[PVP]_0 = 0.15 \text{ g l}^{-1}$ saturation takes place around $[SDBS] = 1.8 \text{ mmol l}^{-1}$, whereas this is approximately 4.0 mmol l^{-1} of SDBS at $[PVP]_0 = 0.5 \text{ g l}^{-1}$. As a result, complexes formed in the case of $[PVP]_0 = 0.15 \text{ g l}^{-1}$ possess, at equal surfactant content, a higher average charge than those formed in $[PVP]_0 = 0.5 \text{ g l}^{-1}$. When this fact is combined with the patchwise charge character of the clay, insight into the observations of figures 4.6 and 4.7 can be obtained.

The adsorption of pure PVP is higher at $[PVP]_0 = 0.5 \text{ g l}^{-1}$ (figure 4.1a). The complexes formed at the lower polymer content have a stronger plate affinity, independent of pH. As a consequence, if only plate adsorption

had to be considered, the differences between the curves would remain constant or even slightly increase. Now consider the edge adsorption. Neutral edges provide no significant coulombic attraction which can mask the trends caused by the plates. Hence, at $\text{pH} = 7$ the PVP curves do not merge with increasing surfactant content. Most of the SDBS adsorbed at this pH is due to electrostatic attraction. At $\text{pH} = 5$ the positively charged edges more strongly attract the complexes formed at $[\text{PVP}]_0 = 0.15 \text{ g l}^{-1}$. As a result, the difference between the PVP curves in figure 4.6 decreases with increasing charge of the complexes. A remarkable accompanying observation of the SDBS adsorption at this pH is the higher adsorbed amount in the case of low polymer content (figure 4.6). We showed already that the SDBS adsorption from a solution containing $[\text{PVP}]_0 = 0.15 \text{ g l}^{-1}$ was mainly governed by charge compensation of the edges (figure 4.3 with discussion). Obviously, this is not the case anymore if more polymer is present. Since the major part of the surfactant molecules are aggregated in condensed structures on a polymer chain, this is most likely due to steric reasons, i.e. the number of complexes required for charge compensation need more area than the surface is able to offer. In other words, the edge aggregates are not able to contain more surfactant molecules than actual complexes in solution. At $\text{pH} = 7$ there are less positive charges present at the edges, which can therefore be easily compensated by surface complexes.

For the plateau adsorption of pure PVP on kaolinite, we proposed a model discriminating between edges and plates (chapter 2). Adsorption on the former is strongly pH -dependent at a level of roughly 0.2 mg m^{-2} at $\text{pH} = 7$. When this compared with the $\Gamma_{\text{PVP}} \approx 0.4 \text{ mg m}^{-2}$, observed at $\text{pH} = 7$, $[\text{PVP}]_0 = 0.5 \text{ g l}^{-1}$ and high surfactant concentrations (figure 4.7), it may be concluded that this amount cannot be completely adsorbed on the edges. Hence, it is likely that the siloxane plates are partly covered by PVP that is hardly associated with SDBS. This again supports the conclusion that the composition of adsorbed species is not imposed by the solution but adjusted to the surface characteristics.

4.4 Conclusions

The mixed adsorption of PVP and SDBS on kaolinite is a very complex process, governed by various interactions between the polymer, the surfactant and the clay, and further complicated by its patchwise surface heterogeneity. The overall result depends on the pH, the electrolyte concentration, and the amounts of polymer and surfactant. Studying the results of the variation of these parameters yields valuable information about the adsorption mechanisms and the surface types onto which adsorption takes place. In this way, a fairly detailed picture can be constructed.

In the absence of polymer, SDBS adsorbs both by electrostatic and hydrophobic interactions. In the case of a polymer-surfactant mixture, surfactant adsorption is in 10^{-2} M NaCl mainly determined by charge compensation at the edges. At increased electrolyte concentration, adsorption of weakly charged aggregates or single molecules takes place by hydrophobic interactions.

PVP adsorption from the mixture shows similar behaviour under different conditions. With increasing surfactant concentration initially a small increase in the adsorbed amount is observed, followed by a strong decrease and finally flattening off to a plateau. These three regions can be related to the actual species present in the solution and reflect the changing character of charge of the polymer-surfactant complexes with increasing surfactant concentration. This change induces a difference in the adsorption mechanism, from dominated by hydrogen bonding and hydrophobic interactions for uncharged polymers, to electrostatic control for highly charged complexes. A small amount of polymer, without or with hardly any surfactant associated to it, adsorbs on the siloxane plates by hydrophobic interactions.

Over the entire surfactant concentration range, polymer-surfactant aggregates are adsorbed at the edges. The composition of these complexes differs from that in solution, and is controlled by the surface charge.

References

- 1 I. P. Robb, in *Anionic Surfactants, Surfactant Science Series; Vol. 11*, edited by E. H. Lucassen-Reynders, Marcel Dekker, New York (1981), 109.
- 2 E. D. Goddard, *Colloids Surf.* **19**, 255 (1986).
- 3 K. Hayakawa and J. C. T. Kwak, in *Cationic Surfactants, Surfactant Science Series; Vol. 37*, edited by D. N. Rubingh and P. M. Holland, Marcel Dekker, New York (1991), 189.
- 4 J. C. Brackman and J. B. F. N. Engberts, *Chem. Soc. Rev.* **22**, 85 (1993).
- 5 B. Lindman and K. Thalberg, in *Interactions of Surfactants with Polymers and Proteins*, edited by E. D. Goddard and K. P. Ananthapadmanabham, CRC Press, Boca Raton (1993), 203.
- 6 P. Hansson and B. Lindman, *Current Opinion Colloid Interface Sci.* **1**, 604 (1996).
- 7 M. Kawaguchi and A. Takahashi, *Adv. Colloid Polym. Sci.* **37**, 219 (1992).
- 8 G. J. Fleer, M. A. Cohen Stuart, J. M. H. M. Scheutjens, T. Cosgrove, and B. Vincent, *Polymers at Interfaces*, Chapman & Hall, London (1993) .
- 9 L. K. Koopal, in *Coagulation and Flocculation, Surfactant Science Series; Vol. 47*, edited by B. Dobias, Marcel Dekker, New York (1993), 101.
- 10 K. P. Ananthapadmanabhan, in *Interaction of Surfactants with Polymers and Proteins*, edited by E. D. Goddard and K. P. Ananthapadmanabhan, CRC Press, Boca Raton (1993), 5.
- 11 H. Otsuka and K. Esumi, in *Structure-performance Relationships in Surfactants, Surfactant Science Series; Vol. 70*, edited by K. Esumi and M. Ueno, Marcel Dekker, New York (1997), 507.
- 12 J. Ghodbane and R. Denoyel, *Colloids Surf. A: Physicochem. Eng. Aspects* **127**, 97 (1997).
- 13 N. V. Sastry, J.-M. Sequaris, and M. J. Schwuger, *J. Colloid Interface Sci.* **171**, 224 (1995).
- 14 M. Sjöberg, L. Bergström, A. Larsson, and E. Sjöström, *Colloids Surf. A: Physicochem. Eng. Aspects* **159**, 197 (1999).
- 15 K. Esumi and M. Oyama, *Langmuir* **9**, 2020 (1993).
- 16 K. Esumi, A. Masuda, and H. Otsuka, *Langmuir* **9**, 284 (1993).

- 17 I. Rachas, Th. F. Tadros, and P. Taylor, *Colloids Surf. A: Physicochem. Eng. Aspects* **161**, 307 (2000).
- 18 C. Ma and C. Li, *J. Colloid Interface Sci.* **131**, 485 (1989).
- 19 H. Otsuka, K. Esumi, T. A. Ring, J.-T. Li, and K. D. Caldwell., *Colloids Surf. A: Physicochem. Eng. Aspects* **116**, 161 (1996).
- 20 H. Otsuka and K. Esumi, *Langmuir* **10**, 45 (1994).
- 21 C. Ma, *Colloids Surf.* **16**, 185 (1985).
- 22 K. Esumi, Y. Takaku, and H. Otsuka, *Langmuir* **10** (1994).
- 23 K. Esumi, K. Sakai, K. Torigoe, T. Suhara, and H. Fukui, *Colloids Surf. A: Physicochem. Eng. Aspects* **155**, 413 (1999).
- 24 D. J. Neivandt, M. L. Gee, C. P. Tripp, and M. L. Hair, *Langmuir* **13**, 2519 (1997).
- 25 B. M. Moudgil and P. Somasundaran, *Colloids Surf.* **13**, 87 (1985).
- 26 E. S. Pagac, D. C. Prieve, and R. D. Tilton, *Langmuir* **14**, 2333 (1998).
- 27 K. Esumi, M. Iitaka, and Y. Koide, *J. Colloid Interface Sci.* **208**, 178 (1998).
- 28 J. Wang, B. Han, H. Yan, Z. Li, and R. K. Thomas, *Langmuir* **15**, 8207 (1999).
- 29 H. van Olphen, *An Introduction to Clay Colloid Chemistry*, second ed., Wiley-Interscience, (1977) .
- 30 T. M. Herrington, A. Q. Clarke, and J. C. Watts, *Colloids Surf.* **68**, 161 (1992).
- 31 B. Braggs, D. Fornasiero, J. Ralston, and R. S. Smart, *Clays Clay Miner.* **42**, 123 (1994).
- 32 P. V. Brady, R. T. Cygan, and K. L. Nagy, *J. Colloid Interface Sci.* **183**, 356 (1996).
- 33 T. Mehrian, A. de Keizer, and J. Lyklema, *Langmuir* **7**, 3094 (1991).
- 34 T. Mehrian Isfahany, Thesis, Wageningen Agricultural University, 1992.
- 35 H. S. Hanna and P. Somasundaran, *J. Colloid Interface Sci.* **70**, 181 (1979).
- 36 J. F. Scamehorn, R. S. Schechter, and W. H. Wade, *J. Colloid Interface Sci.* **85**, 463 (1982).
- 37 K. P. Ananthapadmanabhan and P. Somasundaran, *Colloids Surf.* **77**, 105 (1983).
- 38 P. A. Siracusa and P. Somasundaran, *J. Colloid Interface Sci.* **114**, 184 (1986).
- 39 P. A. Siracusa and P. Somasundaran, *J. Colloid Interface Sci.* **120**, 100 (1987).
- 40 P. A. Siracusa and P. Somasundaran, *Colloids Surf.* **26**, 55 (1987).
- 41 W. A. House and I. S. Farr, *Colloids Surf.* **40**, 167 (1989).
- 42 J. E. Poirier and J. M. Cases, *Colloids Surf.* **55**, 333 (1991).

- 43 J. R. Marchesi, W. A. House, G. F. White, N. J. Russell, and I. S. Farr, *Colloids Surf.* **53**, 63 (1991).
- 44 B. Alince and T. G. M. v. d. Ven, *J. Colloid Interface Sci.* **155**, 465 (1993).
- 45 R. S. Chow, *Colloids Surf.* **61**, 241 (1991).
- 46 J. Lyklema, *Fundamentals of Interface and Colloid Science, Vol. II*, Academic Press, London (1995) Chapter 5, section 2.

Chapter 5

Cellulose Films as Model Systems for Adsorption Studies

Abstract

A thick cellulose film can be produced by chemical regeneration of trimethylsilyl cellulose. The TMSC-films are produced by the spincoating technique which gives reproducible, rapidly prepared films with a reasonable smoothness. Stability against detachment in water is provided by a PVP-PS block copolymer which anchors the TMSC-film on a hydrophilic substrate. The films are characterized by their thickness, roughness, stability, swelling behaviour, charge and wetting properties. They are reasonable smooth, amorphous in nature, slightly charged and rather hydrophilic. The adsorption properties resemble those of ordinary cellulose surfaces. Clearly, a cellulose surface has been obtained that shows good promises for model adsorption studies.

5.1 Introduction

Cellulose is a major constituent of wood, plant material, and cotton, with applications in amongst others the paper and textile industry. Interactions between cellulose and several other components are of great practical relevance. Much research has been addressed to its adsorption properties, i.e. the adsorption of water-soluble cellulose derivatives at solid/liquid interfaces¹⁻⁹ and the adsorption of a variety of adsorbates on cellulose-like surfaces¹⁰⁻¹⁷. For such surfaces, most of the obtained results are very difficult to compare, since the cellulose surfaces are often not well defined, differing greatly in chemical composition, topology, and crystallinity. Despite its abundance, there is less systematic knowledge about cellulose surfaces than, for example, about those of mineral oxides.

A main problem with cellulose lies in obtaining smooth, well defined, and stable surfaces. In recent years, several groups have tried to overcome this problem. Neumann et al.¹⁸ spincoated cellulose layers from a trifluoroacetic acid (TFA) solution on mica and used them in a surface force apparatus. The cellulose layers thus obtained in this way were not very stable and probably had some dangling tails protruding in solution which strongly influenced their behaviour. Wegner's group^{19,20} solved these problems. They hydrophobized cellulose by hexamethyldisilazane (HMDS) into trimethylsilyl cellulose (TMSC). This product can either be spun in an aqueous acid to obtain fibres, or deposited on a solid substrate to obtain films which are subsequently regenerated into cellulose. Deposition was carried out by the Langmuir-Blodgett technique. The resulting films were more smooth and more stable than those obtained by spincoating²¹. A disadvantage of the Langmuir-Blodgett technique is that it is very time consuming when thick films are needed: every layer has to be brought up separately.

In this chapter the rapid preparation of stable cellulose films by a combination of the above-mentioned techniques is reported. Use is made of the speed of the spincoating technique and the procedure of Wegner. To reduce roughness and stability problems, a block copolymer is used to

anchor the cellulose films onto the substrate. The produced films will be characterized by their thickness, roughness, stability, swelling behaviour, charge, and wetting properties. To investigate whether these films can be used as model substrates for cellulose surfaces, three different polymers and two surfactants will be adsorbed on the films.

5.2 Experimental

5.2.1 Chemicals

Silicon wafers with a native oxide layer of 2-3 nm were purchased from Aurel (Germany). Trimethylsilyl cellulose (TMSC) was synthesized according to a procedure described by Stein²² and analyzed by NMR and IR spectroscopy. Starting material for the synthesis was microcrystalline cellulose from Sigma (Sigmacell type 20) which was used as received. Polystyrene-*b*-poly(4-vinylpyridine) (PS-*b*-P4VP), the anchoring polymer, was purchased from Polymer Source, Inc. (Canada) which had number average molecular masses (M_n) of $21.4 \cdot 10^3 \text{ g mol}^{-1}$ and $20.7 \cdot 10^3 \text{ g mol}^{-1}$ for the PS and PVP parts, respectively.

The polymers poly(vinylpyrrolidone) (PVP, $M_n = 17.4 \cdot 10^3 \text{ g mol}^{-1}$, BASF), poly(ethyleneglycol) (PEG, $M_n = 15 \cdot 10^3 \text{ g mol}^{-1}$, Fluka), and sodium carboxymethylcellulose (NaCMC, $M_n = 600 \cdot 10^3 \text{ g mol}^{-1}$, AKZO Nobel) and the surfactants hepta-ethyleneglycol mono *n*-dodecylether ($C_{12}E_7$, Nikko Chemicals, Japan) and sodium dodecylbenzenesulphonate (SDBS, Fluka) were all used as received. Electrolytes were all of analytical grade. Water was purified by passing it through two mixed-bed ion exchangers, a carbon column and a microfilter.

5.2.2 Preparation of the films

Silicon wafers were thoroughly cleaned with demineralized water and put in a plasma cleaner (Harrick Scientific Corp., model PDC-32G) for 45 seconds. They are exposed to a 100 ppm PS-*b*-P4VP solution in chloroform for 30 minutes, rinsed with fresh chloroform and dried with nitrogen. A smooth polymer layer is now adsorbed with PVP segments

bound to the wafer and free PS blocks as anchors (figure 5.1a). A solution of TMSC in chloroform ($[TMSC] = 20 \text{ g l}^{-1}$) is spincoated on these wafers for 20 seconds at 2500 rpm (figure 5.1b). Adequate attachment to the PS blocks is provided by the hydrophobic TMS-groups which are completely wrapped around the cellulose backbone²⁰. Regeneration of the TMSC-film into cellulose is achieved by exposing the films for about 15 min to a gaseous atmosphere of a 10% HCl solution (figure 5.1c). After this exposure time, no further changes of the refractive index and the film thickness could be observed. This is however a much longer time than the 30 seconds reported by Buchholz et al.¹⁹, who prepared ultrathin films with a thickness of a few nm. Our films are much thicker so likely the HCl molecules need more time to reach and cleave the TMS-groups. The completion of the regeneration of cellulose was tested on the absence Si-peaks by infrared spectroscopy. After an experiment the silicon strips with the bound film can be cleaned as described above and recycled, i.e. new block copolymer and TMSC-layers can subsequently be brought up and regenerated.

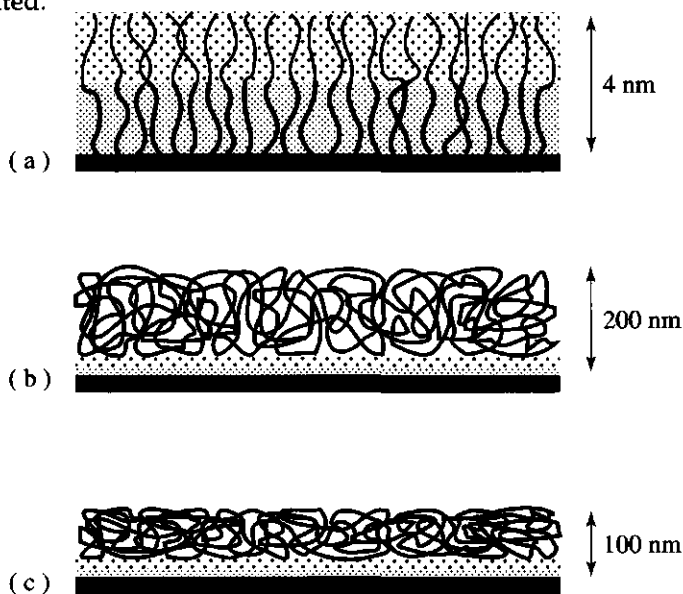


Figure 5.1: Schematic picture of the preparation of the cellulose films: (a): adsorption of PS-b-P4VP on Si-wafer, (b): thick TMSC-layer spincoated on the PS blocks, (c): regeneration of TMSC into cellulose thereby releasing hydrophobic TMS-groups.

5.2.3 Methods

The refractive index and the thickness of every cellulose layer is quantitatively determined by computer-controlled null **ellipsometry** (Sentech SE-400). This technique determines polarization changes occurring at oblique reflection of polarized light from a surface^{23,24}. From the complex reflection coefficients r_p and r_s of the parallel (p) and perpendicular (s) components of the light beam, the ellipsometrical angles Ψ and Δ can be determined by $r_p/r_s = \tan \Psi \exp(i\Delta)$. The mentioned optical properties of the layer can be calculated from these angles assuming a layer model consisting of a series of homogeneous, flat layers. Comparison between measurements carried out in air and in aqueous solutions offer the possibility to study the extent of swelling of the cellulose layer.

Static contact angles (θ) are determined by a Sessile Drop Tensiometer (SDT 200, IT concept). A droplet is formed and deposited onto a solid cellulose surface. For a system consisting of a drop of liquid on a smooth surface in equilibrium with a vapour phase, the contact angle and the surface tensions acting between the different phases, are related by Young's equation²⁵:

$$\gamma_{lv} \cos \theta = \gamma_{sv} - \gamma_{sl} \quad [5.1]$$

where θ is the equilibrium contact angle, and γ_{lv} , γ_{sv} and γ_{sl} are the interfacial tensions of the water/vapour, solid/vapour and solid/water surface, respectively. Combining this equation with the Girifalco-Good expression for γ_{sl} ²⁶, and splitting both γ_{sv} and γ_{lv} into a dispersion and a polar component²⁷, the following equation results^{28,29}:

$$\gamma_{lv}(1 + \cos \theta) = 2\sqrt{\gamma_s^d \gamma_l^d} + \sqrt{\gamma_s^p \gamma_l^p} \quad [5.2]$$

Contact angle measurements of two different liquids with known components γ_l^i , like water and α -bromonaphtalene, provide two equations with two unknowns, i. e. γ_s^d and γ_s^p . The results obtained in this way are sufficient for our purpose. Van Oss²⁹ can be consulted for a discussion of the shortcomings of this concept.

Atomic force microscopy (AFM) is used to investigate the surface roughness of the films. Measurements are carried out on a Digital Instruments Nanoscope III in the contact mode with a spring constant of about 0.58 N m^{-1} using SiN_3 tips. Measurements are carried out both in air (50 - 60% humidity) and in 10^{-2} M NaCl , at room temperature.

Electrokinetic properties of the cellulose surfaces are investigated by **streaming potential experiments** carried out on a home-made apparatus³⁰. In the absence of surface conductance and double layer overlap, and under conditions of laminar flow, streaming potentials can be converted into ζ -potentials according to the Smolukovski equation³¹:

$$\zeta = \frac{E_{\text{str}} \eta K^L}{\epsilon \Delta p} \quad [5.3]$$

where E_{str} is the measured streaming potential, η the viscosity of the liquid medium, K^L the conductivity of the medium, ϵ the dielectric permittivity, and Δp the applied pressure. The linearity between applied pressure and streaming potential was verified up to a pressure maximum of $4.0 \cdot 10^4 \text{ N m}^{-2}$.

Polymer and surfactant adsorption experiments were carried out to relate the observed adsorption characteristics of the cellulose surface to that of commonly used celluloses, i.e. to test whether the surface can be used as a model substrate. These experiments are carried out by **stagnation point flow reflectometry**. This set-up is briefly introduced in chapter 6 and discussed in detail by Dijt et al.^{32,33}. Here, we only recall the equation which is used for the calculation of the adsorbed amount Γ :

$$\Gamma = \frac{\Delta S}{S_0} \frac{1}{A_s} \quad (\text{mg m}^{-2}) \quad [5.4]$$

where ΔS is the output signal, S_0 the initial ratio $\frac{I_{p,0}}{I_{s,0}}$ of the respective parallel and perpendicular intensities of the light beam prior to adsorption, and A_s is a sensitivity factor determined by the optical properties of the layer. It can be calculated by an optical model³⁴ which assumes smooth, homogeneous layers, similarly as for ellipsometry.

5.3 Results and Discussion

5.3.1 Characterization

5.3.1.1 Ellipsometry

The hydrophobic TMSC-films in air are roughly 190 ± 6 nm thick. Such thick layers are desired since in this case the resulting cellulose films are well suited for reflectometry (see section 5.3.2.1). The thickness can be controlled by the concentration of the TMSC-solution during the spincoating process. After regeneration, the thickness decreased to 100 ± 4 nm, almost half the original value. The decrease is comparable to that for the Langmuir-Blodgett films¹⁹ and mainly stems from the loss of mass of the big hydrophobic TMS groups which are hydrolyzed and subsequently transformed into volatile hexamethyldisiloxanes²². Refractive indices yielded 1.460 ± 0.005 for the TMSC film and 1.528 ± 0.003 for the cellulose film, in good agreement with earlier results^{19,21}.

The cellulose film swells when exposed to 10^{-2} M NaCl, resulting in a thickness of 120 ± 8 nm and a refractive index of 1.450 ± 0.005 . To a first approximation, the volume fraction of water ϕ in the swollen cellulose layer can be estimated from the additivity rule:

$$n_{\text{aqueous film}} = \phi n_{\text{H}_2\text{O}} + (1 - \phi) n_{\text{cellulose}} \quad [5.5]$$

which gives $\phi \approx 0.39$. Penetration of water molecules in the film indicates an at least partly amorphous nature of the cellulose layer on the wafer²¹. This is likely since the TMSC-chains do not have much time during the spincoating process to arrange into well organized layers.

5.3.1.2 Contact angle measurements

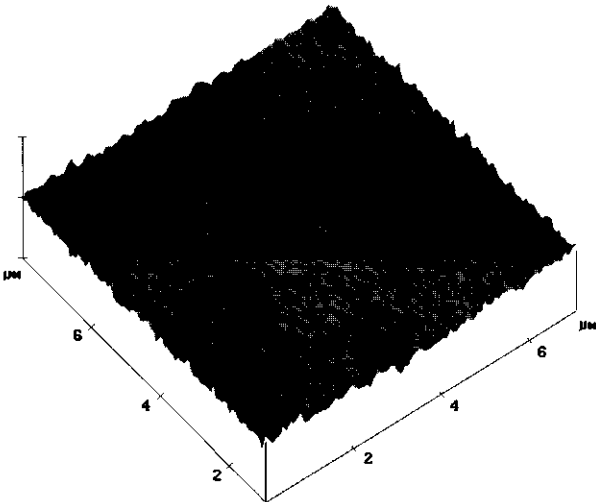
Table 1 shows the measured contact angles on the TMSC-film and the regenerated cellulose film. For cellulose also the calculated surface free energy components are shown. The contact angles against water show regenerated cellulose to be rather hydrophilic. This is confirmed by the surface free energy which possesses both a polar and a dispersion component.

Table 5.1: Contact angles for water and α -bromonaphtalene, and calculated polar and dispersion components of the surface free energies.

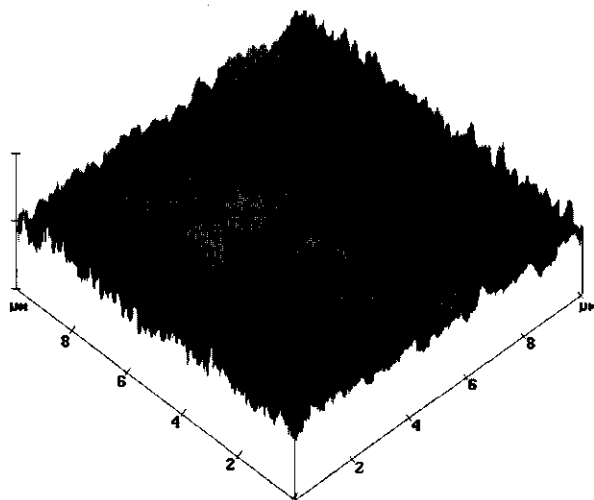
Surface	θ_{water}	$\theta_{\text{Br-Napht}}$	$\gamma_s^p / \text{mJ m}^{-2}$	$\gamma_s^d / \text{mJ m}^{-2}$
TMSC	89.0			
regenerated cellulose	36.4	14.3	24.0	43.0
cellulose in water	22.6	28.0	32.3	39.5
cellophane	19.6	26.6	33.1	40.0

The polar character can be accounted for by surface charges and hydroxyl groups. A hydrophobic nature can be linked with crystalline regions at the surface. The contact angle decreased overnight when the surface was immersed in water (table 5.1). The polar component of the surface free energy drastically increased, whereas the dispersion one changed only little. We suggest that this is due to dissociation of surface groups, which emphasizes the polar character of the cellulose surface. The values are in reasonable agreement with those found for cellophane, confirming our conclusion that the regenerated upper-surface consists of pure cellulose.

5.3.1.3 Atomic Force Microscopy



(a)



(b)

Figure 5.2: AFM pictures of a cellulose film in air (a) and in 10^{-2} M NaCl (b).

Figure 5.2a and b shows oblique AFM pictures of a regenerated cellulose film in air (50–60% humidity) and in 10^{-2} M NaCl, respectively. No big structural defects can be observed.

The root mean square roughness of the dry film is 1.0 nm and its maximum thickness variation compared to a perfectly flat plate is ± 4.6 nm. This is slightly less smooth than the values reported for the corresponding thin LB-films²¹ (i.e. 0.16 nm and 3.64 nm, respectively) and probably comparably smooth as the spincoated films of Neumann et al.¹⁸, although it is not clear how their variation in thickness was defined.

When the films are immersed in 10^{-2} M NaCl for 10 minutes, these properties become 2.5 nm for the root mean square roughness, and ± 9.0 nm for the thickness variation, respectively. Clearly, the roughness increases when the films are exposed to water. This is not surprising, since in air the films are in a collapsed-like state. In contact with water, solvent molecules and/or electrolytes diffuse into the films causing them to swell, leading to an increased roughness. A preferred in-layer organization cannot be observed, probably because the spincoating technique does not allow the chains to find their most favorable conformations. This is in

contrast with the ultrathin LB-films, where the polymer backbones are preferentially oriented parallel to the dipping direction²⁰. For the thicker LB-films, there was little indication for the existence of a preferred orientation²¹.

5.3.1.4 Streaming Potential Measurements

Figure 5.3 shows the ζ -potential of the cellulose surfaces as a function of pH in solutions containing different types and amounts of electrolytes. The isoelectric point (iep) of cellulose is found around pH = 3.8. This corresponds well to the points of zero charge of microcrystalline cellulose, obtained potentiometrically by Van de Steeg¹⁴. Obviously, small monovalent and divalent ions do not specifically adsorb on cellulose. This is in agreement with the observation that monocarboxylic acids only weakly interact with earth-metal cations. The ζ -potential decreases with increasing pH and levels off for pH > 7 reaching -35 mV at [KCl] = 10^{-3} M. This corresponds to an electrokinetic charge of approximately $0.4 \mu\text{C cm}^{-2}$, which makes it far less charged than many well-known oxides^{35,36}.

In the presence of 10^{-3} M NaCl and $3 \cdot 10^{-3}$ M sodium dodecylsulfate (SDS), no iep has been observed. Within the pH range 2-10 the surface remains negatively charged, whereas at pH > 7 no significant differences could be observed between the curves of SDS and KCl. From this, we infer that at low pH, SDS specifically interacts with the cellulose. This interaction vanishes at about pH = 7. The levelling off of the ζ -potential at high pH is surprising, since the surface charge may well be enhanced. Counter-currents could be developed in the vicinity of the interface giving rise to a decrease of the absolute value of the streaming potential, and hence of the ζ -potential. Further insight into the electrokinetic behaviour of the cellulose surfaces may be obtained by surface conduction measurements.

The origin of the surface charge is still under debate. Literature^{37,38} suggests that cellulose is charged over almost the complete pH-range, but this may be due to the presence of hemicelluloses and/or lignin³⁹. By infrared spectroscopy these species have not been identified in our

cellulose. Holmberg et al.²¹ proposed acid hydrolysis of glycoside bonds to occur in the Neumann-films due to the using of TFA as the solvent. The solvent we used (i.e. DMA/LiCl) is milder and is not supposed to lead to any polymer degradation. We assume that the charge arises from some oxidation of the sugar ring into carboxylic acids. The small positive charges observed at $\text{pH} < \text{iep}$ may stem from proton adsorption onto sugar-hydroxyls.

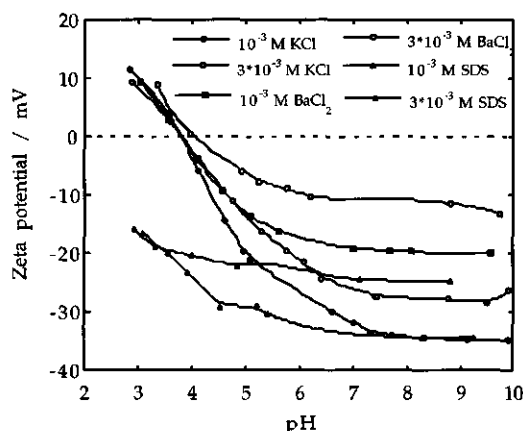


Figure 5.3: ζ -potential of cellulose surfaces as a function of pH in the presence of different types and concentrations of electrolyte; lines are drawn as a guide to the eye.

5.3.2 Adsorption

5.3.2.1 Stability and swelling

Until now, adsorption studies by reflectometry were carried out on mineral oxides^{40,41} or polystyrene^{7,42}. None of these surfaces swells in aqueous solutions. However, cellulose films do swell which leads to a change in the optical properties of the surface layers and hence to a change in the sensitivity factor A_s (equation [5.4]). In order to estimate the influence of swelling on the calculated adsorbed amount, sensitivity factors are calculated by the method of Hansen³⁴. These factors are determined for both a dry cellulose layer ($n_{\text{cell}} = 1.53$) and a swollen layer ($n_{\text{cell}} = 1.45$) as a function of its thickness. In figure 5.4, inverse sensitivity factors are calculated as a function of the thickness of the layer. The optical

properties of the adsorbing layer which are used in the calculation, are typical values for a nonionic surfactant (see the legend of figure 5.4). The results show a considerable difference in A_s^{-1} for a dry and a swollen layer. For a correct determination of the adsorbed amount, it is therefore necessary to use the thickness and refractive index of a swollen layer.

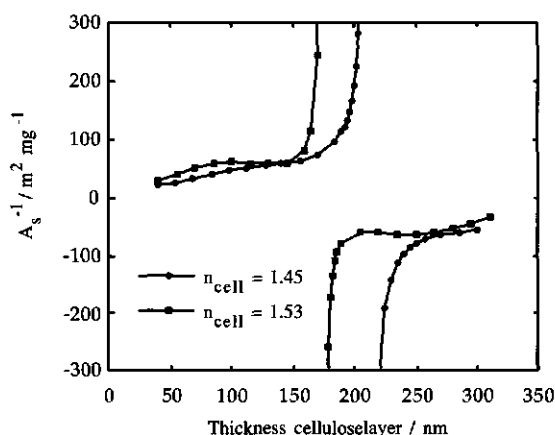


Figure 5.4: Inverse sensitivity factors as a function of the thickness of the cellulose layer at two refractive indices: $n_{\text{cell}} = 1.45$ corresponds to a swollen layer, $n_{\text{cell}} = 1.53$ corresponds to a dry layer. Used model parameters: $n_{\text{Si}} = 3.85$, $n_{\text{PVP-PS}} = 1.46$, $d_{\text{PVP-PS}} = 6$ nm, $n_{\text{NIO}} = 1.45$, $d_{\text{NIO}} = 4$ nm, $dn/dc = 0.135$, referring to an optical five-layer model (silicon, block-copolymer, cellulose, nonionic surfactant, water; a 2 nm SiO_2 -layer is accounted for with the block copolymer layer ($n_{\text{SiO}_2} = 1.46$)).

Furthermore, figure 5.4 shows that for a swollen layer, a thickness in the range 110-150 nm is most suitable, yielding good sensitivity for the output signal³³ whereas small thickness variations do not drastically change A_s^{-1} in this region. We therefore prefer to use films with a swollen layer thickness of roughly 120 nm (see section 5.3.1.1). The singularities observed in figure 5.4 are caused by the fact that $d(R_p/R_s)$ of the parallel and perpendicular reflectivities approaches zero³³, thereby losing all sensitivity.

If anchoring with the block copolymer was omitted, a strong decrease in the output signal with time was observed, indicating detachment of the layer from the wafer. Within roughly 30 minutes, there was hardly any

cellulose left. In the case of anchoring the layer with a block copolymer, stability problems were not observed in any experiment.

5.3.2.2 Polymer adsorption

Figure 5.5 shows typical adsorption measurements as a function time of the uncharged polymers PVP and PEG and the polyelectrolyte NaCMC on the cellulose films. Hardly any adsorption could be detected for the nonionic polymers. This is in line with our observations that PVP and PEG neither adsorbed on microcrystalline cellulose particles (Sigmacell type 20) nor on pre-washed cotton swatches (results not shown), although both polymers are able to interact with certain surface hydroxyl groups^{43,44}. Ishimaru and Lindström¹⁰ did find adsorption of PVP onto unbleached kraft pulp and groundwood pulp, but not onto bleached kraft pulp, where in the bleaching process lignin and hemicelluloses are removed. Therefore, these species were held responsible for adsorption which probably took place by specific interactions between proton-accepting groups of the polymers and phenolic structures present in lignin. Our results are in line with the absence of these species in our cellulose sample.

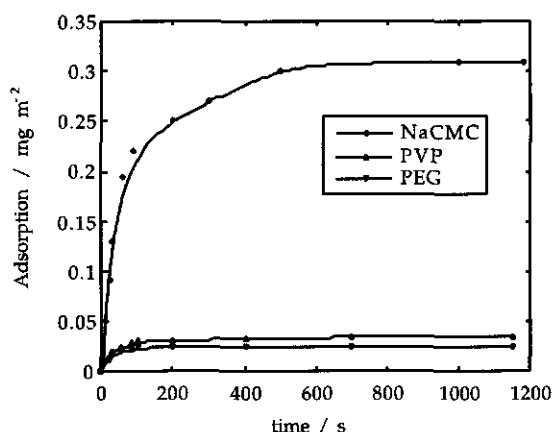


Figure 5.5: Evolution of the adsorbed amount of polymer with time; [NaCMC] = 100 ppm, $I = 10^{-1}$ M NaCl, pH = 4.0; [PVP] = 100 ppm, $I = 10^{-2}$ M NaCl, pH = 5.0; [PEG] = 100 ppm, $I = 10^{-2}$ M NaCl, pH = 5.0.

In contrast to the nonionic polymers, NaCMC does adsorb at the cellulose surface in 10^{-1} M NaCl leading to a clear plateau with a reasonable adsorbed amount. The fact that NaCMC adsorbs on cellulose is known for a long time, think only of its use as an antiredeposition agent in detergency⁴⁵. The likely reason for adsorption is the close molecular resemblance between adsorbent and adsorbate. The electrolyte concentration of 10^{-2} M NaCl apparently screens the charge-charge repulsion sufficiently.

5.3.2.3 Surfactant adsorption

Figure 5.6 shows typical evolutions of the adsorption of an anionic and a nonionic surfactant on the cellulose film with time. For both surfactants, the concentration is about one third of their CMC. SDBS and $C_{12}E_7$ readily adsorb on cellulose showing well-defined plateau values. The adsorption of SDBS has been reported before⁴⁶.

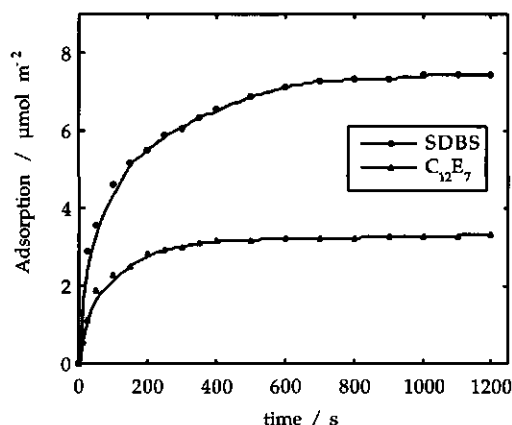


Figure 5.6: Typical evolutions of the adsorption of surfactants with time; $[\text{SDBS}] = 2.4 \cdot 10^{-4}$ M, $[\text{C}_{12}\text{E}_7] = 2.7 \cdot 10^{-5}$ M; pH = 5.0, $I = 10^{-2}$ M NaCl.

It is noted that C_nE_m molecules do adsorb on cellulose (already observed some time ago⁴⁷), whereas the polymer PEG does not. Apparently, the aliphatic chains are essential in the adsorption process. For a detailed discussion on the adsorption of nonionic surfactants on cellulose, see

chapter 6. For the purpose of this paper, it is sufficient to note that the results of the polymer and surfactant adsorption show that the films mimic the behaviour of typical cellulose surfaces, and thus that they can be used as a representative.

5.4 Conclusions

A thick cellulose film can be produced by chemical regeneration of trimethylsilyl cellulose. The TMSC-films are produced by the spincoating technique which gives reproducible, rapidly prepared films with a reasonable smoothness. Stability against detachment in water is provided by a PVP-PS block copolymer which anchors the TMSC-layer on a hydrophilic substrate. Characterization of the final film proved its cellulose-like nature. The cellulose film is amorphous in nature, slightly charged and has both hydrophilic and hydrophobic surface characteristics. The adsorption properties resemble those of ordinary cellulose surfaces. Clearly, a cellulose surface has been obtained that shows good promises for model adsorption studies.

Acknowledgements

Dr. C. G. Geffroy is greatly acknowledged for pioneering work in the development of the cellulose films. Mr. J. H. Maas is acknowledged for performing the AFM-measurements.

References

- 1 P. A. Williams, R. Harrop, G. O. Philips, G. Pass, and I. D. Robb, *J. Chem. Soc., Faraday Trans. I* **78**, 1733 (1982).
- 2 M. Malmsten and B. Lindman, *Langmuir* **6**, 357 (1989).
- 3 M. Huldén and E. Sjöblom, *Prog. Colloid Polym. Sci.* **82**, 8 (1990).
- 4 E. P. G. Arêas and F. Galembeck, *J. Colloid Interface Sci.* **147**, 370 (1991).
- 5 V. Shubin, *Langmuir* **10**, 1093 (1994).
- 6 Y. Yamanaka and K. Esumi, *Colloid Surf. A: Physicochem. Eng. Aspects* **122**, 121 (1997).

- 7 M. A. Cohen Stuart, R. G. Fokkink, P. M. van der Horst, and J. W. T. Lichtenbelt, *Colloid Polym. Sci.* **276**, 335 (1998).
- 8 C. W. Hoogendam, I. Derks, A. de Keizer, M. A. Cohen Stuart, and B. H. Bijsterbosch, *Colloids Surf. A: Physicochem. Eng. Aspects* **144**, 245 (1998).
- 9 C. W. Hoogendam, A. de Keizer, M. A. Cohen Stuart, B. H. Bijsterbosch, J. G. Batelaan, and P. M. van der Horst, *Langmuir* **14**, 3825 (1998).
- 10 Y. Ishimaru and T. Lindström, *J. Appl. Polym. Sci.* **29**, 1675-1691 (1984).
- 11 L. Winter, L. Wågberg, L. Ödberg, and T. Lindström, *J. Colloid Interface Sci.* **111**, 537 (1986).
- 12 L. Wågberg, L. Winter, L. Ödberg, and T. Lindström, *Colloids Surf. A: Physicochem. Eng. Aspects* **27**, 163 (1987).
- 13 L. Wågberg, L. Winter, T. Lindström, and R. Aksberg, *J. Colloid Interface Sci.* **123**, 287 (1988).
- 14 H. G. M. van de Steeg, A. de Keizer, M. A. Cohen Stuart, and B. H. Bijsterbosch, *Colloids Surf. A: Physicochem. Eng. Aspects* **70**, 77 (1993).
- 15 H. G. M. van de Steeg, A. de Keizer, M. A. Cohen Stuart, and B. H. Bijsterbosch, *Colloids Surf. A: Physicochem. Eng. Aspects* **70**, 91 (1993).
- 16 L. M. Ilharco, A. R. Garcia, J. L. da Silva, M. J. Lemos, and L. F. V. Ferreira, *Langmuir* **13**, 3787 (1997).
- 17 M. Müller, I. Grosse, H. J. Jacobatsch, and P. Sams, *Tenside Surf. Det.* **35**, 354 (1998).
- 18 R. D. Neumann, J. M. Berg, and P. M. Claesson, *Nord. Pulp Paper Res. J.* **8**, 96 (1993).
- 19 V. Buchholz, G. Wegner, S. Stemme, and L. Ödberg, *Adv. Mater.* **8**, 399 (1996).
- 20 M. Schaub, G. Wenz, G. Wegner, A. Stein, and D. Klemm, *Adv. Mater.* **5**, 919 (1993).
- 21 M. Holmberg, J. Berg, S. Stemme, L. Ödberg, J. Rasmusson, and P. Claesson, *J. Colloid Interface Sci.* **186**, 369 (1997).
- 22 A. Stein, Thesis, University of Jena, 1991.
- 23 R. M. Azzam and N. M. Bashara, *Ellipsometry and Polarized Light*, Elsevier Science, Amsterdam (1989) .
- 24 H. G. Tompkins, *A User's Guide to Ellipsometry*, Academic Press, New York (1993) .

- 25 P. C. Hiemenz and R. Rajagopalan, *Principles of Colloid and Surface Chemistry*, third ed., Marcel Dekker, New York (1997) Chapter 6.
- 26 R. J. Good and L. A. Girifalco, *J. Phys. Chem.* **64**, 561 (1960).
- 27 F. M. Fowkes, *Ind. Eng. Chem.* **56**, 40 (1964).
- 28 D. K. Owens and R. C. Wendt, *J. Appl. Polym. Sci.* **13**, 1741 (1969).
- 29 C. J. van Oss, *Interfacial forces in aqueous media*, Marcel Dekker, New York (1994) Chapter IX.
- 30 A. J. van der Linde and B. H. Bijsterbosch, *Colloids Surf.* **41**, 345 (1989).
- 31 J. Lyklema, *Fundamentals of Interface and Colloid Science, volume II: Solid-Liquid Interfaces, Vol. II*, Academic Press, London (1995) Chapter 4, 28.
- 32 J. C. Dijt, M. A. Cohen Stuart, J. E. Hofman, and G. J. Fleer, *Colloids Surf.* **51**, 141 (1990).
- 33 J. C. Dijt, M. A. Cohen Stuart, and G. J. Fleer, *Adv. Colloid Interface Sci.* **50**, 79 (1994).
- 34 W. N. Hansen, *J. Optical Soc. Am.* **58**, 380 (1968).
- 35 R. J. Hunter, *ζ -potential in Colloid Science*, Academic Press, London (1988).
- 36 J. Lyklema, *Fundamentals of Interface and Colloid Science, volume II: Solid-Liquid Interfaces*, Academic Press, London (1995) Chapter 2, 75.
- 37 T. M. Herrington and B. R. Midmore, *J. Chem. Soc., Faraday Trans. I* **80**, 1525 (1984).
- 38 J. Budd and T. M. Herrington, *Colloids Surf.* **36**, 273 (1989).
- 39 E. Sjöström, *Nord. Pulp Paper Res. J.* **4**, 90 (1989).
- 40 N. G. Hoogeveen, M. A. Cohen Stuart, and G. J. Fleer, *J. Colloid Interface Sci.* **182**, 133 (1996).
- 41 H. D. Bijsterbosch, M. A. Cohen Stuart, and G. J. Fleer, *Macromolecules* **31**, 9281 (1998).
- 42 J. G. Göbel, N. A. M. Besseling, M. A. Cohen Stuart, and C. Poncet, *J. Colloid Interface Sci.* **209**, 129 (1999).
- 43 M. A. Cohen Stuart, G. J. Fleer, and B. H. Bijsterbosch, *J. Colloid Interface Sci.* **90**, 310 (1982).
- 44 S. Behl and J. A. Kitchener, *J. Colloid Interface Sci.* **161**, 443 (1993).
- 45 R. C. Davis, in *Detergency, Surfactant Science Series; Vol. 20*, edited by W. G. Cutler and R. C. Davis, Marcel Dekker, New York (1972), 269.

- 46 A. Fava and H. Eyring, *J. Phys. Chem.* **60**, 890 (1956).
47 H. Schott, *J. Colloid Interface Sci.* **23**, 46 (1976).

Chapter 6

Nonionic Surfactants approaching Cellulose Surfaces: Kinetics and Adsorbed Amount

Abstract

Kinetic and equilibrium aspects of three different polyethyleneglycol alkylethers near a cellulose surface are measured. The equilibrium adsorption isotherms look very similar for these surfactants, each showing three different regions with increasing surfactant concentration. At low surfactant content both the head group and the tail contribute to the adsorption and the monomers adsorb in a fairly flat state. At higher surface concentrations, lateral interactions become dominant, leading to the formation of half-micelles on the surface. The cellulose surface shows features in between those for typical hydrophilic and hydrophobic surfaces. The adsorption and desorption kinetics are strongly dependent on surfactant composition. At bulk concentrations below the CMC, the initial adsorption rate is transport-controlled. Above the CMC, the micellar diffusion coefficient and the micellar dissociation rate play a crucial role. For the most hydrophilic surfactant, $C_{12}E_7$, both parameters are relatively large. In this case, the initial adsorption rate increases with increasing surfactant content, also above the CMC. For $C_{12}E_5$ and $C_{14}E_7$ there is no micellar contribution to the initial rate. The initial desorption kinetics are governed by monomer detachment. The desorption rate coefficients scaled with the CMC, indicating an analogy between the surface aggregates and those formed in solution.

6.1 Introduction

The adsorption of nonionic surfactants at solid/liquid interfaces is of great practical importance and it has therefore been extensively studied¹⁻¹⁵. Not in the least due to the availability of homodisperse polyethyleneglycol alkylethers, usually denoted as C_nE_m , their adsorption behaviour is well understood nowadays. Some of the studies concerned hydrophilic⁶⁻¹¹ surfaces, others hydrophobic¹²⁻¹⁵ surfaces.

Silica is by far the most studied hydrophilic adsorbent. At low surfactant concentrations, C_nE_m adsorption is driven by attraction between the head groups and the surface. The adsorbed amount remains rather low, which implies that the interactions are weak. For bulk concentrations close to the critical micelle concentration (CMC), the adsorption increases towards a plateau value^{9,10}. This increase in adsorption is due to hydrophobic attraction between the hydrocarbon moieties of the adsorbed surfactant molecules. For small head groups this increase is step-wise, while it is more gradual for surfactants with longer head groups. The concentration at which the adsorption strongly increases, indicates the onset of aggregate formation at the surface. The amount adsorbed in the plateau and the structure of the adsorbed layer depend on the relative sizes of head and tail group. This can be understood using the critical packing parameter concept introduced by Israelachvili^{16,17}. As a rule of thumb, the plateau adsorption increases with decreasing size of the head group, and increasing length of the alkyl chain^{6,8,10}. For the composition of the adsorbed layer, the trend is that extended cylindrical structures are formed by surfactants with a short head group, whereas smaller surface aggregates are formed when the head group is larger^{4,9,10}. These aggregate shapes resemble those formed in solution. Since the attraction between head groups and the surface is weak, the whole process may be viewed as a surface-induced self-assembly.

Carbon black surfaces are the most studied among the hydrophobic adsorbents. Measured isotherms mostly show a Langmuir-type shape, although it is clear that the conditions for ideal Langmuir behaviour are

not met¹³. It has been suggested that surfactant molecules lie flat on the surface at low concentrations whereas at higher concentrations surface aggregates are formed^{14,15}, in which the alkyl chains are oriented towards the surface and head groups towards the solution. The influence of the composition of the surfactants on the adsorbed amount is equal to that for hydrophilic surfaces, i.e. the adsorption increases with decreasing size of the head group and increasing size of the tail^{12,14,15,18}. Calculations based on a self-consistent field lattice theory for surfactant adsorption show that only at relatively high concentrations the isotherms are Langmuir-like¹⁹. Co-operative transitions take place at very low bulk concentrations. This might be the reason that in experimental studies this phenomenon has been largely overlooked.

In addition to knowing the equilibrium adsorbed amount, information about the kinetics is very useful to obtain further insight into the aggregation behaviour of surfactants at interfaces. However, the number of kinetic studies on surfactant systems in the literature are scarce. One of the first was carried out by Klimenko et al.²⁰, focusing on the adsorption of a polyethyleneglycol alkylphenolether, $C_8\phi E_{10}$ and $C_{12}E_{23}$ onto a silica gel. They did not find any effect of micelles on the kinetics. More recent work on the adsorption kinetics of surfactants^{21,22} and diblock copolymers²³⁻²⁵ showed that monomers and micelles may both contribute to the initial rate. The micellar contribution was interpreted either by direct adsorption, or by breaking up of micelles near the surface, thereby acting as suppliers of monomers. An extensive study to the kinetics of surfactants on bare and hydrophobic silica was carried out by Tiberg et al.^{4,21,26}. These authors identified five regimes in their adsorption-desorption curves, each having its own time-characteristic. Initially both the adsorption and the desorption rate are limited by diffusion of monomers and micelles. At intermediate adsorption values the rate of adsorption decreases because the driving force goes down: there are fewer open sites on the surface and, as equilibrium is approached, the concentration gradient over the stagnant layer also decreases²¹.

This chapter focuses on nonionic surfactants approaching a cellulose surface. Despite its practical relevance e.g. in detergency and papermaking, no systematic study of this system could be found in the literature. A reason for this lack might be the difficulty to obtain well-defined cellulose surfaces. Chapter 5 describes a method that has been developed to overcome this problem by coating wafers with a cellulose film. The availability of such surfaces allows us to study both the kinetics and the equilibrium adsorption of nonionic surfactants on cellulose by stagnation point flow reflectometry. In order to study the effects of the size of the head and tail group on both kinetic and equilibrium aspects, we investigated surfactants of different composition.

6.2 Experimental

6.2.1 Materials

Homodisperse polyethyleneglycol alkylethers, $C_{12}E_5$, $C_{12}E_7$, and $C_{14}E_7$ were purchased from NIKKO Chemicals (Japan) and used as received. The c.m.c.'s and optical properties of these surfactants are shown in table 6.1. The preparation of thick cellulose layers, based on Wegner's method^{27,28}, is described in detail in chapter 5. Layers exposed to 10^{-2} M NaCl had a thickness of 120 nm with a root mean square roughness of 2.5 nm. The refractive index of the swollen layers was 1.45 and the contact angle against water equalled 25°. HCl and NaCl were of analytical grade. Water was purified by passing it through two mixed-bed ion exchangers, a carbon column and a microfilter.

Table 6.1: Critical micelle concentration (c.m.c.)²⁹, refractive index (n)²⁹, and refractive index increment (dn/dc)³⁰ of the nonionic surfactants.

Surfactant	c.m.c. / 10^{-5} M	n / -	$\frac{dn}{dc}$ / ml g ⁻¹
$C_{12}E_5$	6.5	1.443	0.131
$C_{12}E_7$	8.0	1.446	0.138
$C_{14}E_7$	1.0	1.447	0.139

6.2.2 Methods

Surfactant adsorption is studied by stagnation point flow reflectometry. The reflectivity of a flat surface changes due to adsorption. For details about this set-up we refer to Dijt et al.^{31,32}. Incoming polarised light from a He-Ne laser is reflected by a surface at the Brewster angle in a hydrodynamically well-defined position (stagnation point) of the incoming fluid. The reflected beam is split into its parallel (p) and perpendicular (s) component and the ratio $S = I_p/I_s$ of the respective intensities is continuously recorded. Adsorption results in a change ΔS of the output signal. Under appropriate conditions, the relation between ΔS and the adsorbed amount Γ is to a very good approximation linear³²:

$$\Gamma = \frac{\Delta S}{S_0} \frac{1}{MA_s} \quad [\text{mmol m}^{-2}] \quad [6.1]$$

where S_0 is the initial ratio prior to adsorption, M is the molecular weight of the surfactant, and A_s is a sensitivity factor determined by the optical properties of the surface layers. The parameter A_s can be calculated by an optical model in which every layer i is assumed to be homogeneous and characterised by a thickness d_i and refractive index n_i following the method of Hansen³³ which is based on the exact matrix method of Abeles. A five-layer model (silicon, block-copolymer, cellulose, nonionic surfactant, and water) is used to represent our system. Actual values of thicknesses d_i and refractive indices n_i were measured by ellipsometry (see chapter 5). It is noted that reflectometrically only adsorbed amounts are measured. The implications are that (i) conformational transitions in the adsorbate, taking place at given Γ , are not observable but (ii) changes in Γ resulting from such transitions are visible.

All experiments are carried out at a flow rate of 1.0 ml min^{-1} , pH = 5.0 and an electrolyte concentration of 10^{-2} M NaCl . The adsorbed amounts which will be reported in section 6.3.2.1 are taken 12 minutes after start of the experiment. At this time, the adsorption rate is very low, if not negligible.

6.3 Results and discussion

6.3.1 Kinetic Aspects

6.3.1.1 Adsorption and desorption as a function of time

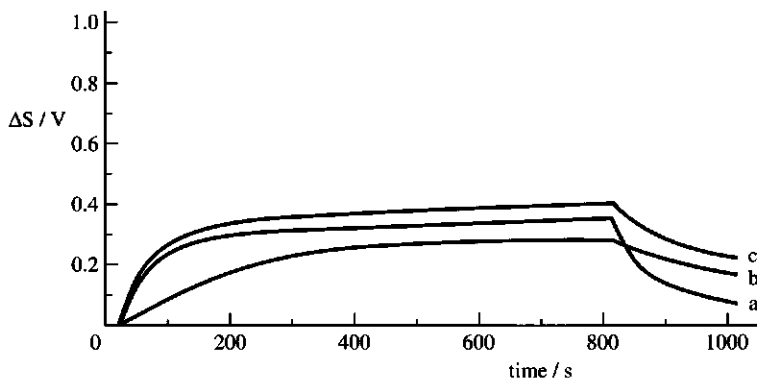


Figure 6.1: Typical adsorption-desorption curves of nonionic surfactants onto cellulose surfaces at concentrations below the c.m.c.; $1.5 \cdot 10^{-5}$ M $C_{12}E_7$ (a), $2.4 \cdot 10^{-6}$ M $C_{14}E_7$ (b), $1.3 \cdot 10^{-5}$ M $C_{12}E_5$ (c); pH = 5.0, 10^{-2} M NaCl.

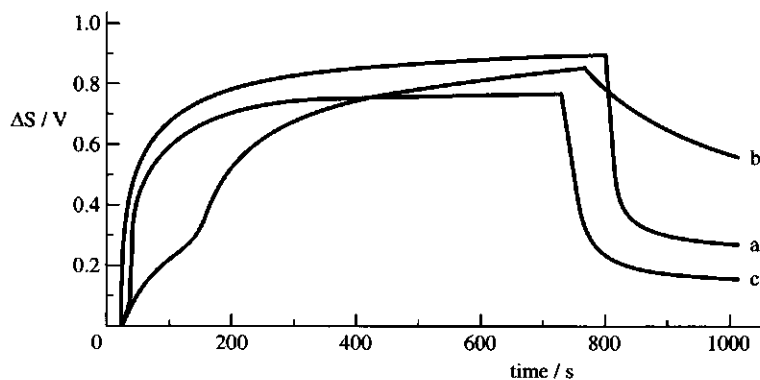


Figure 6.2: Typical adsorption-desorption curves of nonionic surfactants onto cellulose surfaces at concentrations above the c.m.c.; $4.6 \cdot 10^{-4}$ M $C_{12}E_7$ (a), $4.0 \cdot 10^{-5}$ M $C_{14}E_7$ (b), $5.6 \cdot 10^{-4}$ M $C_{12}E_5$ (c); pH = 5.0, 10^{-2} M NaCl.

Figures 6.1 and 6.2 show typical sets of adsorption-desorption curves of the nonionic surfactants at concentrations below and above their c.m.c.'s, respectively. In all experiments an adsorption time of at least twelve

minutes was allowed, thereafter pure electrolyte solution was led into the cell to study the desorption.

The kinetic curves plotted in figure 6.1 initially show a short linear region followed by a decrease in slope thereby reaching a (pseudo-) plateau. The same observations can be made for the desorption curves, i.e. initially a linear decrease with time, followed by a more gradual decay. It takes a very long time before desorption is complete. The $C_{14}E_7$ -curves have much lower initial adsorption and desorption rates than those of the C_{12} -surfactants. The general shapes of the curves can be explained by the fact that in the adsorption part the driving force, i.e. a chemical potential difference between adsorbed and bulk surfactants, $\mu_s - \mu_b$, decreases with increasing surface coverage. This leads to a decrease in the rate. By the same principle, the desorption rate decreases with lowering of the adsorbed amount.

At surfactant concentrations above the c.m.c. (figure 6.2), the curves also initially show a linear region, but at longer times the curves for $C_{14}E_7$ are more complex than those at low surfactant concentrations. This surfactant shows a clear inflection point around 150 s. Further investigations (data not shown) indicate that this point reproducibly recurs at concentrations ≥ 0.6 -c.m.c. and at an adsorbed amount of $2.4 \pm 0.2 \mu\text{mol m}^{-2}$. In general, this specific behaviour can either be a solution or a surface phenomenon. The observation that the inflection point is more pronounced at increased flow rates and increased surfactant concentrations, and that it occurs at an approximately fixed adsorbed amount, indicates that it is a surface feature. Most probably, just before the inflection point is observed, a rearrangement of adsorbed molecules into energetically more favourable aggregates takes place (surface self-assembly). Upon this rearrangement, more area becomes available for adsorption and/or molecules arriving near the surface experience a weaker energetic adsorption barrier. As a result, the adsorption rate increases. The fact that this behaviour is only observed for the longest aliphatic chain indicates that hydrophobic interactions are involved.

The initial adsorption and desorption rates will now be discussed in more detail.

6.3.1.2 Initial adsorption and desorption kinetics

Initial adsorption and desorption rates $(d\Gamma/dt)_0$ are determined from the slopes of the sets of curves shown in figures 6.1 and 6.2, right after the injection of the surfactant solution or the pure solvent, respectively:

$$\left(\frac{d\Gamma}{dt}\right)_0 = \left(\frac{d(\Delta S)}{dt}\right)_0 \left(\frac{1}{S_0 M A_s}\right) \quad [6.2]$$

The resulting initial adsorption rates as a function of the surfactant concentration are plotted in figure 6.3. The three surfactants behave differently. However, below the c.m.c. they show a nearly linear increase of the initial adsorption rate with surfactant concentration. These rates are higher for $C_{12}E_7$ and $C_{14}E_7$ than for $C_{12}E_5$. Above the c.m.c., the adsorption rates of $C_{14}E_7$ and $C_{12}E_5$ remain constant, whereas those of $C_{12}E_7$ continue to increase, though less steeply than below the c.m.c.. Obviously, micelles have no influence on the initial adsorption rates of $C_{12}E_5$ and $C_{14}E_7$. These rates are completely determined by the monomer concentration. However, for $C_{12}E_7$ it follows that micelles also contribute to the adsorption rate.

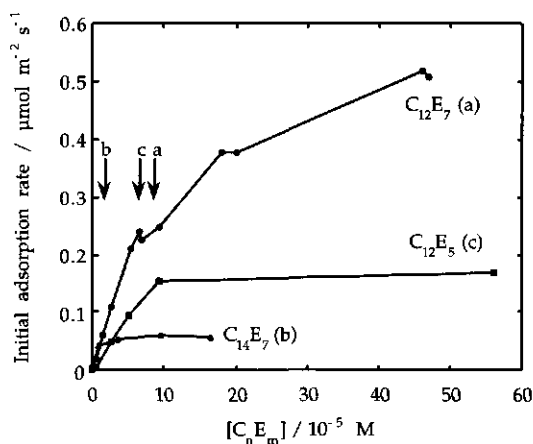


Figure 6.3: Initial adsorption rates as a function of the surfactant concentration; pH = 5.0, $I = 10^{-2} \text{ M NaCl}$; the arrows indicate the c.m.c.'s; lines are only a guide to the eye.

Figure 6.4 shows the initial desorption rates. For all three surfactants, these increase linearly with the adsorbed amount. The desorption rates of $C_{12}E_7$ are slightly higher than those of $C_{12}E_5$, while they are both much higher than those of $C_{14}E_7$. Obviously, the desorption rates primarily depend on the length of the hydrophobic tail and to a much lesser extent on the size of the head group.

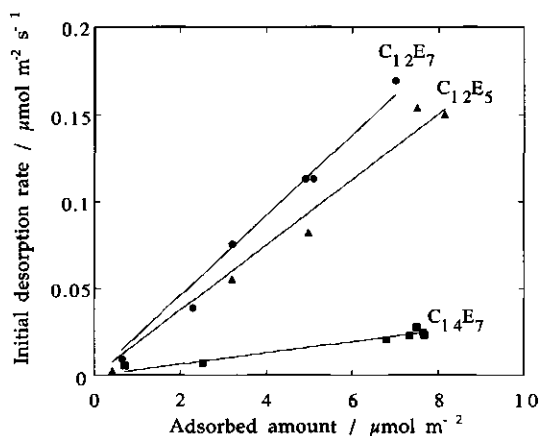


Figure 6.4: Initial desorption rates as a function of the surfactant concentration; pH = 5.0, $I = 10^{-2}$ M NaCl.

6.3.1.3 Modelling and discussion

To further explain these results, the adsorption/desorption process can be divided into a (1) surfactant transport from a bulk phase over a stagnant layer, and vice versa, and (2) surfactant attachment on or detachment from the surface. These contributions are separately considered, and connected by the notion of a subsurface. In the analysis, a distinction will be made between concentrations below and above the c.m.c..

(i) $[C_n E_m] < \text{c.m.c.}$

In the given experimental set-up, transport takes place by convection and diffusion, which is generally called 'convective diffusion'. The starting equation is^{34,35}:

$$J_{tr} = -D\nabla c + vc \quad [6.3]$$

where D is the diffusion coefficient, c the monomer concentration and v the bulk velocity. It is noted that although the real gradient in the diffusion term in equation [6.3] is a chemical potential difference, $\nabla\mu$, a concentration gradient may be used for dilute solutions³⁴.

Flow fields due to convective diffusion are reviewed for different collectors and flow fields³⁵. For stagnation point flow, a (stagnant) diffusive boundary layer with a thickness δ_d arises near the surface. Outside this layer is a bulk phase with constant monomer concentration c_b . In the stagnant layer (i.e. from the bulk to the subsurface), the concentration varies with the distance to the surface. The monomer flux over the stagnant layer may be expressed as²⁵:

$$J_{tr} = k_{tr}(c_b - c_s) \quad [6.4]$$

where k_{tr} is the transport coefficient and c_s the monomer concentration at the subsurface. For convective diffusion, the transport coefficient can be expressed as^{25,31}:

$$k_{tr} = CD^{2/3} \quad [6.5]$$

where C accounts for the cell geometry and the hydrodynamics of the flow field, and D is the monomer diffusion coefficient. Equations [6.4] and [6.5] are the counterpart of Fick's law for diffusion: $J_{tr} = D \frac{dc}{dx} \approx D \frac{\Delta c}{\delta}$ [6.6], where δ is the diffusion layer thickness. The dependence of D on the flux differs between equation [6.5] and Fick's law, since $\delta \propto D^{1/3}$ for convective diffusion³⁶.

The net adsorption rate as a result of monomer attachment on and detachment from the surface depends on the surface coverage³⁷:

$$\left(\frac{d\Gamma}{dt}\right)_a - \left(\frac{d\Gamma}{dt}\right)_d = k_a(1-\theta)(c_s - c_{eq}) \quad [6.7]$$

where k_a is the adsorption rate coefficient, θ is the fractional surface coverage, i.e. $\theta = \Gamma/\Gamma_{max}$, and c_{eq} is the equilibrium concentration^{38,39} corresponding to the actual value of the adsorbed amount.

As there will not be any monomer accumulation at the subsurface, the transport flux [6.4] must equal the net adsorption rate [6.7]. By combining these equations the subsurface concentration can be eliminated, leading to the following general expression for the monomer adsorption/desorption rate in terms of the experimentally accessible parameters c_b , c_{eq} , θ and $t^{37,40}$:

$$\frac{c_b - c_{eq}}{d\Gamma/dt} = \frac{1}{k_{tr}} + \frac{1}{k_a(1-\theta)} \quad [6.8]$$

The left hand side of this equation expresses a measure of the driving force divided by the rate. This ratio is equal to the sum of two resistances, one due to transport and one due to attachment/detachment.

We will now focus on the initial adsorption and desorption rate.

Initial adsorption rate

At the initial stages of the adsorption process $c_{eq} = 0$ and $\theta = 0$ and equation [6.8] yields a proportionality between the initial adsorption rate and the bulk concentration. This is also observed experimentally until roughly the c.m.c. (figure 6.3). Since the only barrier for monomer adsorption is the detachment of water from the surface which is relatively fast, it is most likely that the initial adsorption rate is transport-limited. At a given bulk concentration, rate differences are then caused by differences in the transport coefficient of the different surfactants. Equation [6.5] shows an expression for this coefficient. Since the geometry of the cell and the flow rate of the solutions were not changed in the experiments, C is a constant. As a result, the slopes of the curves in figure 6.3 reflect the relative magnitudes of the monomer diffusion coefficients. Schönhoff and Södermann⁴¹ found a monomer diffusion coefficient of $C_{12}E_5$ at 25°C of $3.9 \cdot 10^{-10} \text{ m}^2 \text{ s}^{-1}$. Using this value for a calibration, we find $C = 4.1 \text{ m}^{-1/3} \text{ s}^{-1/3}$ and diffusion coefficients for $C_{12}E_7$ and $C_{14}E_7$, equal to $1.1 \cdot 10^{-9} \text{ m}^2 \text{ s}^{-1}$ and $1.2 \cdot 10^{-9} \text{ m}^2 \text{ s}^{-1}$, respectively. These values are included in table 6.2.

It follows that D increases with increasing size of the polar head group whereas it is hardly affected by an increase in the tail length. This result is in line with that obtained by Lange⁴² who observed $D_{C_{12}E_7} < D_{C_{12}E_9}$ in

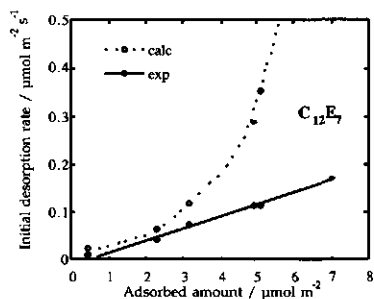
dynamic surface tension measurements. This trend may be caused by an increased hydration of the more hydrophilic monomer.

Initial desorption rate

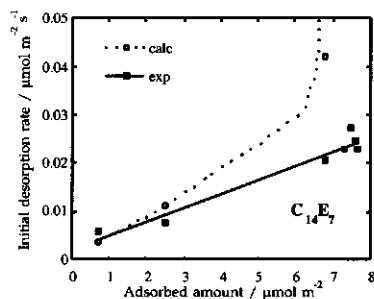
In the desorption process, the bulk solution contains no surfactant molecules. For a reasonably high surface coverage this means that the driving force initially is very large. Since the observed initial desorption rates are finite, there must be a resistance (either limited by detachment or transport) to moderate the desorption rate. It is likely that initially the detachment of a molecule from a surface aggregate suppresses the desorption rate. According to figure 6.4, the initial desorption rate is a first order process, being proportional to the adsorbed amount:

$$\left(\frac{d\Gamma}{dt}\right)_{d,0} = -k\Gamma \quad [6.9]$$

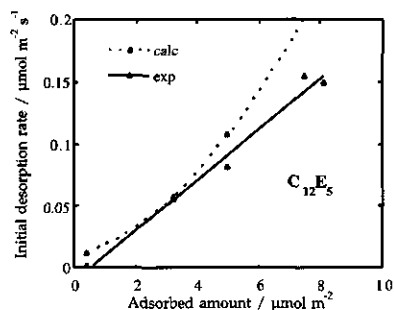
which directly yields an exponential decay for desorption in time. Equation [6.9] suggests a detachment-controlled process (see also expression [6.8]). In order to quantitatively check whether detachment is indeed rate-limiting, the initial desorption rate for a transport-controlled process is calculated. Equation [6.8] yields for this situation $\left(\frac{d\Gamma}{dt}\right)_{tr,0} = -k_{tr}c_{eq}$, which can be calculated since both k_{tr} (equation [6.5]) and c_{eq} (from the equilibrium adsorption isotherms in figure 6) are known. Figures 5a-c show for every surfactant these calculated initial transport-controlled desorption rates together with the observed rates, as a function of the adsorbed amount.



(a)



(b)



(c)

Figure 5: Calculated and observed initial desorption rate contributions of nonionic surfactants.

The three surfactants show similar behaviour despite the large differences in the absolute rates. The observed and calculated desorption rates fairly well coincide up to a surface coverage of 2.5-3.0 $\mu\text{mol m}^{-2}$ ($\theta \approx 0.35$ -0.40) whereas at higher adsorbed amounts, the calculated rates substantially overestimate the experimental ones. The initial desorption rate is at low surface coverages in the same order of size of a transport-controlled process, whereas at higher adsorbed amount it becomes clearly detachment-controlled. As a result, the slopes of the lines directly yield the desorption rate coefficient k_d . These values are included in table 6.2. In order to interpret the relative magnitudes of these coefficients, their meaning must be clearly understood. The adsorption and desorption rate coefficients stem from the equilibrium constant for adsorption, $K = k_a/k_d$, which is a measure of the surface affinity of a molecule. It can be related to the adsorbed amounts by, for example, the Langmuir equation: $\frac{\theta}{1-\theta} = Kc$.

At low θ , k_a is diffusion-controlled. In other words, every molecule arriving at the surface adsorbs, provided it arrives at an open site which leads to the factor $(1-\theta)$ in equation [6.8]. Under these conditions, k_a is a generic parameter, independent of the type of surface. This is experimentally confirmed for the adsorption kinetics of nonionic surfactants at hydrophobic and hydrophilic surfaces⁴³. As a consequence, kinetic differences (observed in K) which do not originate from diffusion,

are due to differences in k_d , i.e. the ease by which a molecule can detach from an adsorbed layer. This concept for the association/dissociation of aggregates at the solid/liquid interface, is analogous to that put forward by Aniansson et al.⁴⁴ for that of ionic surfactants in solutions. They derived $k^-/k^+ = \text{c.m.c.}$, with k^+ and k^- the micellar association and dissociation rate constants, respectively, with k^+ close to being diffusion controlled.

With this in mind, the magnitudes of k_d -values has been considered (table 6.2). It follows that their ratio's (i.e. $C_{14}E_7 : C_{12}E_5 : C_{12}E_7 = 1.0 : 6.5 : 7.9$) equal that of the c.m.c.'s (table 1), an observation also noted by Tiberg²¹. A high k_d means that a molecule can easily be detached from a surface aggregate. Since a high c.m.c. means that molecules have no strong tendency to form aggregates in solution, it is not surprising that we observe a coupling between k_d and the c.m.c..

Table 6.2: Monomer diffusion coefficients and surface micellar dissociation rate constants of different nonionic surfactants.

Surfactant	$C_{12}E_5$	$C_{12}E_7$	$C_{14}E_7$
$D^{\text{mon}} / 10^{-10} \text{ m}^2 \text{ s}^{-1}$	3.9 ^a	11	12
k_d / s^{-1}	0.022	0.027	0.0034

^a value obtained from Schönhoff and Södermann⁴¹.

Table 6.2 shows that the addition of one ethylene group to the molecule decreases k_d by one order of magnitude while the number of ethylene-oxide groups have only little effect. The same trends have been found by Aniansson et al.⁴⁴ for the association/dissociation of sodium alkylsulfates in solution and by Tiberg for the desorption of polyethyleneglycol alkylethers from silica²¹. Our absolute values are lower by a factor of five than those of Tiberg, but this difference may be caused by stronger binding of aggregates at the cellulose surface compared to that onto silica. The observation that the desorption rates scale with the c.m.c. is a strong indication that the surface aggregates resemble the aggregates formed in solution.

(ii) $[C_n E_m] > \text{c.m.c.}$

It is recalled that at bulk concentrations above the c.m.c., the initial adsorption rates gradually increased for $C_{12}E_7$ whereas they remained constant for $C_{12}E_5$ and $C_{14}E_7$ (figure 6.3). In solution, micelles and monomers are in dynamic equilibrium. The micelle concentration increases with increasing surfactant concentration, while the monomer concentration is roughly constant.

Micelles can contribute to the adsorption kinetics in two ways: (1) by diffusing through the stagnant layer and subsequent adsorption, or (2) by diffusing through this layer till $c_b < \text{c.m.c.}$, after which they dissociate thereby acting as a source of monomers, causing an additional flux of surfactant towards the surface. Since the affinity of the head groups for the surface is low (see section 6.3.2), it is not likely that micelles directly adsorb onto the surface. By excluding direct adsorption, three processes remain that may contribute to the adsorption rate: monomer and micellar diffusion, and micellar dissociation. Bijsterbosch et al.²⁵ solved the corresponding transport equations for relatively slow and rapid dissociation of the micelles, showing that the contribution of micelles to the adsorption kinetics depends on their dissociation rate. If this dissociation is relatively slow, adsorption kinetics is simply determined by the adsorption rate of monomers. If it is rapid, a gradual increase of the adsorption rate as function of the surfactant concentration is observed above the c.m.c.. For the systems under study, the latter is only the case for $C_{12}E_7$ (figure 6.3), i.e. the most hydrophilic surfactant. So it is inferred that the $C_{12}E_7$ -micelles dissociate more rapidly than those containing only five EO-groups.

In order to relate the observations of figure 6.3 to the composition of the surfactants, the magnitude of the monomer diffusion coefficients should be compared to the corresponding micellar diffusion coefficients and micellar dissociation rates.

The relative magnitudes of the monomer diffusion coefficients have been obtained from figure 3. Their ranking is: $D_{C_{14}E_7}^{\text{mon}} \geq D_{C_{12}E_7}^{\text{mon}} > D_{C_{12}E_5}^{\text{mon}}$.

Micellar diffusion coefficients are determined by the size and the shape of the micelles. These are, in turn, determined by the relative sizes and shapes of head and tail group^{16,17}. It is known that $C_{12}E_7$ forms spherical micelles, whereas $C_{12}E_5$ -micelles have a more prolate shape^{45,46}. Most probably, the size and shape of $C_{14}E_7$ will be between those of $C_{12}E_7$ and $C_{12}E_5$. For particles of similar shape, the Stokes-Einstein equation states that the hydrodynamic radius is inversely proportional to the diffusion coefficient³⁴. If this is the case, for the relative magnitude of the micellar diffusion coefficients, the following order should hold: $D_{C_{12}E_7}^{\text{mic}} > D_{C_{14}E_7}^{\text{mic}} > D_{C_{12}E_5}^{\text{mic}}$.

The dissociation rate constant of micelles, k_d , is mainly determined by the length of the aliphatic chain⁴⁷ and increases with decreasing hydrophobicity^{44,48}. This can be intuitively understood when k_d is looked upon as a measure of the stability of the micelle, i.e. k_d should be related to the c.m.c.. We therefore expect the following order: $k_{d,C_{12}E_7} > k_{d,C_{12}E_5} \gg k_{d,C_{14}E_7}$.

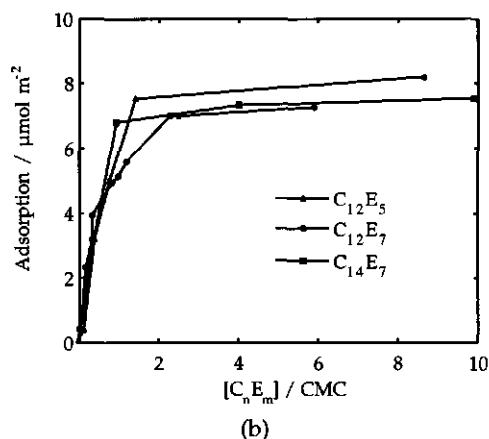
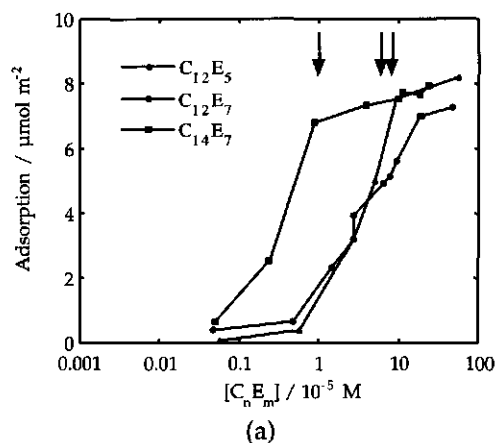
Summing up, it follows that for the most hydrophilic surfactant, $C_{12}E_7$, the micellar diffusion coefficient and the micellar dissociation rate constant are relatively large. In this case, micelles play a crucial role in the adsorption kinetics and the initial adsorption rate increases with increasing surfactant concentration, also above the c.m.c.. The low micellar dissociation rate constant of $C_{14}E_7$, the most hydrophobic surfactant, is the likely reason for the observation that $C_{14}E_7$ -micelles do not contribute to the initial adsorption rate. In this case the initial adsorption rate is dominated by the adsorption of monomers and above the c.m.c. the rate can be obtained from equation [6.8] by $c_b \approx \text{c.m.c.}$ and $k_a \gg k_r$. Surfactant $C_{12}E_5$ has a moderate dissociation rate, but a relatively low micellar diffusion coefficient. Apparently, neither do in this case micelles significantly contribute to the adsorption rate.

In general, it can be concluded that the role of micelles in the adsorption kinetics is determined by the relative magnitudes of the monomer diffusion coefficient on the one hand, and the micellar dissociation rate and the micellar diffusion coefficient on the other.

6.3.2 Equilibrium aspects

6.3.2.1 Adsorbed amount

Adsorption isotherms after an equilibration time of twelve minutes are shown with a linear (b) and a logarithmic (a,c) concentration axis in figure 6.6. In figures 6.6b and c, the concentration axis is scaled to the c.m.c.. Figure 6.6a shows that the surfactants $C_{12}E_5$ and $C_{14}E_7$ reach about the same saturation concentration value, whereas that for $C_{12}E_7$ is slightly lower.



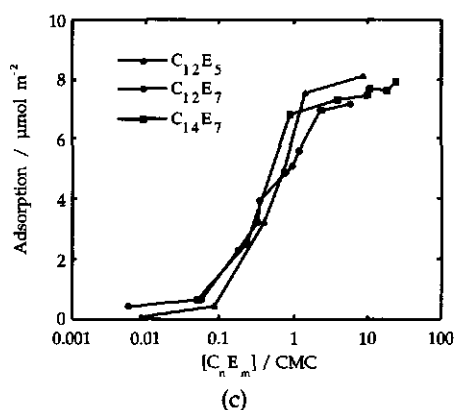


Figure 6.6: Adsorption isotherms of nonionic surfactants on a cellulose surface plotted on a logarithmic (a, c) and linear (b) concentration axis; pH = 5.0, $I = 10^{-2}$ M NaCl; the arrows in figure (a) indicate the c.m.c..

Apart from these small differences in the saturation adsorption, the isotherms hardly differ. This also follows from figure 6a and c, which put more emphasis on the low concentration region. Figure 6a shows the specific differences between the surfactants most clearly. The lower the c.m.c., the lower the concentration at which the adsorption starts.

The semi-logarithmic plots show three distinct regions. At low concentrations (< 0.1 -c.m.c.) there is a small but finite adsorption which is slightly higher for the hepta-ethyleneglycols. At about one tenth of the c.m.c. the adsorption increases steeply till the c.m.c. is reached. After the c.m.c., a (pseudo-)plateau is observed. The three above-mentioned regions will now be discussed by comparing the results with those from literature for typical nonionic surfactant adsorption onto hydrophilic and hydrophobic surfaces.

At low concentrations (< 0.1 -c.m.c.), adsorption likely takes place as isolated molecules since the surface concentration is too small for self-assembly. This means that there should be an attraction between single surfactants and the surface. On a typical hydrophilic surface like silica, adsorption of these nonionic surfactants only starts at 0.6–0.9-c.m.c.⁹⁻¹¹. Hence, it can be concluded that the affinity of the surfactants for cellulose

is larger than that for a typical hydrophilic surface. Probably, on cellulose the hydrophobic tails significantly contribute to the surfactant-surface attraction. Additional support for this conclusion is obtained from adsorption experiments of poly(ethylene oxide) (PEO) which show that PEO does not adsorb onto cellulose. This indicates that the attraction Gibbs energy of an EO-segment with the cellulose surface is less than the critical adsorption Gibbs energy required for polymer adsorption. However, the slightly higher initial adsorption of $C_{12}E_7$ and $C_{14}E_7$ over $C_{12}E_5$, however indicates that the head groups also contribute. It is thus likely that both the EO-head group and the aliphatic tail contribute to the initial adsorption. Therefore, at concentrations < 0.1 -c.m.c. the molecules adsorb fairly flat.

Beyond 0.1-c.m.c. a strong increase in adsorption is observed. The onset of this increase scales with the c.m.c. or the hydrophobicity of the surfactant (figure 6a, c). In this region surface aggregates are formed, of which some features are similar to micellization in solution, i.e. the driving force is the same viz. hydrophobic bonding of the hydrocarbon chains. The slopes of the curves are somewhat steeper than that for a Langmuir isotherm, pointing towards a lateral attraction. To quantify this, an analysis based on the Frumkin-Fowler-Guggenheim (FFG) adsorption isotherm⁴⁹, which is basically a Bragg-Williams isotherm, may be used:

$$\frac{\theta}{1-\theta} = Kxe^{-B\theta} \quad [6.10]$$

where B is a lateral interaction parameter. The values of K and B may be obtained by replotting equation [6.10] as $\ln\left(\frac{\theta}{1-\theta} \frac{1}{x}\right) = \ln K - B\theta$. Such a plot yields a straight line with slope B and intercept $\ln K$. In figure 6.7 the data are plotted in this way, the results correspond reasonably well with straight lines. The slopes of the curves are roughly independent of the length of the aliphatic chain and lead to $B = 2.2 \pm 0.2$, which indicates a moderate lateral attraction⁵⁰. The data are not sufficiently accurate to discriminate between surfactants of differing chain length.

Figure 6.7 further shows that the affinity constant K increases with increasing length of the alkyl chain. This is because hydrophobic bonding increases with chain length. From $\ln K = \Delta G^\circ / RT$, where ΔG° is the standard free energy of adsorption, we obtain a contribution of 1.1 kT per hydrophobic segment. As expected from figure 6c, this value corresponds very well with the contribution of an aliphatic segment to the Gibbs energy of micellization.

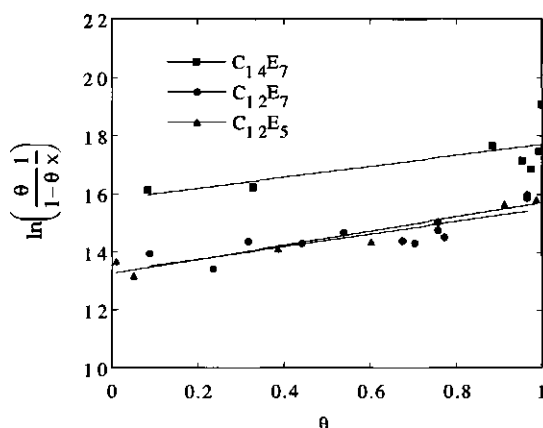


Figure 6.7: Adsorption isotherms of nonionic surfactants plotted according to the linearized form of the FFG-equation.

The third part of the isotherms is the (pseudo-)plateau which is reached around the c.m.c.. The absolute value is slightly higher for $C_{12}E_5$ than for the molecules with the longer head group. These trends are comparable to those found on hydrophilic surfaces and are ascribed to be a packing phenomenon (i.e. denser packing in surface aggregates of molecules with a smaller head group).

A final remark that has to be made is that the plateau values are rather high. Typical values for surfactant adsorption on silica⁹⁻¹¹ are in the range of $4-6 \mu\text{mol m}^{-2}$ whereas for hydrophobic surfaces values of $2-4 \mu\text{mol m}^{-2}$ are found^{4,13,15}. The origin of the high adsorbed amount is not clear. The isotherms have usual shapes and adsorption is reversible. There may be a shortcoming of the optical model (see section 6.2.2), problems could be

surface roughness or swelling of the cellulose layer due to adsorbing molecules. Both will affect the value of A_s and hence Γ . However, an earlier study regarding the adsorption of poly(vinylamine) on a similar cellulose did not show exceptionally large adsorption values⁵¹. An explanation may be that some molecules partly penetrate into the cellulose layer.

6.3.2.2 Molecular packing at the surface

In this section, all results are combined in order to picture the structure of the adsorbed layer throughout the adsorption process. At low surfactant concentrations single molecules adsorb in a rather flat conformation. In the early stages of the steep part of the adsorption isotherm, molecules may still be adsorbed in such a flat state, where they interact to form two-dimensional surface aggregates. At increased adsorption values, where the inflection point in the kinetic curves of $C_{14}E_7$ occurs, surfactant-surfactant attractions become increasingly important. This results in the detachment of head groups and part of the hydrocarbon segments from the surface. It is seen as a transition in the adsorption isotherms which reflects the difference between surfactant-surfactant attraction, and the surfactant-surface attraction. In this way, large three-dimensional aggregates (half-micelles) are formed at the surface. The higher plateau adsorption for $C_{12}E_5$ corresponds with the more prolate micellar structures this surfactant forms compared to the more curved shapes of $C_{12}E_7$ and $C_{14}E_7$. Important evidence for the existence of half-micelles is also obtained from the initial desorption rates of the different surfactants, i.e. they were proportional to the c.m.c.'s.

The inflection point in the adsorption curve of $C_{14}E_7$ (figure 6.2) is likely caused by self-assembly on the surface. A denser packing of molecules (either two- or three-dimensional, where parts of a molecule detach from the surface) due to lateral attractions, increases the area available for adsorption and hence the net adsorption rate. This gain in area is most substantial for the largest molecule, i.e. $C_{14}E_7$.

6.4 Conclusions

Nonionic surfactants readily adsorb onto cellulose, thereby showing three distinct regions which are most visible if their concentration is plotted on a logarithmic scale. Single molecules lie more or less flat on the surface at low concentrations. At increased concentrations, lateral attraction between surfactant molecules dominates and leads to the formation of half-micelles at the surface. These associates resemble the structures formed in solution. Above the c.m.c., the adsorption does not further increase.

The adsorption of the nonionic surfactants on cellulose shows features which are somewhat in between those for a hydrophilic and a hydrophobic surface but may also display some specific features. A good illustration is the moderate lateral attraction in the steep part of the adsorption isotherms.

The adsorption and desorption kinetics sensitively depend on surfactant composition. Below the c.m.c., the initial adsorption rate is transport-controlled. Above the c.m.c., the relative magnitude of monomer diffusion compared micellar diffusion and micellar dissociation, determines whether micelles play a role or not. Micelles contribute as monomer-suppliers to the adsorption kinetics if D^{mic} and k_d are sufficiently large. This is the case for $C_{12}E_7$, the most hydrophilic surfactant. The desorption kinetics are governed by the dissociation rate of surface aggregates.

References

- 1 J. S. Clunie and B. T. Ingram, in *Adsorption from Solution at the Solid/Liquid Interface*, edited by G. D. Parfitt and C. H. Rochester, Academic Press, New York (1983), 105.
- 2 W. von Rybinsky and M. J. Schwuger, in *Nonionic Surfactants, Surfactant Science Series, volume 23*, edited by M. J. Schick, Marcel Dekker, New York (1987).
- 3 J. Lyklema, *Fundamentals of Interface and Colloid Science, volume II: Solid-Liquid Interfaces*, Academic Press, London (1995) Chapter 2, 75.
- 4 F. Tiberg, *J. Chem. Soc., Faraday Trans.* **92**, 531 (1996).

- 5 B. Jönsson, B. Lindmann, K. Holmberg, and B. Kronberg, *Surfactants and Polymers in Aqueous Solution*, John Wiley & Sons, Chichester (1998).
- 6 S. Partyka, S. Zaini, M. Lindheimer, and B. Brun, *Colloids Surf.* **12**, 255 (1984).
- 7 P. Levitz, H. van Damme, and D. Keravis, *J. Phys. Chem.* **88**, 2228 (1984).
- 8 A. Gellan and C. H. Rochester, *J. Chem. Soc., Faraday Trans. I* **81**, 2235 (1985).
- 9 M. R. Böhmer, L. K. Koopal, R. Janssen, E. M. Lee, R. K. Thomas, and A. R. Rennie, *Langmuir* **8**, 2228 (1992).
- 10 F. Tiberg, B. Jönsson, J. Tang, and B. Lindman, *Langmuir* **10**, 2294 (1994).
- 11 Z. Király, R. H. K. Börner, and G. H. Findenegg, *Langmuir* **13**, 3308 (1997).
- 12 J. M. Corkill, J. F. Goodman, and J. R. Tate, *Trans. Faraday Soc.* **62**, 750 (1966).
- 13 B. Kronberg, *J. Colloid Interface Sci.* **96**, 55 (1983).
- 14 A. Gellan and C. H. Rochester, *J. Chem. Soc., Faraday Trans. I* **81**, 1503 (1985).
- 15 J. M. Douillard, S. Pougnet, B. Faucompre, and S. Partyka, *J. Colloid Interface Sci.* **154**, 113 (1992).
- 16 J. N. Israelachvili, D. J. Mitchell, and B. W. Ninham, *J. Chem. Soc., Faraday Trans. 2* **72**, 1525 (1976).
- 17 J. Israelachvili, *Intermolecular and Surface Forces*, second ed., Academic Press, San Diego (1991).
- 18 B. Kronberg, P. Stenius, and G. Igeborn, *J. Colloid Interface Sci.* **102**, 418 (1984).
- 19 M. R. Böhmer and L. K. Koopal, *Langmuir* **6**, 1478 (1990).
- 20 N. A. Klimenko, A. Permilovskaya, A. A. Tryasokurova, and A. M. Koganovski, *Kolloidn. Zh.* **37**, 972 (1975).
- 21 F. Tiberg, B. Jönsson, and B. Lindman, *Langmuir* **10**, 3714 (1994).
- 22 E. S. Pagac, D. C. Prieve, and R. D. Tilton, *Langmuir* **14**, 2333 (1998).
- 23 J. F. Tassin, R. L. Siemens, W. T. Tang, G. Hadziioannou, J. D. Swalen, and B. A. Smith, *J. Phys. Chem.* **93**, 2106 (1989).
- 24 M. R. Munch and A. P. Gast, *Macromolecules* **23**, 2313 (1990).
- 25 H. D. Bijsterbosch, M. A. Cohen Stuart, and G. J. Fleer, *Macromolecules* **31**, 9281 (1998).
- 26 J. Brinck, B. Jönsson, and F. Tiberg, *Langmuir* **14**, 1058 (1998).
- 27 M. Schaub, G. Wenz, G. Wegner, A. Stein, and D. Klemm, *Adv. Mater.* **5**, 919 (1993).

- 28 V. Buchholz, G. Wegner, S. Stemme, and L. Ödberg, *Adv. Mater.* **8**, 399 (1996).
- 29 N. M. van Os, J. R. Haak, and L. A. M. Rupert, *Physico-chemical Properties of Selected Anionic, Cationic and Nonionic Surfactants*, Elsevier, Amsterdam (1993).
- 30 Y. C. Chiu and L. J. Chen, *Colloid Surf.* **41**, 239 (1989).
- 31 J. C. Dijt, M. A. Cohen Stuart, J. E. Hofman, and G. J. Fleer, *Colloids Surf.* **51**, 141 (1990).
- 32 J. C. Dijt, M. A. Cohen Stuart, and G. J. Fleer, *Adv. Colloid Interface Sci.* **50**, 79 (1994).
- 33 W. N. Hansen, *J. Optical Soc. Am.* **58**, 380 (1968).
- 34 J. Lyklema, *Fundamentals of Interface and Colloid Science, volume I: Fundamentals*, Academic Press, London (1991) Chapter 6, 54.
- 35 A. Adamczyk, T. Dabrós, J. Czarnecki and T. G. M. v. d. Ven, *Adv. Colloid Interface Sci.* **19**, 183 (1983).
- 36 R. F. Probstein, *Physicochemical Hydrodynamics, an introduction*, Butterworth Publishers, Stoneham (1989).
- 37 M. A. Cohen Stuart and A. de Keizer, in *Oxide Surfaces, Surfactant Science Series*, edited by J. Wingrave, Marcel Dekker, New York (2000), in press.
- 38 J. C. Dijt, M. A. Cohen Stuart, and G. J. Fleer, *Macromolecules* **25**, 5416 (1992).
- 39 J. C. Dijt, M. A. Cohen Stuart, and G. J. Fleer, *Macromolecules* **27**, 3207 (1994).
- 40 M. J. Avena and L. K. Koopal, *Environ. Sci. Technol.* **33**, 2739 (1999).
- 41 M. Schönhoff and O. Södermann, *J. Phys. Chem. B* **101**, 8237 (1997).
- 42 H. Lange, *J. Colloid Sci.* **20**, 50 (1965).
- 43 M. J. Avena, A. de Keizer and L. K. Koopal, *to be published* (2000).
- 44 E. A. G. Aniansson, S. N. Wall, M. Almgren, H. Hoffman, I. Kielmann, W. Ulbright, R. Zana, J. Lang, and C. Tondre, *J. Phys. Chem.* **80**, 905 (1976).
- 45 P.-G. Nilsson, H. Wennerström, and B. Lindman, *J. Phys. Chem.* **87**, 1377 (1983).
- 46 B. Lindman, in *Surfactants*, edited by T. F. Tadros, Academic Press Inc., London (1984), 83.
- 47 J. H. Clint, *Surfactant Aggregation*, Blackie & Son, Glasgow (1992).
- 48 S. Kato, H. Nomura, H. Honda, R. Zielinski, and S. Ikeda, *J. Phys. Chem.* **92**, 2305 (1988).

- 49 R. H. Fowler and E. A. Guggenheim, *Statistical Thermodynamics*, University Press, Cambridge (1965) 429.
- 50 L. K. Koopal, in *Coagulation and Flocculation, Surfactant Science Series; Vol. 47*, edited by B. Dobias, Marcel Dekker, New York (1993), 101.
- 51 C. Geffroy, M. P. Labeau, K. Wong, B. Cabane, and M. A. Cohen Stuart, *Colloids Surf. A: Physicochem. Eng. Aspects*, in press (2000).

Summary

This thesis deals with detergency-related adsorption phenomena of (mixtures of) polymers and surfactants. Both types of molecules play an important role in the removal and subsequent stabilization of soil from a substrate. Starting with a model detergency system consisting of polymers, surfactants, soil and a substrate, a division is made into a set of sub-systems, each focusing on the interactions of two or more of these model components.

The first chapter gives a short introduction on the typical behavior of polymers and surfactants in solution and at interfaces, and touches upon the physicochemical principles of detergency.

In a washing process it is important to prevent the redeposition of soil, which in an earlier stage has been removed from a substrate. A way to keep particles dispersed in solution is to cover them with a thick polymer layer providing electrostatic and/or steric stabilization. The adsorption of the uncharged polymer poly(vinylpyrrolidone) (PVP) on Na-kaolinite has been studied in chapter 2. The surface of this clay mineral is patchwise heterogeneous with respect to its charge and chemical composition. In order to reveal these charge characteristics, potentiometric acid-base titrations were performed on samples at different concentrations of sodium chloride. An interpretation of the proton adsorption/desorption in terms of the contributions of the individual surface types, i.e. edges and plates, has been given. At the latter type, protons are strongly favored over sodium ions. Striking similarities were observed between the proton adsorption and the PVP adsorption experiments. PVP readily adsorbs with high affinity on at least part of the kaolinite surface. Studying the effect of the pH, the electrolyte concentration, and the presence of multivalent ions on the amount adsorbed at the plateau has given further insight into the adsorption mechanisms. Increasing the pH or the electrolyte concentration

leads to a decrease in PVP adsorption. A model is proposed in which PVP adsorbs on edges and basal planes by different mechanisms. The adsorption of PVP on the edges is strongly pH dependent, but that on the plates only weakly. Specifically adsorbed protons at the plates act as anchor sites for PVP segments. Multivalent ions do not influence the proposed adsorption mechanism directly, but primarily change the surface area accessible for PVP.

Before studying adsorption of a polymer-surfactant mixture, information on the interaction between the polymer and the surfactant in solution is indispensable. Chapter 3 covers the interaction between the anionic surfactant sodium dodecylbenzenesulphonate (SDBS) and the uncharged polymer poly(vinylpyrrolidone) (PVP) by titration microcalorimetry. Since hydrophobic attractions are typically dependent on temperature, which is in general not the case for other types of interaction, measurements carried out at different temperatures have yielded information on the nature of the associations. The interaction enthalpy of mixed PVP/SDBS systems clearly showed a consecutive endothermic and exothermic region with increasing surfactant concentration. The endothermic part can be looked upon as an incremental binding isotherm and reflects the number of surfactant molecules involved in the process. The exothermic region features the inverse of hydrophobic bonding behaviour. In our opinion, this is due to conformational changes of the polyelectrolyte complexes. With increasing amount of surfactants bound to the chain, electrostatic repulsion of neighbouring surfactant head groups tends to expand the complexes, whereas hydrophobic interactions do the opposite. Beyond a certain coverage, the coulombic repulsion forces the chains to swell. This is accompanied by losing hydrophobic inter- and intrachain linking. Additional surfactants continue to adsorb on the vacant hydrophobic adsorption sites. The influence of the initial amount of polymer and the electrolyte concentration support our proposals.

The results and the knowledge obtained with this study has helped to understand the mixed adsorption of PVP and SDBS on kaolinite, which is the subject of chapter 4. Both components adsorb from their mixture on the clay. This process is sensitive to the pH, the electrolyte concentration, and the amounts of polymer and surfactant. In the absence of PVP, SDBS adsorbs on the clay by electrostatic and hydrophobic interactions. When polymers are present, the adsorbed amount of SDBS is at 10^{-2} M NaCl mainly determined by charge compensation on the edges.

Under different conditions PVP shows similar behaviour as a function of the surfactant concentration. With increasing SDBS concentration three subsequent regions in the PVP adsorption can be distinguished: initially a small increase, followed by a strong decrease, which finally flattens off to a plateau. These regions are related to the surface affinity of the species actually present in solution. They reflect the changing character of the charge of the polymer-surfactant complexes with increasing surfactant concentration. At low surfactant content, the polymer chains are not or hardly charged, and they adsorb on the clay by hydrogen bonding and hydrophobic interactions. At high surfactant concentrations, the adsorption of polymer-surfactant complexes is dominated by coulombic attraction. There is experimental evidence for the presence of mixed surface aggregates at the edges. The composition of these complexes differs from that in solution and is controlled by the surface charge. With increasing electrolyte concentration, this difference becomes smaller.

After a detailed look at the solution side of the washing process, we have to focus on the substrate. In order to carry out some fundamental studies, a flat and well-defined surface was needed which was a good mimic for cotton. To that end, a cellulose surface was developed which was able to function as a model for cotton. Chapter 5 describes the preparation of thick cellulose films. The method is based on the attachment of hydrophobized cellulose on a wafer and subsequent chemical regeneration to cellulose. With the spincoating technique, reproducible, rapidly prepared, and flat cellulose surfaces can be obtained. These are characterized by their

thickness, roughness, swelling behaviour, stability, charge, and wetting and adsorption properties. The root mean square roughness of dry surfaces was 1.0 nm. When immersed in water, the layers swell which indicated an at least partly amorphous nature, and the root mean square roughness increased to 2.5 nm. Stability of the layer against detachment by water was provided by a block copolymer which anchored the layer onto a wafer. Streaming potential measurements showed an iso-electric point of $\text{pH} = 3.8$. No specific adsorption of mono- and divalent ions was observed. Contact angle measurements showed the surface to be rather hydrophilic. The former can be linked with charges and polar groups, whereas the latter can be related to crystalline regions. Adsorption of familiar polymers and surfactants on the cellulose layer showed that it mimics the behaviour of an ordinary cellulose surface.

So far, all studies concerned equilibrium aspects. However, in a washing process, the dynamics of processes, such as adsorption, removal, and stabilization, are very important. Kinetic and equilibrium aspects of nonionic surfactant adsorption on cellulose surfaces just described, are studied in a stagnation point flow cell (chapter 6). Nonionic surfactants readily adsorb on cellulose, thereby showing three distinct regions. At low surface coverages, molecules adsorb more or less in a flat state, with a contribution from both the head group and the tail. At increased concentrations, lateral attraction between surfactant molecules is dominant, leading to the formation of half-micelles at the surface. In line with the results of chapter 5, the adsorption features of cellulose are in between those for a hydrophilic and a hydrophobic surface.

The kinetics of nonionic surfactant adsorption depends on the composition of the surfactant. Below the CMC, the initial adsorption rate is determined by monomer diffusion. Above the CMC, the magnitudes of the micellar dissociation rate and the micellar diffusion coefficient, should be compared to that of the monomer diffusion coefficient. If the micellar properties are sufficiently large, micelles acts as monomer-suppliers. This was observed for the most hydrophilic surfactant under study. The

desorption rate depends on the surface coverage. Initially, it is controlled by monomer detachment. The desorption rate coefficients of different surfactants scaled with the CMC, suggesting an analogy between the surface aggregates to those formed in solution.

So far we focused on *sub*-systems of the washing process, related to the solution and the substrate part, respectively. By way of conclusion, we give a small illustration which connects these parts (see figure S1).

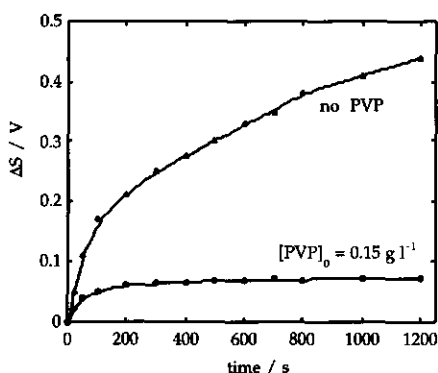


Figure S1: Deposition of bare and PVP-pre-adsorbed kaolinite on cellulose as a function of time in a stagnation point flow cell; pH = 5.0, $I = 10^{-2}$ M NaCl.

The figure shows the deposition of bare and PVP-pre-adsorbed kaolinite particles on cellulose. The bare particles readily deposit, whereas the deposition is greatly reduced if PVP is pre-adsorbed. We know that PVP adsorbs on kaolinite (chapter 2), whereas it does not adsorb on cellulose (chapter 5). This explains the observations in figure S1. A thick polymer layer is adsorbed on the clay, thereby providing steric stabilization against (re)deposition onto cellulose.

This set-up of the cellulose surfaces in a stagnation point flow cell can be used for a variety of adsorbates and serve as a model for (re)deposition studies.

Samenvatting

Het wassen van kleren is een proces waar iedereen mee te maken heeft. Desondanks vragen maar weinig mensen zich af wat er nu precies in een wasmachine gebeurt. We stoppen onze vuile was erin, voegen wasmiddel toe, en verwachten dat het er volledig schoon en fris uitkomt. Bij nadere bestudering wordt al snel duidelijk dat wassen niet zo eenvoudig is als het op het eerste oog misschien lijkt. Een van de oorzaken is de grote variëteit in zowel kleding (katoen, polyester, wol, etc.) als vuil (gras, klei, koffie, bloed, etc.). Aan het wasmiddel de taak om deze vlekken op te sporen en te verwijderen, en de kleding niet aan te tasten.

Een wasmiddel bevat een groot aantal componenten zoals oppervlakte-actieve stoffen (ook wel 'surfactanten' of zepen genoemd), polymeren, enzymen, bleekmiddelen en waterontharders, die elk hun eigen functie in het proces hebben. Vaak vertonen ze ook onderlinge interacties, die zowel positieve als negatieve effecten op het eindresultaat kunnen hebben.

Dit proefschrift gaat over het gedrag van twee van deze componenten, namelijk polymeren en surfactanten, aan vast-vloeistof oppervlakken. Polymeren zijn grote molekulen die opgebouwd zijn uit een groot aantal segmenten (monomeren). Ze spelen een belangrijke rol in het stabiliseren van reeds verwijderd vuil. Surfactanten hebben een tweeslachtige structuur, bestaande uit een waterminnende (hydrofiele) kop en een watervrezende (hydrofobe) staart, zie figuur 1.2 op bladzijde 4. Een gevolg van deze tweeslachtigheid is dat ze de neiging hebben zich op te hopen (te adsorberen) aan grensvlakken, zoals een lucht-water of een olie-water grensvlak. Als surfactanten in contact met water worden gebracht, voelen de hydrofiele delen zich hier goed thuis, terwijl de hydrofobe delen het liefst elkaar opzoeken. Als er voldoende surfactantmolekulen aanwezig zijn, lossen ze dit probleem op door aggregaten (micellen) te vormen, waarbij de koppen naar de waterfase worden gericht en de staarten naar

elkaar toe (zie figuur 1.3 op bladzijde 5). De concentratie waarbij micellen worden gevormd wordt de kritische micel concentratie (doorgaans aangeduid als c.m.c., afkomstig van het Engelse 'critical micelle concentration') genoemd. De c.m.c. is de meest karakteristieke eigenschap een surfactant.

Adsorptie van surfactantmolekulen aan een grensvlak verlaagt de grensvlakspanning, zodat de verwijdering van vuil vergemakkelijkt wordt. Veel soorten vuil kunnen worden opgenomen in de hydrofobe kern van micellen waarmee wordt voorkomen dat het op een andere plaats op de kleding neerslaat.

Om het gedrag van polymeren en surfactanten in relatie tot het wasproces goed te kunnen bestuderen, is gekozen voor een modelsysteem, bestaande uit polymeren, surfactanten, vuildeeltjes en een substraat (modeloppervlak voor textiel). Omdat dit systeem nog steeds erg complex is, zijn subsystemen onderzocht. Hoofdstuk 2 behandelt de adsorptie van het ongeladen polymeer poly(vinylpyrrolidon) (PVP) op een kleisoort, kaolinet, dat wordt gebruikt als modeloppervlak voor vuil. Kaolinetdeeltjes hebben een zeshoekige vorm, waarbij randen en platen te onderscheiden zijn. Deze oppervlakken verschillen in chemische samenstelling en ladingsgedrag. De platen hebben een constante negatieve lading, terwijl de randen een variabele lading hebben, afhankelijk van de pH. Als gevolg van deze heterogeniteit is kaolinet een interessant oppervlak om te bestuderen. De adsorptie van ongeladen PVP is sterk afhankelijk van de pH en de ionsterkte. PVP adsorbeert op de verschillende oppervlakken van kaolinet via verschillende mechanismen: op de randen treedt adsorptie op via de vorming van waterstofbruggen, terwijl op de platen binding plaatsvindt tussen hydrofobe delen van het oppervlak en hydrofobe groepen in het polymeer. Het blijkt dat de platen een sterke voorkeur hebben voor protonen ten opzichte van natriumionen. Als protonen adsorberen, vormen ze ankerpunten voor PVP. Kenmerkend voor de adsorptie van polymeren is dat ze zich op meerdere plaatsen hechten aan een oppervlak (zie figuur 1.1 op bladzijde 2) en dikke

lagen vormen. Het zijn deze lagen die polymeren erg geschikt maken om ze te gebruiken voor het stabiliseren van deeltjes.

De wisselwerking tussen PVP en de negatief geladen surfactant sodium dodecylbenzenesulfonaat (SDBS) is het onderwerp van hoofdstuk 3. Aan een polymeeroplossing is surfactant toegevoegd en de resulterende stijging of daling van de temperatuur is gemeten. Door dit bij verschillende temperaturen te doen, kan informatie worden verkregen over het mechanisme van de wisselwerking tussen PVP en SDBS. Bij lage surfactantconcentratie binden losse molekulen aan de pyrrolidon-ring van het polymeer. Deze losse molekulen fungeren als een kiem waaraan bij hogere concentratie nieuwe molekulen adsorberen. De drijvende kracht is hier identiek aan die voor de vorming van micellen in oplossing, namelijk *hydrofobe binding*. Dit proces, waarin surfactantaggregaten zich vormen aan een keten, wordt bevorderd door polymeren. In ongeladen toestand vormen polymeren in oplossing doorgaans een kluwen waarbij veel ketensegmenten tamelijk dicht bij elkaar in de buurt zitten. Door de adsorptie van surfactantaggregaten wordt de keten opgeladen en komt hierdoor onder spanning te staan door aggregaten die bij elkaar in de buurt zitten. Als gevolg hiervan trekt het polymeer zich bij hoge surfactantconcentratie, waarbij wisselwerkingen, zowel binnen een keten als tussen ketens, worden opgegeven. De keten trekt zich waarbij tijdelijk een verlies aan hydrofobe bindingen optreedt. Nieuw toegevoegde surfactant molekulen vullen deze hydrofobe bindingsplaatsen weer op.

Nadat een goed beeld verkregen was over de wisselwerking tussen PVP en SDBS, is gekeken naar de gemengde adsorptie van deze molekulen op kaoliniet. Beide molekulen adsorberen vanuit hun mengsel op de klei. Het is een complex proces, dat erg gevoelig is voor de pH, de hoeveelheid aanwezige ionen, en de hoeveelheden polymeer en surfactant. De adsorptie van PVP vertoont in veel gevallen een maximum als functie van de surfactantconcentratie. Dit maximum treedt op bij lage surfactantconcentratie. De geladen complexen die in oplossing aanwezig zijn hebben een relatief goede affiniteit voor de randen en ondervinden een

relatief zwakke afstoting van de platen. Bij hogere belading van de complexen, is deze afstoting veel hoger en neemt de totale adsorptie af. Door de wisselwerking met surfactant verschuift het adsorptiemechanisme van PVP op kaoliniet van waterstofbrugvorming en hydrofobe binding voor ongeladen PVP, naar hoofdzakelijk electrostatistische (coulombse) aantrekking voor een geladen polymeer-surfactantcomplex. Deze complexen adsorberen op de randen. De samenstelling van de complexen wordt opgelegd door het oppervlak. In eerste benadering compenseren de complexen de lading op de randen.

In de voorgaande hoofdstukken is veel aandacht besteed aan processen die zich afspelen in de waterfase. De laatste twee hoofdstukken richten zich op de substraatzijde. Om het mogelijk te maken fundamenteel onderzoek te doen, was het van belang een goed gedefinieerd oppervlak te hebben. Hoofdstuk 5 beschrijft de ontwikkeling van een cellulose-oppervlak dat fungeert als modelsysteem voor katoen. Gebaseerd op een bekende procedure wordt een dikke cellulosefilm met behulp van spincoating aangebracht op een silicium plaatje. De films worden verankerd op het plaatje met behulp van een blok-copolymeer. De verkregen films werden gekarakteriseerd ten aanzien van hun dikte, ruwheid, zwellingsgedrag, stabiliteit, bevochtiging, ladingsgedrag en adsorptie-eigenschappen. De films zijn voldoende glad, amorf, licht negatief geladen en tamelijk hydrofiel. Het adsorptiegedrag is vergelijkbaar met dat van doorsnee cellulose oppervlakken.

De adsorptie van ongeladen surfactants op deze cellulose films is beschreven in hoofdstuk 6. Met behulp van reflectometrie is zowel gekeken naar de geadsorbeerde hoeveelheid als naar de adsorptiesnelheid. Ongeladen surfactants adsorberen goed op cellulose. In de adsorptieisothermen kunnen drie gebieden worden onderscheiden. Bij lage surfactantconcentratie adsorberen losse molekulen nagenoeg vlak op het oppervlak (i). Bij verhoging van de concentratie, treedt een sterke stijging van de adsorptie op, veroorzaakt door surfactant-surfactant aantrekking (ii). Dit proces is gedreven door hydrofobe binding en is te vergelijken met

micellisering in oplossing en de wisselwerking van surfactants met polymeren in hoofdstuk 4. In het eerste geval bevinden de surfactants zich alleen in oplossing, in het tweede geval fungeert het polymeer als een flexibel oppervlak en in het derde geval is cellulose een vast oppervlak. Verdere verhoging van de concentratie resulteert in een plateau, dat wordt bereikt rondom de c.m.c. (iii). Hier bevinden zich halve micellen op het oppervlak, met de staarten richting cellulose en de koppen naar de waterfase gericht.

De snelheid waarmee de molekulen adsorberen en desorberen, hangt sterk af van de moleculaire samenstelling van de surfactant. Bij lage concentratie is de adsorptiesnelheid in het begin volledig bepaald door diffusie. Boven de c.m.c. bepaalt de snelheid waarmee micellen uiteenvallen, ten opzichte van de diffusiesnelheid van monomeren, of de snelheid nog verder kan toenemen. Als micellen snel bewegen en snel uit elkaar vallen ten opzichte van de snelheid van monomeren, zal de adsorptiesnelheid nog toenemen boven de c.m.c.. Dit is het geval voor een relatief hydrofiele surfactant. Een surfactant die meer hydrofoob is, valt doorgaans minder snel uit elkaar. In dat geval wordt de adsorptie volledig bepaald door de snelheid waarmee monomeren zich richting het oppervlak bewegen.

De desorptiesnelheid hangt sterk af van de hoeveelheid molekulen op het oppervlak. Initieel is het losmaken van een surfactant molecuul de snelheidsbepalende stap in het desorptieproces. Deze snelheid is voor verschillende onderzochte surfactanten evenredig met de c.m.c.. Dit suggereert een sterke analogie tussen de aggregaten die in oplossing gevormd worden, en de aggregaten op het cellulose-oppervlak.

De resultaten en de kennis opgedaan in de voorgaande hoofdstukken kunnen worden gecombineerd. Cellulosefilms in een reflectometer met een stromingscel bieden een flexibele techniek voor allerlei adsorptie- en depositiestudies.

Curriculum Vitae

Lubertus Henricus Torn werd geboren op 6 maart 1971 te Rijssen. In 1989 behaalde hij het VWO-diploma aan het 'College Noetsele' te Nijverdal. Hij ging hierna Chemische Technologie studeren aan de Universiteit Twente in Enschede. Zijn studie rondde hij af in 1995. Zowel stage als afstudeeropdracht voerde hij uit bij DOW Benelux N.V. in Terneuzen, op het gebied van materiaalkunde en technologie van polymeren. Vanaf december 1995 tot februari 2000 was hij als Assistent-in-Opleiding werkzaam bij het laboratorium voor Fysische Chemie en Kolloïdkunde van de Universiteit Wageningen. In deze periode werd het in dit proefschrift beschreven onderzoek uitgevoerd. Sinds februari 2000 is hij in dienst bij Unilever Research Vlaardingen bij de afdeling Home and Personal Care.

Dankwoord

Bij het terugkijken op de afgelopen vier-en-een-half jaar klinkt zowel een euforische ('het boekje' is af: ☺☺) als een bespiegelende ondertoon (vertrek uit Wageningen: ☹). Door de open en gemoedelijke sfeer die op het lab heerst, heb ik me direct thuis gevoeld. Voordat ik mensen in het bijzonder wil aanspreken, daarom eerst een oprecht woord van dank aan de vakgroep (desnoods leerstoelgroep) als geheel.

Een aantal mensen heeft meer van dichtbij mijn stappen gevolgd. In de eerste plaats mijn promotor, Hans Lyklema. Hans, het duurde even voor ik je vrijuit kon tutoyeren. Ik wil je danken voor alle ruimte en vrijheid die ik de afgelopen vier jaar gekregen heb. Bij m'n aanstelling vroeg je me of ik er geen bezwaar tegen zou hebben als je m'n promotor zou zijn. Ik kan nu antwoorden dat ik me geen betere heb kunnen wensen.

Arie en Luuk, jullie vormen een bijzonder copromotor-koppel. Als al onze geplande werkbesprekingen werkelijk waren doorgegaan, waren we nu waarschijnlijk nog bezig geweest. Aan het eind konden we het altijd weer redelijk in elkaars opvattingen vinden en waren we inhoudelijk weer wat wijzer geworden. Ik zal onze besprekingen missen.

Luuk, ik heb veel geleerd van je kritische en grondige blik op experimentele resultaten en conceptteksten, en ik denk met plezier aan diverse stellingnames van je, over diverse onderwerpen, op diverse plaatsen en op diverse momenten; toegegeven, ik was het redelijk vaak met je eens.

Arie, ondanks inter- en intralabverhuizingen waren onze kamers nooit ver van elkaar. Altijd was je bereid te helpen met alledaagse problemen en had je een scherpe kijk op experimentele (on)mogelijkheden.

Gedurende het hele project is er een keer of vier per jaar overleg met Unilever Research Vlaardingse geweest. Ondanks een principiële verschillende oriëntatie verliepen deze besprekingen altijd bijzonder goed. Rode draad gedurende de gehele periode was Flip van der Hoeven. Naast hem in het bijzonder, wil ik ook Paul Birker, Wilfried Blokzijl, Pascale Lazare en John van de Pas hartelijk danken voor hun inbreng en interesse.

Op het lab is een aantal mensen onmisbaar voor het welslagen van een project. Ben Spee, naast het delen van voetbal- en andere levenswijsheden, zorgde je dat alle chemicaliën en apparatuur er op tijd waren; van de diverse weddenschappen die we hebben afgesloten is er tot nog toe maar één werkelijk uitbetaald; ik meen me echter te herinneren dat je er NU precies weer één verloren hebt..... Bert Bouman, Gert Buurman, en Rob Vullings waren altijd bereid om op de meest ongeschikte momenten te helpen met plaatjes, tekeningen, computertroubles of layoutbeslommingen.

Geen AIO zonder (ex-)lab/lotgenoten. Zonder volledig te zijn wil ik in elk geval Marcelo Avena, Desiree Barten, Monique Bremer (ik durf je bijna niet te noemen), Remco Fokkink, Cedric Geffroy, Carla Giacomelli, René Hoogendam (als collega-poolorganisator weet je als geen ander de termen 'betrouwbaar' en 'corrupt' te combineren), Joanne Klein Wolterink, Joost Maas, Martijn Oversteegen (het begrip 'gekromd oppervlak' is voor mij plotseling gaan leven), Maarten van de Wielen (dit keer geen spelletje.....) en Mara Winkels bedanken voor een gezellige en onvergetelijke tijd.

M'n chronologische kamergenieters Henk Huinink, Raquel Barchini en Marijn van der Veen (het zit me nog steeds dwars dat je het minesweep-record bezit) zorgden ieder voor een geheel verschillende, maar steeds prima (werk?)sfeer.

Met veel plezier heb ik Sytske Moolenaar, Stefan van der Burgh, Ben Dijk en deels Ebbing de Jong begeleid bij een afstudeervak. Om uiteenlopende redenen is hier helaas weinig terug te vinden van jullie werk, maar alle onderwerpen waren leuk en leerzaam. Goede herinneringen bewaar ik aan vele al dan niet serieuze uitstapjes, en het volleyballen (nu eindelijk een Kollosolexer). Heel positief kijk ik terug op het geven van onderwijs, wat voor mij bestond uit het practicum en het werkcollege 'Algemene en Fysische Chemie'. Het was erg intensief, maar zeker alle moeite waard.

Bijna aan het eind gekomen, wil ik m'n ouders danken voor hun jarenlange steun en betrokkenheid.

Ten slotte, Marije, de laatste loodjes waren langer en zwaarder dan verwacht; vaak was ik er niet, of misschien wel, maar dan toch eigenlijk ook weer niet; m'n laatste woorden en de komende tijd zijn voor jou.